THE EFFECTS OF NEUROPATHY-INDUCING ORGANOPHOSPHATE ESTERS ON CHICK DORSAL ROOT GANGLIA CELL CULTURES.

By

Christiane Massicotte

Dissertation submitted to the Faculty of the Virginia Polytechnic institute & State University in partial fulfillment of the requirements for the degree of

Doctor of Philosophy

in

Veterinary Medical Sciences

APPROVED

Marion F. Ehrich (Chairman)	Bernard S. Jortner
Cornelis Van der Schyf	Bradley Klein
Jeffrey Bloomquist	Karen D. Inzana

September 2001
Blacksburg, Virginia

Keywords: Organophosphate, Neuropathy, ATP, mitochondria

i. ABSTRACT

THE EFFECTS OF NEUROPATHY-INDUCING ORGANOPHOSPHATE ESTERS ON CHICK DORSAL ROOT GANGLIA CELL CULTURES.

By: Christiane Massicotte

Committee Chairman, Dr. Marion F. Ehrich
Veterinary Medical Sciences

Cultures of dorsal root ganglia (DRG) can achieve neuronal maturation with axons, making them useful for neurobiological studies. They have not, however, previously been used to investigate subcellular events that occur following exposure to neuropathy-inducing organophosphorus (OP) esters. Recent studies in other systems demonstrated alterations of ATP concentrations and changes in mitochondrial transmembrane potential ($\Delta\Psi m$) following exposure to neuropathy-inducing OP compounds, suggesting that mitochondrial dysfunction occurs. The present dissertation proposed an investigation using chick embryo DRG cultures to explore early mechanisms associated with exposure to these toxicants. This approach uses an *in vitro* neuronal system from the species that provides the animal model for OP-induced delayed neuropathy (OPIDN). DRG were obtained from 9-10 day old chick embryos, and grown for 14 days in minimal essential media (MEM) supplemented with bovine and human placental sera and growth factors. Cultures were then treated with 1 μM OP compounds, or the DMSO vehicle control. OP compounds used were phenylsaligenin phosphate (PSP) and mipafox, which readily elicit OPIDN in hens, and paraoxon, which does not cause OPIDN. Confocal microscopic evaluation of neuronal populations treated with PSP and mipafox showed opening of mitochondrial permeability transition (MPT) pores, and significantly lower mitochondrial tetramethylrhodamine fluorescence, suggesting alteration of mitochondrial structure and function. This supports our conclusion that mitochondria are a target for neuropathy-inducing OP compounds by inducing mitochondrial permeability transition. For further evaluation of mitochondrial

function, mitochondrial respiratory chain reactions were measured. *In situ* evaluation of ATP production measured by bioluminescence assay showed decreased ATP concentrations in neurons treated with PSP and mipafox, but not paraoxon. This low energy state was present in several levels of the mitochondrial respiratory chain, including complexes I, III and IV, although complex I was the most severely affected. For morphological studies, the media containing the aforementioned toxicants was removed after 12 hours, and cultures maintained for 4 to 7 days post-exposure. Morphometric analysis of neurites in DRG was performed by inverted microscopy, using a system that was entirely computerized. Morphometric estimation of neurites treated with mipafox or PSP but not with paraoxon suggested that reversible axonal swelling at day 4 post-exposure had reversed by 7 days post-challenge. Ultrastructural alterations were described by electron microscopy. Damage to neurons was more severe following exposure to PSP and mipafox, with mitochondrial swelling and rarefaction of microtubules and neurofilaments observed within the cytoplasm. This study supports others that suggested mitochondria are a primary target for neuropathy-inducing OP compounds. We suggest that mitochondrial permeability transition (MPT) induce abrupt changes in mitochondrial membrane potentials, altering the proton gradient across the mitochondria membrane, decreasing ATP production within the cell. In addition, reduction in ATP production can be related to specific-complex alteration of the mitochondria respiratory chain following neuropathy-inducing OP compounds. The profound ATP depletion and the induction of MPT can induce the release of apoptotic factors and intramitochondrial ions, leading to axonal damage observed later in the course of OPIDN. This study provides evidence that chick DRG cell cultures are an excellent model to study early structural and functional features of OPIDN. It is likely that the alteration in energy lead to ultrastructural defects in these cells. These early events can contribute to alteration in neuronal ATP production previously reported in OPIDN.

ii. ACKNOWLEDGMENTS

First and foremost, I would like to dedicate this work to my parents, immediate family members and loved ones, with whom I have been blessed. Without their unconditional love, understanding and support, I would not have completed this program and become the person I am. They taught me to persevere and never give up. For these reasons, I thank them infinitely.

I would like to particularly thank the members of my committee, Dr. Marion F. Ehrich, and Dr. Bernard S. Jortner, whom were greatly supportive of my work throughout my graduate program. Dr. Jortner's willingness to teach me patiently the art of pathology was above and beyond the call of duty. I could always rely on his kindness and understanding. He always put my interests as a graduate student above his own, making time to answer all my questions thoroughly, and to help me in all aspects of my graduate studies. The tremendous amount of knowledge I acquired during this program reflects the importance he attributes to each of his graduate students. Dr. Ehrich showed me the true meaning of friendship. The energy and enthusiasm she displays towards her work and the work of her graduate students were my source of motivation. She always provided me with constant educational, emotional and financial support, more than was ever needed to complete my formation. Her constant encouragement gave me the strength to persevere. She taught me how to see the positive aspects in everything and everyone. Her generosity and kindness have no limits. All the evenings shared at her cheerful home place with family, friends and music contributed to build a very strong bound between us, which will never weakened, no matter the distances or time.

I would also like to acknowledge Dr. Inzana, Dr. Klein, Dr. Bloomquist and Dr. Van der Schyf, which have actively participate in the formation I received as a neurologist. I

consider myself very fortunate to have been exposed to such a wide range of expertise in the neurology field, which has certainly gave me flexibility to combine research and clinical neurology in my future career.

I would like to sincerely acknowledge the generous assistance provided by the following technicians: Linda Correll, Ginny Viers, Kristel Fuhrman, Kathy Lowe, Sandy Perkins and Wen Li. These persons participated actively in this project, sharing their experience, knowledge and skills, which were very important in my scientific development. Without their tremendous help, this study would not have been possible. I would also like to thank all members of the reprographic team, including Don Massey, Terry Lawrence, and Jerry Barber, Dan Ward for their generous assistance regarding the Figures in this work, and also for all the reprographic material they allowed me to use.

I also would like to acknowledge the financial support I had to perform my research. This work was partially supported by USDA Hatch funds. Virginia - Maryland Regional College of Veterinary Medicine, provided additional funding including a graduate stipend.

Dear God,

Give me the faith to accept the things I can not change,

The strength to change the things I can,

And the wisdom to know the difference.

DECLARATION OF WORK PERFORMED

I declare that I, Christiane Massicotte, performed all the work reported in this dissertation except that which is reported below.

Cells designated for ultrastructural observations were collected, fixed and embedded by myself, and then given to Kathy Lowe and Virginia Viers for sectioning.

iv. TABLE OF CONTENTS

PART III: MATERIALS AND METHODS

PART IV: RESULTS

PART V: DISCUSSION

PART VI: GENERAL REFERENCES

PART VII: APPENDIX

PART VIII: VITA

v. LIST OF TABLES

Table **Page**

Part IV, chapter I:

vi. LIST OF FIGURES

FIGURE ..... **PAGE**

Part II, chapter 1:

Part III, chapter 2

Part IV, chapter 3:

LIST OF FIGURES

FIGURE **PAGE**

Part IV, chapter 4:

Part IV, Chapter 5:

Part IV, chapter 6:

vii. ABBREVIATIONS

ACh: Acetylcholine
AChE: Acetylcholinesterase
ANOVA: Analysis of variance
ANT: Adenine translocase
ADP: Adenine dinucleotide
AMP: adenine mononucleotide
ATP: Adenosine triphosphate
ATPase: Adenosine triphosphatase
Calcein-AM: Calcein
CAP: Compound action potential
CB: Maintenance media for Schwann cells
CH: Mantenance media for purified neuronal populations
CO_2: Carbon dioxyde
DMSO: Dimethyl sulfoxide
DBCV: Di-n-butyl-2,2-dichlorovinyl phosphate
DFP: Diisopropyl-fluorophosphate
DTT: Dithiothreitol
DNA: Diribonucleotide acid
DRG: Dorsal root ganglia
EBSS: Essential buffer salt solution
EDTA: Ethylenediaminetetraacetic acid
EMEM: Eagle's minimum essential medium
Epot: Equilibrium potential
EPSP: Excitatory post - synaptic potential
FBS: Fetal bovine serum
FdU: 5-fluoro-2'-deoxyuridine
$FADH_2$ Flavine adenine dinucleotide
HPLC: High performance liquid chromatography
HPS: Human placental serum
IPSP: Inhibitory post - synaptic potential
ISEL: *In situ* end labeling
KCl: Potassium chloride
KD: Kilodalton
L-15: Lebovitz-15
KOH: Potassium hydroxide
LSD: Least significant difference
MAP: Microtubule - associate protein
$MgSO_4$: Magnesium sulfate
MPP^+: 1-methyl-4-phenylpyridinium
MPTP: 1-methyl-4-phenyl-1,2,3,-tetrahydropyridine

ABBREVIATIONS

mRNA: Messenger ribonucleic acid
MPT: Mitochondrial permeability transition
msec: Millisecond
mV: millivolts
NADH: Nicotinic acid dehydrogenase
NCV: Nerve conduction velocity
NGF: Nerve growth factors
NTE: Neurotoxic esterase or neuropathy target esterase
O: Oxygen
OP: Organophosphorus
OPIDN: Organophosphorus-induced delayed neuropathy
P: Phosphorous
PPi: diphenyl phosphate
p: statistical probability
PBS: phsophate buffer solution
PSP: Phenylsaligenin phosphate
rRNA: Ribosomal ribonucleic acid
RIU: Raw intensity unit
RLU: Relative light unit
S: Sulfur
SAS: Statistical analysis software program
SEM: Standard error of the mean
SER: Smooth endoplasmic reticulum
TMDP: N,N,N, N'-tetraethyl-p-phenylene diamine hydrochloride
TMRM: Tetramethylrhodamine methyl ester
TOCP: Tri-o-cresyl phosphate
TOTP: Tri-o-tolyl phosphate
TPP: Tri-phenyl phosphite
TSP: Tolyl saligenin phosphate
TUNEL: Terminal transferase mediated nick-end labeling
US EPA: United States Environmental Protection Agency
Vp : Voltage potential
Ψm: Mitochondrial transmembrane potential

<u>PART 1</u>: INTRODUCTION.

A. Statement of hypothesis:

The hypothesis tested was that exposure to organophosphorus compounds causing delayed neuropathy (OPIDN) could alter the energy production within neuronal and non-neuronal cells. It had been noted previously that some organophosphate (OP) compounds could inhibit mitochondrial enzymes and cause matrix swelling (Holmuhamedov *et al.*, 1996; Antunes-Madeira *et al.*, 1994). Alterations in mitochondrial functions, including electron transport chain reactions, mitochondrial permeability transitions, or the disruption of ATPase enzyme complexes could occur following exposure to neuropathy-inducing compounds and account for the early mitochondrial transmembrane potential modifications noted previously (Carlson and Ehrich, 1999). Furthermore, it was expected that OP-induced effects on energy production would be greater on neuronal rather than non-neuronal cells of the peripheral nervous system. Maintenance of energy metabolism is essential for neuronal cell survival, and slight modifications could cause variations of the ionic gradient across the membrane, leading to necrosis or apoptosis in these high energy-demanding cells. Support of the hypothesis would bring new insight on the early mechanisms involved in the development of OPIDN.

JUSTIFICATION FOR THE STUDY

B. Justification for the study:

Organophosphorus compounds (OPs) are mainly used in agriculture and industries, and some of these OPs have the potential to cause delayed neuropathy (Jortner and Ehrich, 1987; El-Fawal *et al.*, 1988, 1990; Massicotte *et al.*, 1997). Despite extensive enzymatic, clinical and morphological studies described in the literature, mechanisms involved in the development of OPIDN are still unknown. This research was initiated to improve the mechanistic knowledge about organophosphorus-induced delayed neuropathy (OPIDN) by evaluating the effects of different OPs on energy production at the cellular level. Because mechanistic studies at the cellular and subcellular level are difficult in whole animals, this goal was reached by targeting chicken dorsal root ganglion cell cultures with applied physiological concentrations of organophosphates (OPs) capable of producing type I OPIDN.

Adult chickens are susceptible to OPIDN and provide the US EPA-accepted animal model for studying clinical and pathological alterations caused by OPIDN (US EPA, 1991). This is why cells from chickens were used for the studies proposed. Since mechanistic studies at the cellular and subcellular level are not easily done in whole animals, chicken dorsal root ganglia (DRG) provided a very appropriate primary cell culture model to use for toxicity studies (Blood, 1975; Varon *et al.*, 1981; Kleitman *et al.*, 1995). For all the studies proposed, the neuronal and non-neuronal cells contained within DRG, extracted from 9 or 10 day old chicken embryos, respectively, were allowed to mature in cell culture for at least 14 days. Since previous studies showed that few lesions were detected in chicks younger than 35 days (Pope *et al.*, 1992; Funk *et al.*, 1994; Harp *et al.*, 1997), and chicks older than 49 days developed moderate to severe OPIDN (Moretto *et al.*, 1991; Pope *et al.*, 1992; Peraica *et al.*, 1993; Funk *et al.*, 1994), the 14 day maturation-time proposed for DRG cultures should have approached *in vivo* time of onset for susceptibility to OPIDN. In

addition, to ascertain that this *in vitro* model provided biochemical results similar to the ones observed *in vivo*, neurotoxic esterase (NTE) activities were monitored in differentiated neuronal cell cultures from DRG. NTE is a carboxylesterase whose inhibition is now commonly measured to predict the potential of OP compounds to cause OPIDN (Johnson, 1982; US EPA, 1991; Aldridge, 1993; Ehrich, 1996; Ehrich *et al.,* 1995; Silbergeld *et al.,* 1993). Consequently, NTE inhibition in neuronal cell culture of DRG would provide strong evidence for *in vivo* representation of a well known biochemical event occurring following exposure to neuropathy-inducing OP-compounds. It is also worth mentioning that this cell model presented a great advantage, as toxic effects observed in neuronal and non-neuronal cells following exposure to OP compounds could be differentiated. Therefore, OP-induced toxicity to neuronal and non-neuronal cells could be individually monitored in DRG differentiated into neuronal and non-neuronal (Schwann) cells (Blood, 1975; Wood, 1976; Varon *et al.,* 1981; Kleitman *et al.,* 1995).

Investigation of OP effects on energy at the cellular level was justified. Because the hydrolysis of ATP is coupled to several energetically unfavorable reactions, it is possible and even likely that alterations in ATP concentrations are relevant events in the pathogenesis of OPIDN mechanisms. This view was supported by preliminary studies conducted *in vivo*. ATP concentrations were previously measured in sciatic nerves of adult hens treated with neuropathy-inducing OP compounds (Massicotte *et al.,* 2001). This earlier study revealed variations in ATP concentrations prior to the occurrence of both clinical signs and neuropathological alterations of OPIDN (Jortner and Ehrich, 1987, El-Fawal *et al.,* 1990; Massicotte *et al.,* 2000). However, this preliminary study done in hens did not provide information that would localize the sources of ATP concentration changes following OP exposure within the whole sciatic nerve, since the sciatic nerve contains non-neuronal (Schwann cells, fibroblasts) as well as neuronal cells. Differentiated neuronal (Blood, 1975; Varon *et al.,* 1981; Kleitman *et al.,* 1995) and non-neuronal (Wood, 1976) cell cultures

described in this study allowed individual monitoring of OP-induced toxicity on cellular ATP production in these cell populations.

Alteration of ATP in the presence of neuropathy-inducing OP compounds was examined in DRG cultures in the studies proposed. Adenosine triphosphate (ATP) provides continual cellular input of free energy necessary for most energy requiring processes. In the nervous system, ATP plays a central role in energy exchanges for numerous biological reactions, including muscle contraction, synaptic transmission, active transport of molecules and ions across the neuronal membrane and synthesis of biomolecules from simple precursors (Linden, 1998). In addition, ATP has been proposed to fulfill an important part of the metabolic and energetic demands required in all phases of axonal transport (Goodrum and Morell, 1992). Metabolic modifications have been documented to occur following exposure to OP compounds. This include alterations in mitochondrial respiration and inhibition of oxidative phosphorylation (Sitkiewicz *et al.,* 1980; Holmuhamedov *et al.,* 1996). Some OP compounds have even been reported to interfere with enzyme complexes within the citric acid cycle (Knoth-Anderson *et al.,* 1992) and the glycolytic pathway (Hernandez *et al.,* 1989). These findings suggested that metabolic alterations of free energy production could be an early event involved in mechanisms contributing to OPIDN; therefore, an investigation of these aspects was proposed *in vitro* using a primary neuronal cell line from chick embryos, a species used by EPA for OPIDN testing. Studies of cellular events are exceedingly difficult *in vivo.* This could make them useful both for mechanistic studies and toxicity screening.

The mitochondria have an important role in the production of cellular energy. Mitochondria contain the respiratory chain, the enzymes of citric acid and fatty acid oxidation, contributing to oxidative phosphorylation processes in which ATP is formed. Consequently, the cellular role of these organelles is crucial in regard to free energy

production. Structural and functional modifications have been previously reported within mitochondria of cells challenged with OP compounds. These changes included mitochondrial transmembrane potential alterations (Ψm) (Holmuhamedov *et al.,* 1996; Carlson and Ehrich, 1999). Furthermore, earlier studies performed with SH-SY5Y cell cultures showed that modifications in Ψm occurred at much earlier time-points than other indications of cellular damage, such as DNA fragmentation or loss of substrate adhesion (Nostrandt *et al.,* 1992; Carlson and Ehrich, 1999; Carlson *et al.,* 2000). These observations suggest that changes in Ψm could represent an early event in OP-induced cytotoxicity. How these Ψm modifications lead to a cytological insult following OP exposure in cell cultures are unknown, and their role needs further definition. Examination of mechanisms contributing to Ψm changes on mitochondrial structure and functions were part of the studies proposed.

Mitochondrial modifications in Ψm could be the result of several mechanisms. For example, impairment of the mitochondrial respiratory electron transport chain could result in reduction of proton gradient across the inner mitochondrial membrane and lead to ATP depletion secondary to uncoupled oxidative phosphorylation. Furthermore, electron-motive forces coupled to proton gradients are responsible for the formation and maintenance of Ψm across the inner mitochondrial membrane. In fact, electrons from NADH are transferred through series of enzymes (Complexes I, III, IV) located within the inner mitochondrial membrane, resulting in proton translocation outside the mitochondria. The aforementioned proton-motive forces generated by electron transfer via these complexes are subsequently used by ATP synthase (Complex V) for ATP synthesis (Weiss *et al.,* 1991). Following exposure to OP compounds, alterations in mitochondrial oxygen uptake and respiration have been reported in brain synaptosomes (Sitkiewicz *et al.,* 1980; Skonieczna *et al.,* 1980). The importance of mitochondrial respiration for the maintenance of Ψm and ATP production needed further investigations in cells challenged with OP compounds, and

was evaluated in this study. The quantification of mitochondrial respiration was, therefore, used to determine if the electron transport chain was a target associated with OP-induced toxicity.

This research attempted to quantify mitochondrial respiration in differentiated chicken DRG cell cultures, following exposure to OP compounds capable of inducing delayed neuropathy *in vivo*. DRG cultures include neuronal cells, and non-neuronal cell populations as Schwann cells and fibroblasts, which can be examined separately and in combination. The effects of OP compounds on the mitochondrial electron transport chain, including enzymatic functions of complexes I, III, and IV, were measured *in situ* in digitonin-permeabilized neuronal and non-neuronal DRG cell populations, as the amount of ATP produced over time (Ventura *et al.,* 1995; Hofhaus *et al.,* 1996; Robinson *et al.,* 1996; Wanders *et al.,* 1993; Steyn *et al.,* 2000). With this permeabilized cell system, the formation of ATP from ADP and phosphate was measured using malate and glutamate as oxidable substrates. Addition of complex-specific substrates necessary for complex-driven ATP synthesis (*malate* for Complex I; *glycerol-3-phosphate* for Complex III*; N,N,N',N'-tetraethyl-p-phenylenediamine dihydrochloride* for Complex IV), combined with known specific inhibitors of the respiratory chain complexes (*rotenone* for Complex I; *antimycin* for Complex III; *azide* for complex IV) could localized the effect of OP compounds at precise enzymatic-complex level(s) (Wanders *et al.,* 1993-1994; Hofhaus *et al.,* 1996; Robinson *et al.,* 1996; Steyn *et al.,* 2000). ATP concentrations were determined by using a standardized luciferase-luciferin assay and a semi-automatic bioluminometer, as previously reported for NG 108-15 or murine N-2α neuroblastoma cell lines (Shirhatti and Krishna, 1985; Kutty *et al.,* 1991; Steyn *et al.,* 2000).

Possible OP-induced effects on neuronal cell mitochondria have other manifestations as well. Severe mitochondrial dysfunction results in opening of

mitochondrial permeability transition pores (MPT), and causes the proton-motive forces to dissipate across the inner mitochondrial membrane (Hunter and Haworth, 1970; Zoratti and Szabo, 1995; Bernadi, 1996: Niemienen *et al.,* 1995). The rapid change of permeability associated with the MPT allows the Ψm to dissipate, uncoupling the oxidative phosphorylation with secondary reduction of ATP synthesis (Zoratti and Szabo, 1995; Cassarino *et al.,* 1998). Mitochondrial swelling ensues, along with the release of intramitochondrial ions and proteins (cytochrome *c*) within the cytoplasm (Petit *et al.,* 1997; Lemasters *et al.,* 1998; Cai *et al.,* 1998). Previous studies demonstrated alterations in the overall Ψm when SH-SY5Y cells were challenged with OP compounds (Cassarino *et al.,* 1998; Carlson and Ehrich, 1999). These recent findings implicated the MPT as a potential modulator of amplitude and duration of mitochondrial Ψm seen with OP compound exposures. In this study, the role of MPT on mitochondrial Ψm changes was evaluated following neuropathy-inducing OP compounds in differentiated neuronal cell cultures, originating from DRG of 9-day-old chick embryos.

New techniques have been developed to study the physiological role and function of MPT, and its change in permeability following exposure to toxic compounds (Niemienen *et al.,* 1995, Lemasters *et al.,* 1993, 1998).. Visualization of the MPT in living cells can be achieved by using laser scanning confocal microscopy. This technique can create submicron optical slices through living cells, allowing unprecedented resolution of subcellular structures such as mitochondria, within thick cells or tissues. This new method has been used to monitor MPT *in situ* within hepatocytes, during normal incubation and during oxidative stress in the presence or absence of cyclosporin A (Niemienen *et al.,* 1995, Lemasters *et al.,* 1993, 1998). This technique was adapted to evaluate *in situ* MPT in neuronal or Schwann cell cultures originating from DRG of 9 or 10 day old chicken embryos, respectively, during normal incubation and following OP exposure. This method

provided new information concerning the role of MPT in regard to Ψm modifications and mitochondrial functions within the cell cultures exposed to OP compounds.

As mentioned above, some known OPs can induce delayed neuropathy, resulting in axonal and myelinated fiber degeneration within peripheral nerves and spinal cord tracts of susceptible animals seven to fourteen days after exposure (Jortner and Ehrich, 1987; El-Fawal *et al.,* 1990; Massicotte *et al.,* 1997). Techniques such as perfusion fixation, plastic embedding, light microscopy and ultrastructural examinations have been used in the past to study nervous system lesions, including the characteristic morphologic changes observed with OPIDN (Bischoff, 1970, 1985; Bouldin and Cavanagh 1979b; Jortner and Ehrich, 1987; Jortner *et al.,* 1989; Dyer *et al.,* 1991; El-Fawal *et al.,* 1988; El-Fawal *et al.,* 1990; Ehrich *et al.,* 1993; Massicotte *et al.,* 1997). Toxicity at the cellular level has also been demonstrated in immortal cell lines (Mochida *et al.,* 1988; Veronesi and Ehrich, 1993a; Ehrich *et al.,* 1997, Greenman *et al.,* 1997). Subcellular targets for cytotoxicity observed *in vitro* have not been precisely elucidated. Although structural alterations in mitochondria have been demonstrated following OP exposure (Knoth-Anderson *et al.,* 1992; Antuned-Madeira *et al.,* 1994; Carlson and Ehrich, 1999), specific data relating to events contributing to structural effects following exposure to neuropathy-induced OP compounds in primary DRG cultures are not found in the literature. This work investigated whether dorsal root ganglia cell cultures degenerate following exposure to OPs capable of inducing delayed neuropathy, and identified specific biochemical and morphologic changes observed at the ultrastructural level. This could elucidate the subcellular targets involved in OPIDN, and, possibly, provide an additional model for toxicity screening of this type of toxicant to compliment the presently used *in vivo* methods. In addition, studies in primary cultures are valuable because normal cells removed from animal are used. Immortal cell lines are cancer cells, although easier to obtain and use, are not necessarily the best representatives of the tissues to be studied *in vitro* (Kleitman *et al.,* 1995; Varon *et al.,* 1981; Wood, 1976).

SPECIFIC OBJECTIVES

C. Specific objectives:

The specific objectives of the research were as follows:

1. To create an appropriate *in vitro* model for biochemical and morphological studies of OPIDN in myelinated nerve fibers. Embryonic chick dorsal root ganglia (DRG) were dissected from the lumbar intumescence and a neuronal population was prepared, dissociated from their Schwann cells (Kleitman *et al.,* 1991). Schwann cell isolations were performed (Wood method) from DRG of chick embryo at the same level (Weiss *et al.,* 1996). When needed, Schwann cells were added to the previous neuronal cell culture and allowed to myelinate with addition of ascorbate.

2. To determine the metabolic effects of neuropathy-inducing OP compounds on neuronal and non-neuronal cell cultures from embryonic chick DRG. Concentration changes of ATP associated with exposure to phenylsaligenin phosphate (PSP) and mipafox, direct active esterase inhibitors that cause OPIDN in the hen model, and a nonneuropathic-inducing OP, paraoxon, were determined using the luciferin-luciferase bioluminescence assay (Shirhatti and Krishna, 1985; Kutty *et al.,* 1991). The mitochondrial respiratory chain function was evaluated in the presence of substrates and xenobiotics that act on complex I to IV (Steyn *et al.,* 2000; Hofhaus *et al.,* 1996; Robinson *et al.,* 1996; Wanders *et al.,* 1993; Wolvetang *et al.,* 1990).

3. To evaluate the mitochondrial permeability transition pore (MPT) in living cells after exposure of differentiated neuronal cell culture from embryonic chick DRG to PSP, mipafox, and paraoxon, using laser scanning confocal microscopy (Bernadi *et al.,* 1996; Lemasters *et al.,* 1993, 1998; Nieminen *et al.,* 1995).

4. To describe lesions in neuronal cell cultures from chick dorsal root ganglia after exposure to neuropathy-inducing OP compounds, and compare these morphological changes to *in vivo* models described in the literature for sensitive species (Carboni *et al.*, 1992; Bishoff, 1967; Bouldin and Cavanagh, 1979 a, b; Veronesi *et al.*, 1984; Drakontides *et al.*, 1982; Stumpf *et al.*, 1989; Abou-Donia *et al.*, 1981-1990; Jortner *et al.*, 1983; Jortner, 1984; Boyes *et al.*, 1994). The mitochondria were examined because they are the organelles responsible for ATP production.

LITERATURE REVIEW

PART II: CHAPTER 1

LITERATURE REVIEW:

1.1. Axonopathy and neurons.

1. Synthetic activities of perikaryal and dendritic structures.

Knowledge of fundamental neuronal structure is essential in the recognition of neuronal or axonal damage. The fundamental structure of a neuron can be divided into a soma (perinuclear perikaryon and nucleus), a dentritic zone, and an axon. The perikaryon may vary in shape, and can be round, pyramidal or polyhedral, and contains a central ovoid nucleus with a prominent nucleolus (Summers *et al.,* 1995). A series of arborized perikaryal processes called the dentritic zone is defined as the receptive portion of the neuron, where an internal or external stimuli is converted to an electrical impulse in the neuron. These electrical stimuli are transported centrifugally along the axon. The latter is the cell process that courses from the axon hillock, near the cell body, to the pre-synaptic terminal of a neuron. Neuronal perikarya are rich in ribosomes, which can be arranged along stacks of membrane in parallel array forming Nissl bodies. Basophilic Nissl bodies are found in the cytoplasm of all neurons except in very small ones. The neuron has no Nissl bodies in the region of the axon hillock and in the axon. Transmission electron microscopy reveals that the perikaryal cytoplasm contains neuroflilaments, microtubules, a few lysosomes, and a rich complement of rough endoplasmic reticulum and polyribosomes, Golgi and mitochondria (Summers *et al.,* 1995).

Information controlling the synthesis of proteins is encoded in the DNA of the chromosomes within the cell's nucleus (Kandel *et al*., 1991). In the mature neurons, cell division is rare, and most of the chromosomes are responsible only for gene expression. The nucleolus contains the specific portion of DNA encoding the RNA (rRNA) for future

ribosomal synthesis. In addition to the ribosomal genes of the nucleolus, many other genes are also actively transcribed into the nuclear precursors of mRNA. The resulting mRNA gives rise to three classes of proteins: (1) cytosolic proteins, (2) nuclear, mitochondrial and peroxisomal proteins, (3) cell membrane and secretory proteins.

The cytosolic proteins constitute the most abundant group of proteins in the neuronal cell. Cytosolic proteins include (1) fibrillar components that make up the cytoskeleton (neurofilaments, tubulins, actins, and their associated proteins), (2) the enzymes that catalyze the metabolic reactions of the cell (e.g. proteases, choline acetyltransferase in spinal motor neurons). Messenger RNA molecules for cytosolic proteins emerge through the nuclear pores, and become associated with ribosomes, forming free polyribosomes in the cytoplasm of neurons. The cytosolic proteins can be slightly modified by cotranslational processes (changes during polypeptide synthesis as N-acetylation), or posttranslational processes (modifications after the polypeptide chain has been completed, such as phosphorylation of serine, threonine, or thyrosine by specific protein kinases) (Kandel *et al*., 1991).

The nuclear, mitochondrial and peroxisomal proteins are encoded and transcribed in the cell's nucleus and translated on free polyribosomes. They are directed to their proper organelles by posttranslational importation soon after their synthesis has been completed on free ribosomes (Kandel *et al*., 1991). In contrast, most membrane and secretory proteins reach their destination by cotranslational transfer (see below). Furthermore, the distribution of these proteins to the various membrane compartments of the cell depends on amino acid sequences located at the N-terminal end of the protein. Nuclear re-uptake also depends on the sequence of basic amino acid residues that remain on mature proteins.

The cell membrane proteins and secretory proteins are formed on polysomes attached to the endoplasmic reticulum (rough endoplasmic reticulum) in the cytoplasm. Signal sequences of proteins (N-terminal portion), designated for the cell's major membrane system differ in their secondary structure from the presequences of proteins targeted to the nucleus, mitochondria, or peroxisomes (Kandel *et al*., 1991). The peptides can be transported through the lipid bilayer into the lumen of the endoplasmic reticulum by energetic mechanisms and proteolytic cleavage catalyzed by signal peptidase enzymes. Transportation via cotranslational transfer through the membrane continues until a "stop" transfer segment is reached within the polypeptide chain. Axonal transport mechanisms control the distribution of mature proteins produced by cotranslational transfer (membrane and secretory proteins). Such axonal transportation mechanisms are described in subsequent sections.

2. Axonal structures.

The components of an axon can be divided into the axolemma, the axoplasm, and axonoplasmic elements (Waxman, 1978; Peters *et al*., 1991). The axolemma is the excitable membrane of the neuron. The axoplasm constitutes the fluid compartment, in which bi-directional axonoplasmic flows take place at several velocities (described in the subsequent section). The formed axonoplasmic elements include the mitochondria, smooth endoplasmic reticulum, neurotubules, axonal filaments, miscellaneous membrane-bound bodies, and axonal inclusions (glycogen).

In the axon hillock, organelles predominating in the axoplasm include free ribosomes, mitochondria, neurofilaments and microtubules. Ribosomes are generally absent from the remainder of the axon (Peters *et al*., 1991). The axon beyond the initial segment contains mitochondria, microtubules, neurofilaments, agranular endoplasmic

reticulum, and multivesicular bodies, but is devoid of granular endoplasmic reticulum and free ribosomes. The mitochondria are axonoplasmic elements several microns in length. They are continuously generated in the perikaryon and enter the axon, where they are propagated distally. Axonal mitochondria have been observed in association with microtubules via microtubule-associated proteins (MAP 1), and the latter are responsible for energy coupling between microtubules, mitochondria and other membranous organelles (Peters *et al*., 1991). Neurofilaments are macromolecular filaments of indefinite length and approximately 10 nm in diameter (Peters *et al*., 1991). They are responsible for the stabilization of the axon and ensure its radial growth (Fried *et al*., 1970; Lee *et al*., 1994). Vertebrate neurofilaments are made up of three protein subunits of approximately 68, 150 and 200 KD (Hoffman *et al*., 1975; Liem *et al*., 1978). Phosphorylation of these neurofilaments by protein kinase is crucial for the maintenance of cytoskeletal structure (Nixon *et al*., 1991). Microtubules consist of tubular structures larger than the neurofilaments. In transverse sections, microtubules measure approximately 20-26 nm in diameter (Peters *et al*., 1991). They are essentially tubes of a globular polypeptide known as tubulin. Tubulin is found as a dimer of approximately 100 KD, in which each dimer contains two globular polypeptides of about 50 KD, alpha and beta-tubulin. As tubulin is assembled into microtubules, dimer line-up to form 13 protofilaments arranged parallel to each other, forming the wall of the microtubule. The density of microtubules in axons increases as the diameters of the axon decreases. There are approximately 150 microtubules/μm^2 in unmyelinated axons and less than 15 microtubules/μm^2 in large myelinated ones (Fadic *et al*., 1985; Pannese *et al*., 1984). The function of microtubules is to maintain the shape of anisotropic cells. In addition, they are partly responsible for axonal transportation and axoplasmic flow (Kandel *et al*., 1991), especially that associated with synaptic vesicles (Gray, 1975, Kandel *et al*., 1991). Microtubules also participate in subaxolemmal arrangements at the initial axon segment (Westrum, 1976), and are implicated in cell motility and cell division (Peters *et al*., 1991). Microfilaments are formed

from actin monomers, arranged into 4-6 nm diameter fibrils and found throughout neurons, with greater concentration in presynaptic terminals, membrane cytoskeleton, dendritic spine and growth cones. These microfilaments contribute to growth cone motility, neuronal growth and secretion, and axonal transport (Kirkpatrick and Brady, 1999).

The membranous components of the axoplasm consist of the endoplasmic reticulum, mitochondria, vesicles (multivesicular bodies) and lysosomes. The smooth endoplasmic reticulum (SER) of the axon extends continuously from the axon hillock the axon terminal. In the presynaptic terminals, a primary SER system runs just below the plasma membrane, and extends into the terminal (towards the presynaptic grids). The second SER system occupies the core of the axon and breaks up into spherical synaptic vesicles. SER is implicated in bi-directional fast transport of proteins, glycoproteins, neurotransmitters, mucopolysaccharides, gangliosides and phospholipids, all needed to maintain the axonal and nerve terminals (Droz, 1976; Goodrum and Morell, 1991).

3. Axonal injuries and Wallerian degeneration.

Since ribosomes and other organelles essential in protein synthesis are absent from the axons, the integrity of these neurites and their terminals depends on the neuronal cell body for the supply of all structural elements. Thus, the neuronal cell body must synthesize and deliver the needs of the axon, and recycle extraneous products. Wallerian degeneration is a process characterized by fragmentation and dissolution of the distal part of an axon, with digestion and removal of the collapsed myelin tube, secondary to nerve fiber transection or injury (figure 1). In Wallerian degeneration, dissolution of the distal part of the axon is an active process that follows the loss of contact with the perikaryon. In the peripheral nerve, within the first 3-4 days after the fiber injury, the axon swells, initially occurring near one or more nodes of Ranvier in the distal part of the axon. Proximally, this

paranodal swelling moves towards the cell body in a saltatory manner. The associated myelin sheath slowly retracts away from the nodal region as the axon enlarges. The myelin degenerates simultaneously with, but secondary to the axon. The fiber degeneration leads to formation of swellings along the internodes called ellipsoids, and fragmentation of the myelin sheath into chains of myelin ovoids that are slowly removed by phagocytic cells. There also is degeneration over a few internodes proximal to the injury, similar to the changes distal to the site of injury. Furthermore, a reaction is observed in the cell body following axonal injury that is termed the axon reaction. This is characterized by swelling of the cell body, displacement of the nucleus toward the periphery of the soma, and partial dispersion of Nissl substances in the region around the nucleus. This reaction is also referred to as chromatolysis (De Lahunta, 1983). Following the distal axonal disintegration, Schwann cells proliferate within their basal lamina endoneurial covering, and fill the space previously occupied by the axon and myelin forming the band of Buengner. This structure produces a microenvironment, which enhances subsequent axonal regeneration.

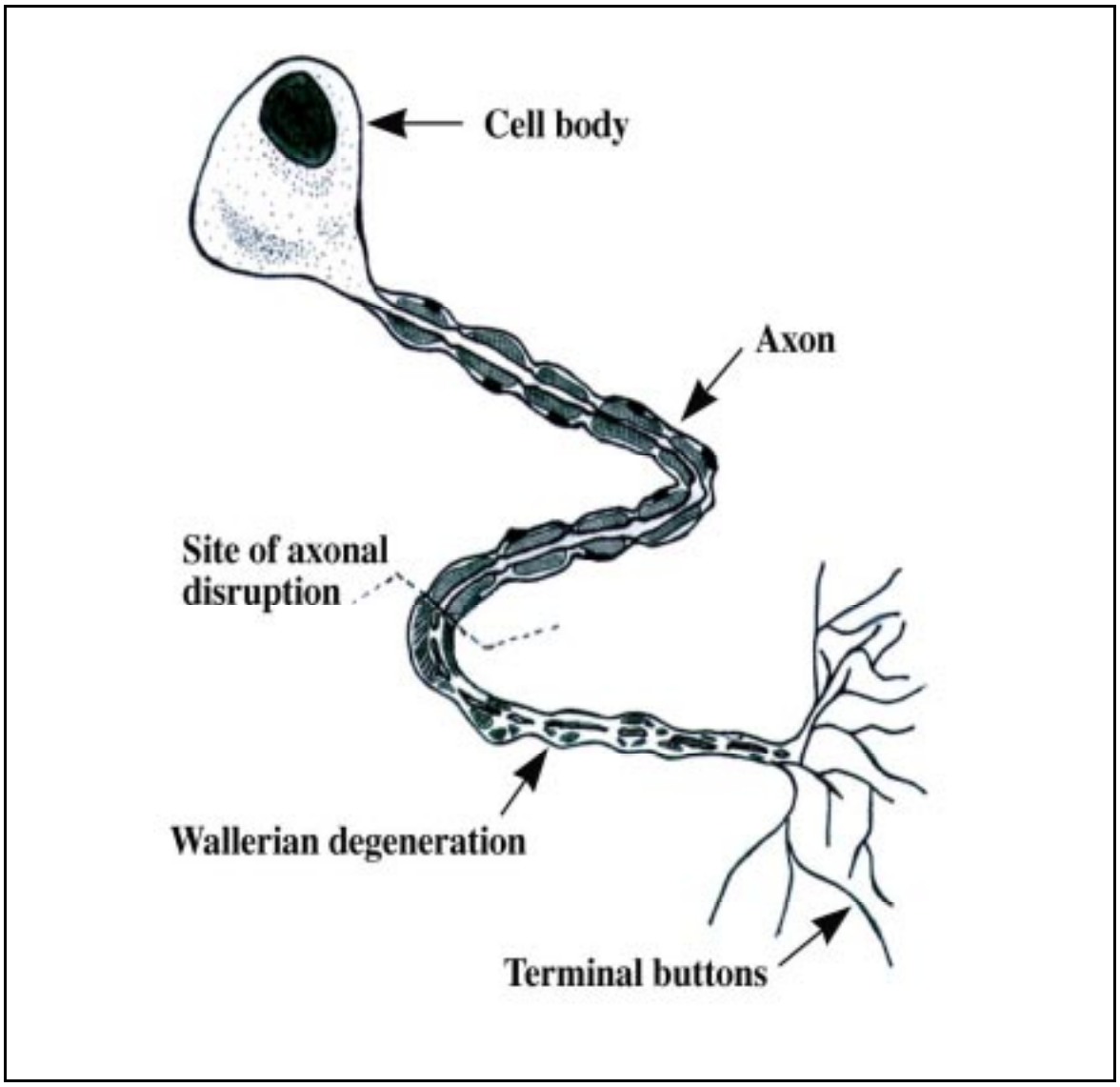

Figure 1: Wallerian degeneration of a neuron showing fragmentation and dissolution of the distal part of the axon, beyond the site of axonal injury (dotted line).

4. General mechanisms of neuronal cell death.

Neuronal cell death may involve apoptotic or oncotic necrosis (Majno and Joris, 1995; Levin *et al.*, 1999; Satry and Rao, 2000). Examples of these mechanisms may be programmed cell death, a form of apoptosis that occurs as a physiological events during development in many growing tissues (Cohen, 1991; Levin *et al.*, 1999; Satry and Rao, 2000), and oncotic necrosis following ischemia or infectious or toxic insults (Sen, 1992; Hockenbery *et al.*, 1995; Kreutzberg *et al.*, 1997; Trump, 1998). Mixed oncotic and apoptotic necrosis can also be observed in neuronal tissues following toxin exposures (Levin *et al.*, 1999).

For apoptotic cell necrosis, nuclear membrane budding or zeiosis, and DNA fragmentation are well-described processes. More commonly, no inflammation or swelling can be detected, and death occurs usually in single cells throughout a given tissue (Majno and Joris, 1995) with this type of cell death, although inflammation and clusters of apoptotic cells have recently been described in apoptotic necrosis. Apoptosis requires *de novo* gene expression, activated by hormones, cytokines, toxins and viruses (Schwart and Osborne, 1993; Martin *et al.*, 1994; Zakeri *et al.*, 1995; Zychlinsky and Sansonetti, 1997), and is dependent on cellular metabolic states (Levin *et al.*, 1999). The biochemical hallmark of apoptosis is internucleosomal DNA fragmentation (Arends *et al.*, 1990). These small fragments (180-200 base pair length) are produced by activation of a Ca^{2+}/Mg^{2+} -dependent endonuclease, giving characteristic DNA laddering. DNA fragmentation can be measured by TUNEL (terminal transferase mediated nick-end labeling), ISEL (*in situ* end labeling), or with DNA-specific fluorochrome propidium iodide (Gavrieli *et al.*, 1992; Gold *et al.*, 1993; Grasl-Kraupp *et al.*, 1995). It has been recently recognized that the TUNEL technique can assist in locating and quantifying dead cells, but when used alone, it is insufficient to distinguish between apoptotic and oncotic cell death (Grasl-Kraupp *et al.*, 1995).

Oncotic necrosis frequently occurs in response to ischemia, toxic insults or infections (Kreutzberg *et al*., 1997). Typically, swelling of cellular components, such as cytoplasm or mitochondria, secondary to increased influx of Ca^{2+} across cell membranes is the pathological hallmark of oncotic necrosis. Light microscopy shows karyolysis with intensive cytoplasmic eosinophilia. In most cases, oncotic necrosis occurs in clusters, and generates an inflammatory response, although it can also be observed in single cells (Levin *et al.*, 1999). Under pathological conditions, however, forms of neuronal cell death may vary considerably, and may operate simultaneously in a given tissue, and differentiation between necrosis and apoptosis may be difficult.

Precise identification of the type of cell death requires cell identification, and both biochemical and molecular biological techniques (Li *et al*., 1995; Kreutzberg *et al*., 1997). *In vitro*, dead cells (whether apoptotic or oncotic) can be detected by their ability to be stained with trypan blue or propidium iodide, because the cell culture does not contain the macrophages that usually phagocytize cells undergoing apoptotic necrosis *in vivo* (Levin *et al.*, 1999). However, there are no universally acknowledged markers of apoptosis, and morphology remain the "gold standard" for distinguishing the type of cell death in tissue. At this time, the most reliable general markers are rapid identification of cell death in fresh tissue by live/dead kits or acridine orange, coupled with shrunken or blebbing nuclear morphology, and perhaps evidence of chromatin condensation or margination (Levin *et al.*, 1999).

5. Neuronal energy metabolism.

a. Mitochondrial respiration.

Mitochondria are oval-shaped organelles (0.5 X 2 μm) located within the neuronal cytoplasm. They contain the respiratory complexes, enzymes of the citric acid cycle and fatty acid oxidation, which are essential for free energy production (Stryer, 1998). Adenosine tri-phosphate (ATP) is the universal currency of free energy in biological systems (Babock and Wikstrom, 1992). Continual free energy production is required for cellular movement, active transport of molecules and ions, and for synthesis of macromolecules and other biomolecules from simple precursors. Oxidative phosphorylation is the process in which ATP is formed as a result of the transfer of electrons from NADH or $FADH_2$ to O_2 by a series of electron carriers and electron-driven proton pumps (Capaldi, 1990; Hofhaus *et al*., 1991; Weiss *et al*., 1991) (Figure 2). Oxidative phosphorylation is the major source of ATP in aerobic cellular systems.

Mitochondria have two membrane structures; the outer permeable membrane facing the cytosolic side, and the highly folded impermeable inner membrane enclosing the centrally located matrix (Figure 2). Reactions of the Kreb cycle and fatty acid oxidation happen within the matrix, whereas oxidative phosphorylation occurs in the inner membrane (Stryer, 1998). Indeed, the respiratory chain, which consists of 3 proton pumps linked by 2 mobile electron carriers, is present within the inner membrane. Electrons from NADH or $FADH_2$ flow through 3 specific transmembrane complexes called NADH-Q reductase (complex I), cytochrome reductase (complex III) and cytochrome oxidase (complex IV). This electron flow results in the pumping of protons out of the mitochondrial matrix and the generation of a transmembrane potential (Capaldi, 1990; Hofhaus *et al*., 1991; Weiss *et al*., 1991). ATP is synthesized when proton flow back to the matrix through the ATP synthase

enzymatic complex (also known as complex V, or FoF1-ATPase, or H^+-ATPase) (Penefsky and Cross, 1991; Fillingame, 1992; Pederson and Amzel, 1993). In this way, the synthesis of ATP is coupled to the flow of electrons from NADH or $FADH_2$ to O_2 by a proton gradient across the inner mitochondrial membrane and concentration of ADP present in the system (Babcock and Wikstrom, 1992; Stryer, 1998).

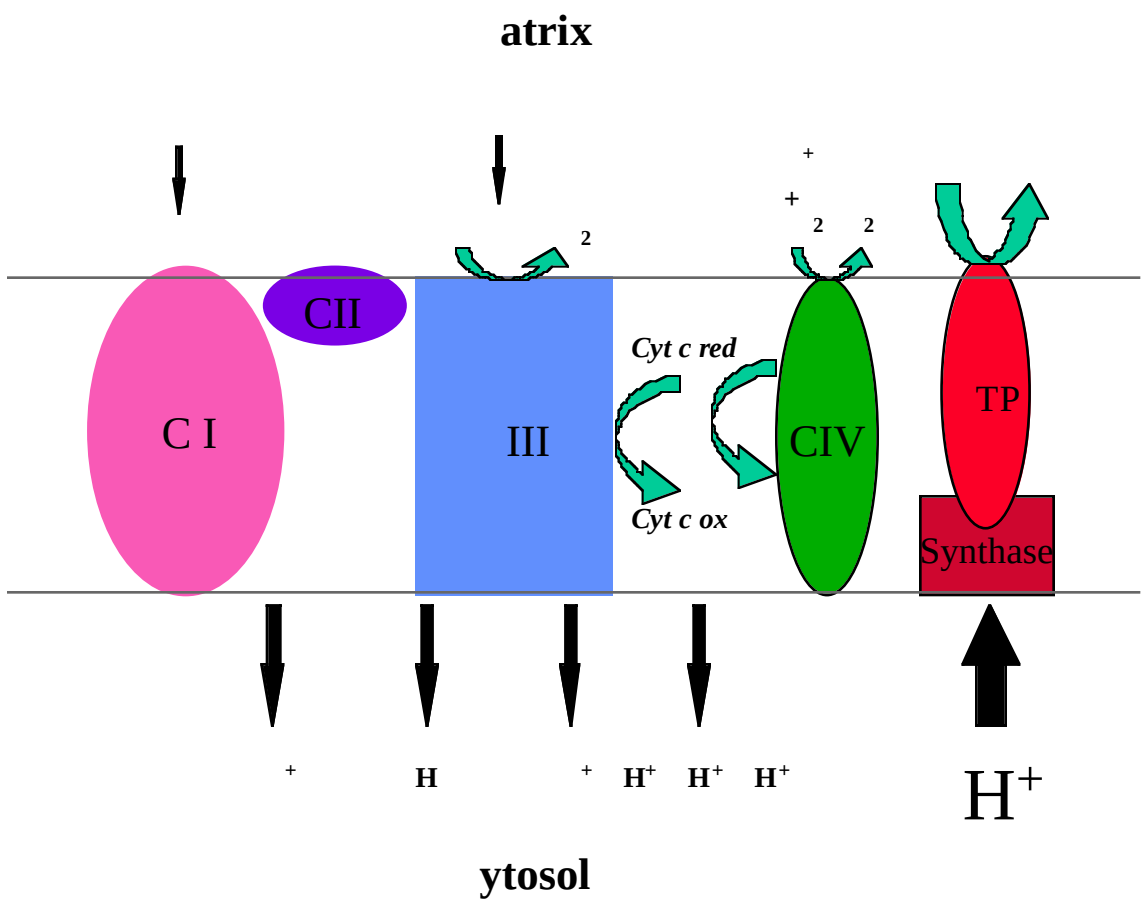

Figure 2. Representation of the electron transport chain and oxidative phosphorylation. Electrons from NADH or $FADH_2$ are transferred through the respiratory chain creating a proton-motive force across the inner mitochondrial membrane that is used to drive ATP synthesis by ATP synthase (Stryer, 1998).

Mitochondrial respiration can be measured in eukaryotic cells using two different methods. The first technique measures mitochondrial respiration as a function of the amount of oxygen consumed by polarography (Rustin *et al*., 1994; Hofhaus *et al*., 1996). The second approach consist of quantifying the amount of ATP produced over time (Bates *et al*., 1994; Wanders *et al*., 1993, 1994; Robinson *et al*., 1996). In the later method, digitonin is used to selectively permeabilize the cell membranes without affecting the mitochondria itself (Ventura *et al*., 1995). Consequently, the mitochondrial electron transport chain within the inner membrane remains unaltered, allowing evaluation of toxicity-induced disorder of the mitochondrial respiration reactions. With this permeabilized cell system, the formation of ATP from ADP and phosphate can be measured using malate and glutamate as oxidable substrates. Addition of complex-specific substrates necessary for complex-driven ATP synthesis (*malate* for Complex I; *glycerol-3-phosphate* for Complex III*; N,N,N',N'-tetraethyl-p-phenylenediamine dihydrochloride* for Complex IV), combined with known specific xenobiotics acting on specific respiratory chain complexes (*rotenone* for Complex I; *antimycin* for Complex III; *azide* for complex IV) can be used to localize the effect of a toxic insult at the exact enzymatic-complex site (s) (Wanders *et al.*, 1993-1994; Hofhaus *et al.*, 1996; Robinson *et al.*, 1996; Steyn *et al.*, 2000). ATP concentrations can be determined by using a standardized luciferase-luciferin assay and a semi-automatic bioluminometer, as previously reported for NG 108-15 or murine N-2α neuroblastoma cell lines (Shirhatti and Krishna, 1985; Kutty *et al.*, 1991; Steyn *et al.*, 2000). This method is very sensitive, with ATP detection limits of 10^{-16} M (Lundin *et al*., 2000; Stanley *et al*., 1986). Chemically, ATP reacts with D-luciferin, releasing PPi and adenylyl luciferin. Then, oxygen reacts with the newly formed adenylyl luciferin to produce CO_2, AMP and electronically excited oxiluciferin (FIG. 2). The quantity of light emitted during relaxation is measured in photons (562 nm), or relative light units (RLU). When ATP is the limiting reagent, the light produced is proportional to ATP concentrations.

$$\text{ATP} + \text{Luciferin} \underset{Mg^{2+}}{\overset{\text{Luciferase}}{\rightleftharpoons}} \text{Adenyl luciferin} + \text{PPi} \qquad (1)$$

$$\text{Adenyl luciferin} + \text{O2} \xrightarrow{\text{Luciferase}} \text{Oxyluciferin} + \text{AMP} + CO_2 + \text{photons} \qquad (2)$$

Figure 3. Reactions involved in the quantification of ATP using the luciferin-luciferase assay. Reaction (1) is reversible, whereas the second one is essentially irreversible (Lemasters and Hackenbrock, 1979).

Mitochondrial respiration can also be evaluated in isolated mitochondrial preparations, by measuring oxygen consumption polarographically at controlled temperature (30°C), by using a Clark oxygen electrode (Clark and Nicklas, 1970, Rosenthal *et al*., 1987; Berman and Hastings, 1999). This method, however, was not used for this dissertation research. The first step involved with this technique is to determine the oxygen consumption in isolated mitochondria of neuronal tissue, with malate and glutamate as sole substrate. Then, active state 3 respiration rates can be measured by the addition of ADP, and resting state 4 respiration rates is recorded after addition of oligomycin to inhibit ATP synthase (Moreadith and Fiskum, 1984, Rosenthal *et al*., 1987). After a short period of rest, the rate of uncoupled respiration can be determine following the addition of carbonyl cyanide p-trifluoromethoxyphenylhydrazone (FCCP). This agent used to maximize the proton permeability of the inner membrane and to provide a rate of uncoupled respiration (State 3_u) limited by electron flow through the electron transport chain. The degree to which the mitochondrial respiration is coupled to oxidative respiration is reflected by the respiratory control ratios defined as the rate of State 3 respiration divided by the rate of state 4 respiration (Rosenthal *et al*., 1987; Berman and Hastings, 1999). The advantages of this

methods over ATP quantification is the functional separation of respiratory State 3 from State 4, and the ability to study oxygen consumption in well-coupled and uncoupled mitochondrial respiration.

b. Mitochondrial transition pore.

The mitochondrial permeability transition pore (MPT) is a calcium-dependent protein that allows the normally impermeable inner mitochondrial membrane to become permeable to solutes of molecular mass less than 1500 DA (Zoratti and Szabo, 1995; Bernadi, 1996). The rapid alteration of membrane permeability associated with MPT leads to depolarization of the transmembrane potential, release of small solutes then proteins, osmotic swelling and loss of oxidative phosphorylation (Gunter and Pfeiffer, 1990). Opening of the MPT has been implicated in several forms of neuronal death including apoptosis, and necrosis secondary to excitotoxicity or ischemia or neurotoxicants (Cai *et al*., 1995; Uchino *et al*., 1995; Niemienen *et al*., 1996; Packer *et al*., 1996; Schinder *et al*., 1996; White and Reynolds, 1996; Zamzami *et al*., 1996, Petit *et al*., 1997; Ouyang *et al*., 1997; Cassarino *et al*., 1998; Lemasters *et al*., 1993, 1998). The conductance of the MTP is extremely high, with typical channel currents of about 1 nanoSiemen. This conductance is much greater than plasma membrane Ca^{2+} and Na^{+} channels, and opening of a single MPT channel may be sufficient to cause mitochondrial depolarization and swelling (Zoratti and Szabo, 1996).

The molecular composition of the MPT remains uncertain. Evidence suggests that the MPT spans both the inner and outer mitochondrial membrane, and proteins from the matrix exist in the pore complex including cyclophilin, a cyclosporin A-binding protein (Hackenbrock, 1968; Halestrap and Davidson, 1990). Indeed, cyclosporin A blocks MPT with high affinity (Crompton *et al.*, 1988; Bernadi, 1996). Visualization of the MPT in

living cells can be achieved by using laser scanning confocal microscopy, by the redistribution of the cytosolic fluorophore, calcein, into individual mitochondria (Lemasters *et al*., 1998). This technique can create submicron thin optical slices through living cells, allowing unprecedented resolution of subcellular structures such as mitochondria, within thick cells or tissues. This new method has been used to monitor MPT *in situ* within hepatocytes, during normal incubation and during oxidative stress (Niemienen *et al.*, 1995, Lemasters *et al.*, 1993, 1998). The studies found that oxidative stress would open the MPT. This technique proved that Ψm modifications and change in mitochondrial functions within these cell cultures involved the MPT.

c. Free energy production and neuronal functions.

Cell viability is highly dependent on the production and utilization of ATP. For example, more than 80% of ATP is generated by mitochondrial oxidative phosphorylation in the brain under aerobic conditions (Fiskum 1983, 1985). As such, mitochondrial synthesis of ATP is essential to maintenance of normal neuronal function.

The long axons spanning the large separation between the cell body and the nerve terminal require specialized axonal transportation systems. Axonal transport controls the distribution of membrane and secretory protein in the neuron, and is characterized by fast anterograde, fast retrograde, and slow axoplasmic systems (Kandel *et al.*, 1991). Five discrete rates of anterograde transport and one of retrograde transport have been recognized. Rapid movement of material (rate between 200-400 mm/day) down the axon is defined as fast axonal anterograde transport (Goodrum and Morell, 1991). This transport mechanism is thought to involve several cytological structures including vesicles and agranular (smooth) endoplasmic reticulum. Proteins, glycoproteins, phospholipids, glycolipids, neurotransmitters and associated enzymes, and several other organelles are moved down the

axon by fast anterograde transport. The latter provides the proteins and lipids essential to maintain the axonal and nerve terminal membranes. The motor molecule for anterograde movement is thought to be kinesin, an ATPase consisting of two large subunits (alpha), and two small subunits (beta). Kinesin forms cross-bridges between the moving membranous organelles. The fast anterograde transport system depends on oxidative metabolism, and is independent of the cell body (Kandel *et al.,* 1991). Furthermore, ATP has been proposed to fulfil an important part of the metabolic and energetic demands required in all phases of axonal transport (Goodrum and Morell, 1992).

Ion transport and gradients, by Na^+-K^+ATPase or Ca^{2+}ATPase pumps, are responsible for maintenance of the electrochemical ionic gradients across the axoplasmic membrane (Augustine *et al.,* 1990). One essential role of the neuron is to generate membrane axon potentials, in order to carry a message, as an electrical signal along the axon. An appropriate ionic intra and extracellular environment around the cell membrane is essential for the neuron to execute its function. At rest, a driving force exists for moving ions across the membrane. Their gradients are generated by ATP-dependent ion pumps. This driving force is defined as the resting membrane potential. The resting membrane potential (Vpot) is present because intra and extracellular ionic concentrations differ on both sides of the membrane, with high concentrations of potassium ions and negatively charged protein molecules inside, and sodium, chloride, and ions calcium outside the neuron. At rest, the membrane potential is more negative inside the neuron (Vpot=-65 mV). In general, the value of the resting potential is closer to the equilibrium potential of the ion for which the membrane is most permeable (Epot), in this case, potassium. Changes in free energy production can lead to alterations of ion transport/gradients (Na^+-K^+ATPase, and Ca^{2+}ATPase pumps) across the plasma membrane (Augustine *et al.,* 1990).

Although mitochondria are pivotal in controlling cell life, these organelles play an important role in the control of cell death. In fact, mitochondria can trigger apoptosis through disruption of electron transport, oxidative phosphorylation and ATP production (Green and Reed, 1998). Disruption of electron transport chain reactions has been recognized as an early feature of cell death (Garcia-Ruiz *et al*., 1997). ATP is required for downstream events taking place in apoptosis. Therefore, although loss of mitochondrial ATP can cause cell death, it is unlikely that this is the sole mechanism for induction of apoptosis, since ATP depletion occurs relatively late in apoptotic processes. In this case, it is more likely that ATP depletion leads to necrotic cell death (Farber, 1982; Borgers *et al*., 1983).

The mitochondrial permeability transition is an important recognized mitochondrial event, involved in both necrotic and apoptotic cell death (Cai *et al*., 1998; Lemasters *et al*., 1998). The MPT occurs in several forms of necrotic cell death including oxidative stress, ischemia, and Ca^{2+} ionophore toxicity (Broekmeier *et al*., 1992; Imberti *et al*., 1993, Griffiths and Halestrap, 1994). Furthermore, the MPT is a critical event associated with the progression of apoptotic cell death, and it does not occur uniformly during apoptosis (Liu *et al*., 1996; Kluck *et al*., 1997; Yang *et al*., 1997; Cai *et al*., 1998; Lemasters *et al*., 1998). Indeed, a variable proportion of mitochondria undergo MPT, and the onset of MPT to increasing numbers of mitochondria within a cell can lead progressively to autophagy, apoptosis and necrotic cell death (Lemasters *et al*., 1998). For example, when the MPT involves a few mitochondria, autophagy is stimulated, leading to lysosomal degradation of the affected mitochondria and removal of the signals stimulating autophagy. As more mitochondria become involved, the MPT initiates the promotion of apoptosis, since the release of pro-apoptotic substances like cytochrome c and AIF can no longer be controlled. Finally, once all mitochondria undergo MPT in a cell, ATP becomes profoundly depleted secondary to uncoupling of oxidative phosphorylation and accelerated ATP hydrolysis by

mitochondrial ATP synthase. The ATP depletion leads abruptly to necrotic cell death. Cyclosporin A, a strong MPT inhibitor, can prevent both necrosis and apoptosis in these cell models.

1.2. Organophosphorus compounds.

1. General considerations.

Organophosphorus ester (OP) compounds have been widely used in industry and agriculture. The extent of their use, mainly as synthetic pesticides, but also in plasticizers, hydraulic fluids, lubricants, and petroleum additives reflects utilitarian features of these compounds. Potentially, over 20 million toxic organophosphorus esters could be synthesized, using Schrader's (1963) generalized formula. It has been estimated that over 200 such toxic compounds, out of 500,000 synthesized organophosphorus pesticides, have been used commercially throughout the world (Spencer, 1973). Two major types of OP toxicity has been recognized. The first type of toxicity is related to the inhibition of acetylcholinesterase, resulting in cholinergic crisis. Cholinergic crisis related to OP compounds has been well described in many species (Chambers and Levi, 1992; Abou-Donia and Lapadula, 1990). One other problem associated with exposure to certain organophosphorus compounds is the potential for the development of delayed neuropathy. OP toxicity have been reported in different species, including humans, domestic and wild animals (Johnson, 1975a,b; Abou-Donia and Lapadula, 1990; Abou-Donia *et al.,* 1986; Veronesi *et al.,* 1984; Lapadula *et al.,* 1985; Soliman *et al.,* 1984; Stumpf, 1989; Smith *et al.,* 1959; Abou-Donia, 1981; Ehrich, 1996). Of these species, the domestic chicken (hens) has proven to be the most reliable animal model to study the delayed effects of organophosphate intoxications, since it readily shows clinical signs and lesions. Thus, the delayed neuropathic potential of OP compounds are usually extrapolated from studies in

this species (Dudek and Richardson, 1979; Dudek *et al*, 1980; Johnson *et al.*, 1981; Lotti *et al.*, 1981; US EPA, 1991).

2. Chemical structure.

Organophosphorus (OP) compounds are a large and diverse family of chemicals. They are organic compounds containing phosphorus-carbon (P-C) bonds. The phosphorus can be trivalent or pentavalent, depending if three or five outer orbital electrons are present, respectively. The trivalent phosphorus configuration is pyramidal and such compounds are considered to be derivatives of phosphines, PH3. The pentavalent phosphorus compounds are tetrahedral (phosphine oxide, phosphinic acid, phosphonic acid). The pyramidal conformation is unstable, and thus undergoes tautomeric changes to a tetrahedral conformation (Abou-Donia and Lapadula, 1990).

OP compounds may be classified as anhydrides, aliphatics, aromatics, and heterocyclics. The majority of OP insecticides are derivatives of phosphoric acids. The partial structures of these 14 types of OP insecticides known are shown in figure 4 (Chambers and Levi, 1992). Triesters of phosphoric acids (phosphates) are considered the prototype of the entire family of OP compounds, in which all 4 atoms surrounding the phosphorus are oxygen. Sulfur-containing OP compounds also exist. Phosphorothionates (parathion, diazinon, chlorpyrifos) and phosphorothioates contain a P=S bond. The phosphorothionothiolates (e.g. phosphorodithioates) constitute a subclass, where one S atom is as P=S, and the other as a thioester. Thioesters can be linked to an alkyl subtituent, or the leaving group can be attached via S atom (e.g., malathion, dimethoate). Phosphoramides constitute another class of OP compounds, where amides are formed instead of esters. Of the seven phosphoramides used as insecticides today, three are

phosphoramidates (fenamiphos, phospholan and mephospholan), two are phosphoramidothionates (propetamphos and isofenphos) and two are phosphoramidothiolates (metamidophos, acephate) (Chambers and Levi, 1992). OP compounds that have one substituent attached by a phosphorus-carbon bond are classified as phosphonates (e.g., trichlorfon), phosphonothionothiolates (fonophos) and phosphonothionates. Phosphinothionates and phosphinates have two P-C bonds.

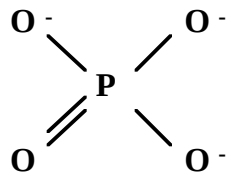

Phosphates

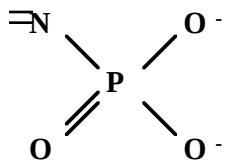

Phosphoramides
Phosphoramidates

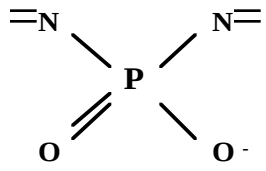

Phosphorodiamidates

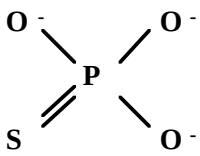

Phosphorothioates
Phosphorothionates

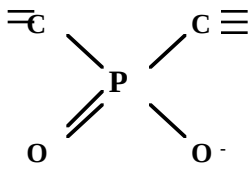

Phosphinates

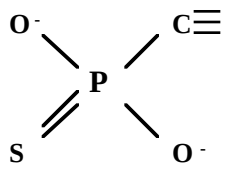

Phosphonothionates

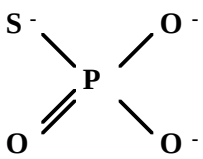

Phosphorothiolates

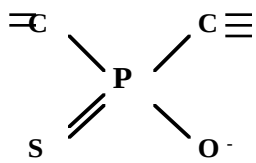

Phosphinothionates

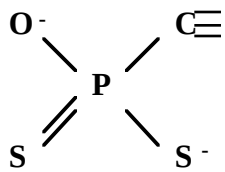

Phosphonothionotiolates

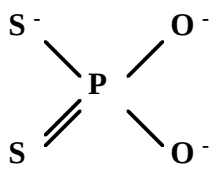

Phosphorodithioates
Phosphorothionothiolates

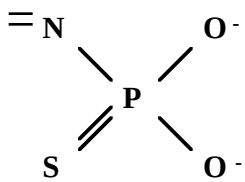

Phosphoramidothionates

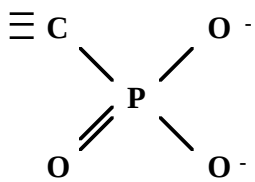

Phosphonates

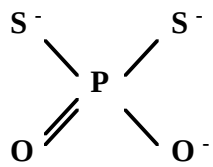

Phosphorothiolates

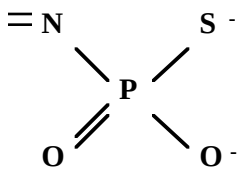

Phosphoramidothiolates

Figure 4: Structural classification of organophosphorus compounds (Chambers H, 1992).

3. Chemical classification related to toxicological effects of OP compounds.

An important deleterious effect of OP compounds is acute toxicity, related to their ability to inhibit acetylcholinesterase (AChE) by phosphorylation. The potency of OP compounds as anti-AChE agents depends on the resulting degree of AChE phosphorylation. As a consequence, exposure to these OP compounds leads to accumulation of ACh in the cholinergic nerve synapses and neuromuscular junctions. The latter results in junctional hyperexcitabilily, and multiple postsynaptic impulses generated by a single presynaptic stimulus in both somatic and autonomic nervous systems. The clinical signs of acute neurotoxicity of OP compounds are described in a subsequent section. A variety of different type of OP classes have the potential to produce acute neurotoxicity (phosphates, phosphorothionates, phosphorothiolates, phosphorothiono- thiolates, phosphorodithiolates, phosphorodithioates, phosphoroamidates, phosphonates, phosphorodiamidates, phosphinates, phosphinothionates, phosphonothionothiolates, phosphoroamidothiolates, phosphoroamidithionates) (Chambers and Levi, 1992). Specific organophosphorus compounds capable of inhibiting acetylcholinesterase and producing acute neurotoxicity include: diisopropyl-fluoro-phosphate (DFP), diazinon, chlorpyrifos, dichlorvos, malathion, parathion, paraoxon (Abou-Donia and Lapadula, 1990; Hern, 1971; Johnson, 1975a,b; Koelle *et al.,* 1946; Majno *et al.,* 1961; Smith *et al.,* 1930; Smith *et al.,* 1959).

Some OP compounds can induce a delayed neuropathy, OPIDN, a toxic effect that is not related to AChE inhibition. These OP compounds are known to inhibit another enzyme called neurotoxic esterase (NTE). Inhibition of NTE is a prerequisite to OPIDN (Johnson, 1974). The mechanism of NTE inhibition is discussed below. Inhibitors of NTE can be divided in two categories depending upon their biological effects. The first group consists of phosphates, phosphonate, and phosphoramidates, compounds which essentially

irreversibly inhibit NTE, and induce delayed neuropathy (OPIDN). Carbamate, sulfonyl fluorides, and phosphinates reversibly inhibit NTE, and do not cause delayed neuropathy (Fig. 4). Among specific organophosphorus products capable of producing delayed neuropathy after NTE inhibition are tri-ortho-tolyl phosphate (TOTP, also known as tri-o-cresyl phosphate, TOCP), cyclic saligenin phosphates such as phenyl saligenin phosphate (PSP), and tolyl saligenin phosphates (TSP), diisopropyl-fluorophosphate (DFP), mipafox, and methamidophos (Chambers and Levi, 1991; Ecobichon, 1994).

Delayed neuropathy induced by OP compounds has been divided into 2 categories; type I and type II (Abou-Donia and Lapadula, 1990). The major difference between type I and type II OPIDN - inducing compounds is that type I compounds have a pentavalent phosphorus atom, whereas type II compounds have a trivalent phosphorus atom. Type I compounds include derivatives of phosphoric, phosphonic and phosphoramide acids, and phosphorofluoridates, with their sulfur analogs. The type II category compounds consist of phosphorus acid derivatives (triphosphites) and their sulfur analogs (Abou-Donia and Lapadula, 1990). Other differences also exist between type I and type II OP compounds. For example, the ortho-methyl group of aromatic type I compounds must be metabolized to saligenin o-tolyl cyclic phosphate, which is considered the potent neurotoxic metabolite. On the contrary, type II aromatic compounds are neurotoxic without the need of metabolic transformation.

The neuropathy induced by type I and type II OP compounds differ based on species susceptibility, onset and nature of clinical signs, and extent of brain, spinal cord lesions. For example, triphenyl phosphite, a type II OP, has been reported to cause ataxia in species both susceptible to (hens, ferrets), and relatively resistant to (rats) type I OPIDN (Abou-Donia and Lapadula, 1990). The latent period is also shorter for Type II OPIDN compared to type I, and clinical signs are usually more generalized and severe with

neuropathy induced by triphosphites (Lehning *et al.,* 1986; Veronesi and Dvergsten, 1987; Carrington *et al.,* 1988). The spectrum of lesions induced by pentavalent type I compounds also differs from the pattern observed with triphosphite and its sulfur analogs. In chickens, lesions of type II OPIDN are more widespread than injury caused by type I OPIDN, in that higher order centers responsible for processing and integrating sensorimotor, visual and auditory information were damaged (Tanaka *et al.,* 1992). Indeed, neuronal cell body lesions of chromatolysis and necrosis which are prominent characteristics of type II OPIDN were not a feature of type I OPIDN. In type I OPIDN, the primary lesion consisted of degeneration of axon terminals, primarily affecting large myelinated central and peripheral nerve fibers. On the contrary, type II OPIDN in chickens produced extensive terminal axonal degeneration. prominent in the spinal cord gray and white matter, selected medullary brain stem nuclei, cerebellar granular layer folia I-VI, and several midbrain and forebrain structures (Tanaka and Bursian, 1989; Tanaka *et al.,* 1992). The classical OPIDN syndrome described in the literature and in this dissertation proposal, regarding clinical and morphological changes, generally refers to type I OPIDN (Bishoff, 1967; Bishoff, 1970; Cavanagh, 1954; Cavanagh, 1964; Itoh *et al.,* 1984; Jortner and Ehrich, 1987; Krinke *et al.,* 1979; Prineas. 1969; Tanaka and Bursian, 1989).

Approximately 60% of the aliphatic OP compounds tested produced delayed neurotoxicity (type I OPIDN). The descending order of neurotoxic potential as regards the 12 subclasses known to produce OPIDN are: phosphonates = phosphorofluoridates = phosphonofluoridates = phophorodiaminodofluoridates = phosphoroamidofluoridates > phosphates > phosphorotrithioates > phosphorothioates = phosphonothioates = phosphinofluoridates > phosphorochloridates (Chambers and Levi, 1992). Forty-six percent of the aliphatic aromatic compound group tested have the potential to produce OPIDN and the neurotoxic effect descending order is : phophorodiamidofluoridates > phosphonates > phophonothioates > phosphates > phosphorothioates > phosphinates.

Delayed neurotoxicity was observed as 35 % of triarylphosphates were evaluated (Chambers and Levi, 1992). Most triarylphosphate esters with one or more phenyl rings substituted in the ortho position or an ethyl group in the para position produce OPIDN. Saligenin cyclic phosphorus compounds are the more neurotoxic products with 62 % producing OPIDN. Compared to type I pentavalent OP compounds, few type II chemical products have been tested. Delayed neurotoxicity have been reported in hens with all four type II compounds tested (triphenyl phosphite, tri-o-cresyl phosphite, tri-m-cresyl phosphite, and tri-p-cresyl phosphite) (Abou-Donia and Lapadula, 1990).

4. Cyclic phenylsaligenin phosphate (PSP).

Phenyl saligenin phosphate (PSP), an active congener of tri-*ortho*-tolyl-phosphate (TOTP) (Eto *et al.,* 1961), has been well studied for its ability to produce delayed neurotoxicity in hens (Ehrich and gross, 1983; Jortner and Ehrich, 1987; Abou-Donia and Lapadula, 1990; El-Fawal *et al.,* 1988, 1990; Ehrich *et al.,* 1993;, 1997; Massicotte *et al.,* 1999, 2000). A proposed pathway showing the transformation of TOTP to PSP is presented in Figure 3 and 4. Advantages of PSP were related to its capability to produce clinical signs and lesions of delayed neuropathy with few acute cholinergic effects and its ability to induce OPIDN without a need for metabolic activation (Aldridge *et al.,* 1981). PSP is thus considered an excellent compound for experimental evaluation of the clinico-pathological courses of OPIDN, hence its choice for this study.

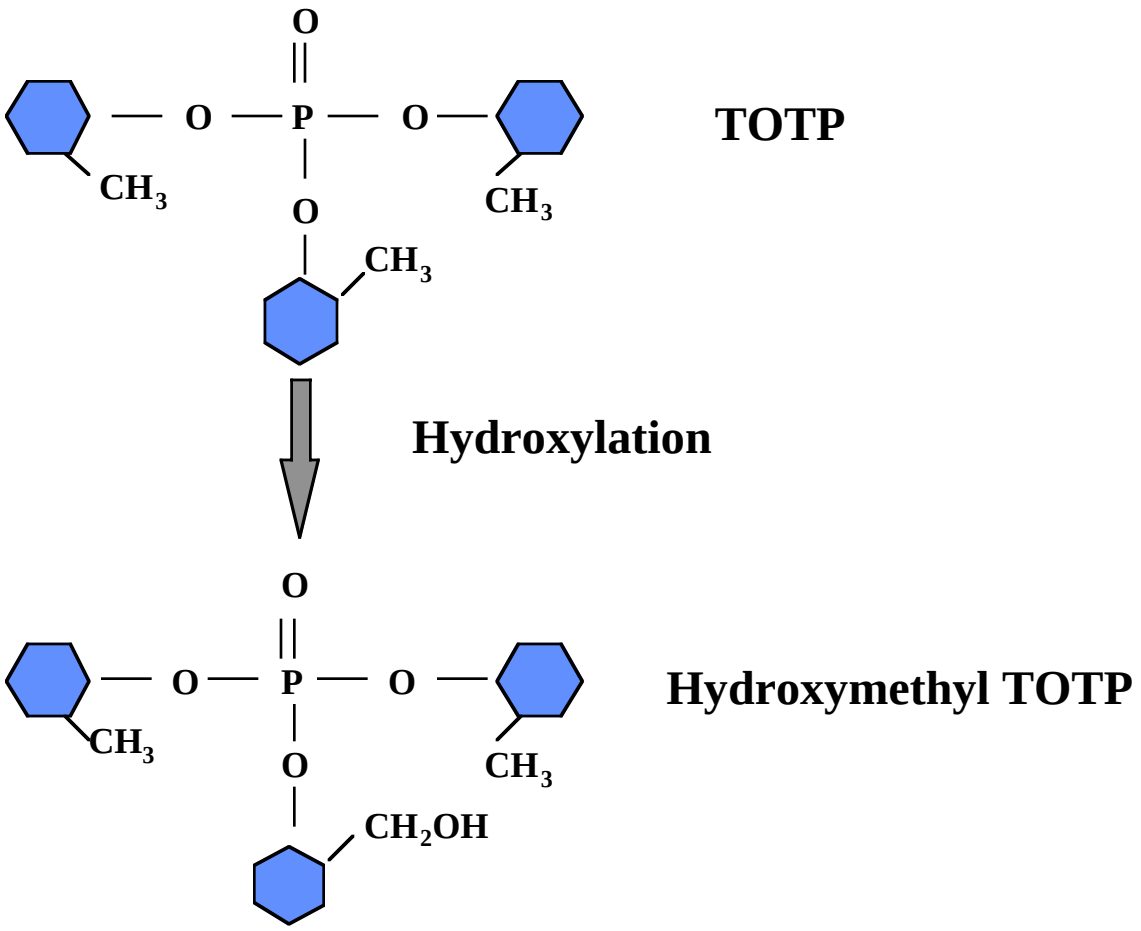

Figure 5: Proposed pathway for hydroxylation of TOTP (Eto *et al.*, 1961).

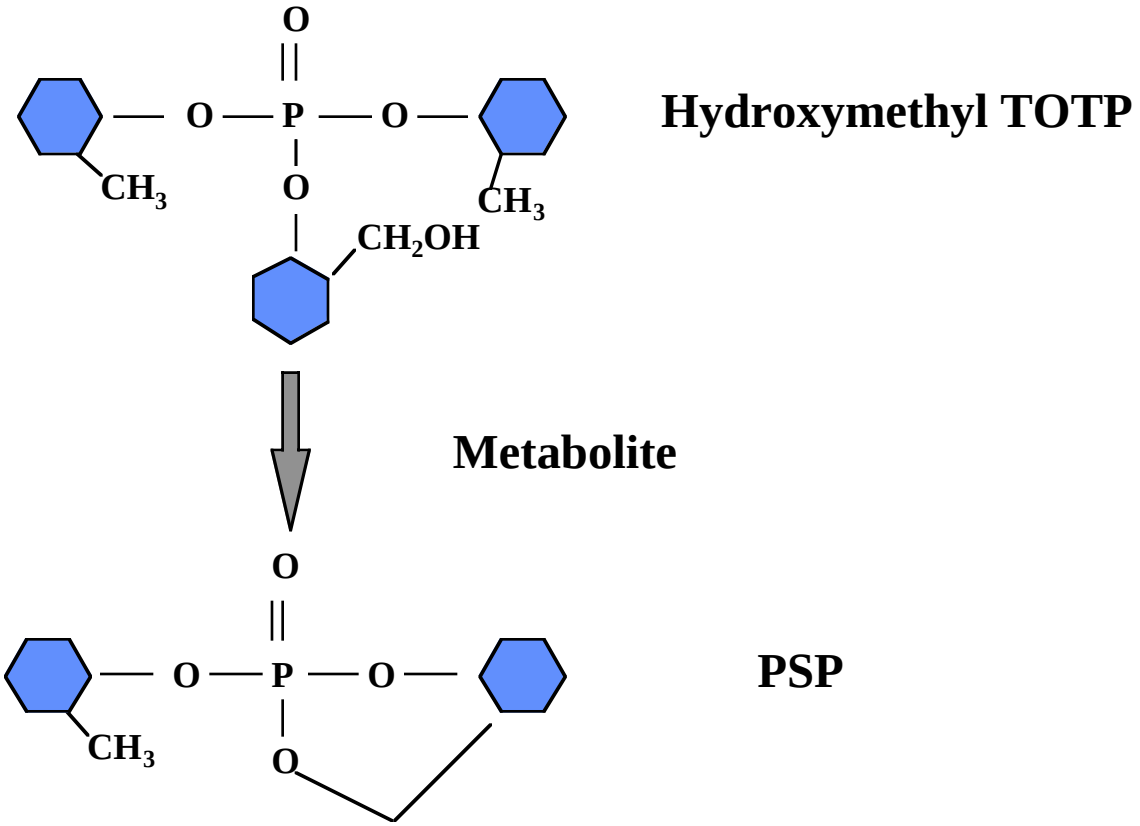

Figure 6: Proposed pathway for cyclization reactions of TOTP, continued from Figure 5 (Eto *et al.*, 1961).

1.3. Organophosphate - induced delayed neuropathy (OPIDN).

1. Outbreaks of OPIDN in humans and animals.

In addition to acute (cholinergic) poisoning, another neurotoxic condition has been observed with exposures to some, but not all, organophosphorus esters. This neurotoxic syndrome was eventually characterized as distal myelinated nerve fiber degeneration occurring several days following exposure to certain organophosphates (Cavanagh, 1954). The common term used to describe the resulting syndrome is organophosphorus-induced delayed neuropathy (OPIDN). This toxic neuropathy sporadically affects humans exposed to the OP compounds. The syndrome was originally noticed following treatment of tubercular patients with phosphocresote, a mixture of esters formed from phosphoric acid and coal-tar phenols (Davis *et al.*, 1980; Lorot, 1944). A widespread human outbreak of organophosphorus induced delayed neuropathy (OPIDN) was observed in mid and southern United States in the late 1920s and early 1930s, characterized by ataxia/weakness, and paresis/paralysis, occurring 10-21 days after ingestion of ginger extracts. The causative agent, tri-ortho-cresyl phosphate (TOCP), was a contaminant in some batches of the extracts of Jamaican ginger, hence the name "Ginger Jake syndrome". At least 20,000 human victims suffered from this syndrome to diverse degrees (Smith *et al.*, 1930). In 1959, another serious epidemic of TOCP induced neuropathy occurred in North Africa, afflicting more than 10,000 persons (Davis, 1963). Other organophosphorus compounds have also been implicated in OPIDN induction in humans: mipafox, leptophos, trichlorfon, parathion, fenthion (Bidstrup, 1953; Johnson *et al.*, 1981; Metcalf, 1975, 1984). Due to their neurotoxic effects, the production and sale of many of these compounds has ended. There are other less definitive reports suggesting that OPIDN in humans has come from consumption of or occupational exposures to OP neurotoxicants, but the full extent of these events cannot be ascertained.

OPIDN has also been seen in domestic animals exposed to appropriate toxicants. As an example, in 1971, leptophos was responsible for the death of 1300 water buffalo in Egypt. Clinical signs were manifested by ascending paralysis, with exposure following massive application of this product to control cotton leaf-worms (Abou-Donia *et al.,* 1974).

Despite the fact that effects of OP compounds on NTE and AChE have been well documented, little is known about early biochemical pathogenic events in OPIDN. Because of much reported discordance between NTE inhibition and OPIDN, alteration of some hypothesized trophic factors in the progression of the neuropathy has been suggested. These trophic factors include ^{3}H-DFP-binding protein within the active subunit site of NTE (Carrington *et al.,* 1985; Pope *et al.,* 1992; Pope *et al.,* 1993; Escurdo *et al.,* 1995), and ornithine decarboxylase since activity of this enzyme within the spinal cord was dramatically reduced after DFP exposure (Pope *et al.,* 1995).

2. Clinical manifestations associated with OPIDN.

Not every animal species is susceptible to clinical manifestations of OPIDN. The condition has been observed in humans and other primates, cattle, sheep, water buffaloes, cats, chickens, ferrets, and turkeys. Other species such as quail, rats, mice, rabbits, guinea pigs, hamsters and gerbils are more resistant, or show inconsistent delayed neurotoxicity (Abou-Donia, 1981; 1982; Bursian *et al.,* 1983; Jortner *et al.,* 1983; Larsen *et al.,* 1986; Veronesi *et al.,* 1991). Due to its reliability and clarity of responses, the domestic hen is the animal utilized in regulatory testing of chemicals for their ability to elicit OPIDN (US EPA, 1991). Age also influences the susceptibility of a subject to OPIDN, with younger animals less affected (Moretto *et al.,* 1991; Funk *et al.,* 1994). In addition, high social stress enhances the clinical severity of TOCP-induced neuropathy (Ehrich *et al.,* 1983). The general progression of clinical signs in susceptible species consists of incoordination, ataxia and weakness, with progression to complete flaccid paralysis. In hens, for example, ataxia

develops 6-14 days after exposure to a neurotoxic dose of PSP (2.5 mg/kg), a type I OPIDN-inducing agent. Clinical signs progress to complete paralysis and prostration within a 3-week period (El-Fawal *et al.,* 1990). Variation in dosages of delayed neurotoxicants also causes different degrees of clinical signs (Dyer *et al.,* 1992).

3. Neuropathological effects of organophosphorus compounds.

a. Light microscopic lesions of type 1 OPIDN.

Many pathological studies on different animal species (rats, cats, monkey, sheep, and chickens) have been conducted, generally using TOTP, diisopropyl-fluoro-phosphate (DFP) or mipafox as the toxicant (Carboni *et al.,* 1992; Bishoff, 1967; Bouldin and Cavanagh, 1979 a, b; Veronesi *et al.,* 1984; Drakontides *et al.,* 1982; Stumpf *et al.,* 1989; Abou-Donia *et al.,* 1981-1990; Jortner *et al.,* 1983; Jortner, 1984; Boyes *et al.,* 1994). All OP compounds that induce delayed neurotoxicity cause lesions in both the central and peripheral nervous systems. Morphological characteristics and distribution of the damage depends on several factors including the type or chemical structure of the OP compound, species, age, dosages, frequency and duration of exposure, but major alterations occur in distal levels of long myelinated fibers. In type I OPIDN, Wallerian-type degeneration of specific ascending and descending tracts of sensorimotor pathways of the brain stem, spinal cord and peripheral nerves were observed without changes in nerve cell bodies. Light microscopy of central nervous system lesions revealed swollen degenerating argyrophilic myelinated axons, progressing to destruction of the affected fibers distally. Distal axonopathy affecting larger myelinated fibers of peripheral nerves is also a common feature (Lapadula *et al.,* 1992; Krinke *et al.,* 1979). Breakdown of the fiber proceeds, accumulation of axonal debris, formation of multiple myelin-rich ovoids, and increased number of microglia, macrophages, and reactive astrocytes, fibroblasts or Schwann cells (depending on whether peripheral or central fibers are involved) (Jortner, 1982, 1984; Jortner and Ehrich

1987; Cavanagh, 1964; Pressing *et al.,* 1978). The concept of "chemical transection" of distal axons is suggested as the term to describe the pathogenesis of OPIDN (Bouldin and Cavanagh, 1979a,b). In this, the Wallerian-like degeneration occurs distally to the site of a putative distal non-terminal axonal injury, the "chemical transection". This nerve fiber alteration (Wallerian-like) resembles classical Wallerian degeneration, which is a trophic degeneration that occurs in the neurons distal to a site of traumatic axonal injury (De Lahunta, 1983), in that axonal degeneration and secondary demyelination are observed simultaneously, resulting in axonal swelling along the internodes (ellipsoids), and fiber fragmentation into myelin-rich ovoids (Bouldin and Cavanagh, 1979a). In peripheral nerve Wallerian degeneration, Schwann cells are thought to initiate myelin degradation by sequestering myelin fragments into ovoids and by beginning degradation of the myelin. Later on, macrophages phagocytosis and further degrade the myelin (Goodrum *et al.,* 1996; Griffin *et al.,* 1993).

Prior to 1979, "Dying Back" neuropathy was the name given to describe the characteristic axonal degenerating pattern produced by certain organophosphorus compounds. Erroneously, the selective degeneration was thought to begin at the axon's terminal, progressing in the direction of the cell body (Tanaka *et al.,* 1989). In 1979, Bouldin and Cavanagh studied the spatio-temporal spread of axonal degeneration in the neuropathy induced by DFP, by means of the peripheral nerve teased-fiber technique. This technique offers several advantages including assessment of proximo-distal lengths of individual fibers. Results of this study showed that focal axonal degeneration was localized distally along the axon, away from the cell body, but these lesions were not at the axon terminal. Therefore, 'chemical transection' of distal axons was suggested as the term to describe the pathogenesis of OPIDN (Bouldin and Cavanagh, 1979a,b).

Chickens are considered the most appropriate animal for the study of OPIDN because they exhibit locomotor deficits associated with distinct well defined bilateral lesions in the spinal cord (mainly long tracts), brain stem, cerebellum, and peripheral nerves. The primary site of injuries has been reported to be in the distal, non-terminal axon, affecting longer and large myelinated fibers in the spinal cord and cerebellar medullary white matter and peripheral nerves, with subsequent fiber degeneration distally. Thus, the cervical regions of ascending spinocerebellar tracts and fasciculus gracilis, as well as the lumbosacral area of the descending corticospinal (medial pontine spinal tract), reticulospinal and ventromedial tracts are more affected since these regions constitute the distal levels of these tracts (Beresford *et al.,* 1963; Cavanagh, 1954, 1964; Bouldin and Cavanagh, 1979a,b). Degenerating patterns in the hen's central nervous system induced by tri-ortho-tolyl phosphate (TOTP), diisopropyl-fluoro-phosphate (DFP), and phenylsaligenin phosphate (PSP) have been well studied (Olajos *et al.,* 1978; Tanaka *et al.,* 1989; Jortner and Ehrich, 1987).

Tanaka and Bursian (1989), using thicker sections and silver impregnation techniques, also noticed more central nervous system extensive lesions in hens, involving spinal gray matter, brainstem, and cerebellum. For an example, TOTP intoxication (type I OPIDN) induced distal axonal and nerve terminal degeneration involving the spinal cord, medulla and cerebellum. Spinal cord axonal lesions were observed in the cervical level of the fasciculus gracilis and the dorsal and ventral spinocerebellar tracts, in the lumbar region of the medial pontine-spinal tracts and in the lumbar ventral horns (heavy axonal degeneration). Distal axonopathy and terminal degeneration also were present in the medulla at the level of the lateral vestibular, gracile, external cuneate, lateral cervical nuclei, both dorsal and ventral spinocerebellar tract, and spinal lemniscus. The deep cerebellar nuclei and the cerebellar folia of the anterior lobe were also damaged (Tanaka and Bursian, 1989). With DFP, axonal degeneration was seen mostly within the spinal cord white matter

and the brain stem, with extensive lesions in the cervical ascending homolateral, gracilis, vestibulospinal and tectospinal tracts. (Tanaka *et al.,* 1990). In chicken peripheral nerves, the most sensitive regions are the tibial nerve branches to the lateral head of the gastronemius muscle (Krinke *et al.,* 1979) and the nerve to the biventer cervicis muscle (El-Fawal *et al.,* 1988).

Features of the lesions of OPIDN as seen by light microscopy are best observed with appropriately stained sections from epoxy resin embedded tissue. In the early stages of axonal degeneration, there are focal regions of poor axoplasmic staining, swelling, and associated thin myelin sheaths. Dark-staining intra-axonal debris accumulates in the axoplasm, especially in paranodal regions. Fragmentation of damaged fibers ensues as the process evolves into the Wallerian-like stage, with axonal and myelin ovoids, debris accumulation, and phagocytosis by Schwann cells. Axons become shrunken with disorganized and altered myelin sheaths (Jortner and Ehrich, 1987; Prineas, 1969). The onset of and severity of lesions correlates clinical neurological abnormalities (Massicotte *et al.,* 1997). Using standard single neurotoxic dosages, the first lesions are noted approximately on days 4-7, when a few degenerated fibers are observed (Massicotte *et al.,* 1997; El-Fawal *et al.,* 1988; Jortner and Ehrich, 1987). By day 21, severe and extensive degeneration is seen in the majority of subjects exposed to appropriate dosages of the neurotoxicants. In peripheral nerves, weeks after the clinical onset due to single toxic dose, axons of many injured peripheral nerves regenerate (Jortner, 1982; Jortner and Ehrich, 1987). In these previous studies, lesions produced by PSP in hens were similar in nature and distribution to those observed with TOTP intoxication, and consisted of distal axonal degeneration involving the peripheral nerves, spinal cord, medulla and cerebellum (Tanaka and Bursian, 1989; Cavanagh, 1954; Jortner and Ehrich, 1987). Spinal cord axonal lesions were observed in the cervical level of the fasciculus gracilis tract, in the cervical area of the

dorsal and ventral spinocerebellar tracts, in the lumbar region of the medial pontine-spinal tracts.

b. Electron microscopic studies in OPIDN.

Several reports exist on transmission electron microscopic changes observed in OPIDN mainly in axons, myelin and fiber terminals. In distal levels of affected axons, OPs cause early axoplasmic accumulation of branching cisternal membranous structures, resembling agranular reticulum, prior to swelling and further nerve fiber degeneration (Bischoff, 1967,1970; Bouldin and Cavanagh, 1979b; Prineas, 1969). At a later stage of axonal degeneration, changes consisted of loss of neurotubules and neurofilaments, degenerated mitochondria, accumulation of membranous and dense bodies structures, granular transformation and reduction of axoplasm (Bischoff, 1967,1970; Bouldin and Cavanagh, 1979b; Prineas, 1969). End-stage Wallerian-like fiber degeneration revealed the presence of various degrees of axonal and myelin debris in Schwann cells (Prineas, 1969).

Lesions in the myelin sheaths are also seen. In peripheral nerve, intra-myelin vacuoles can also usually be observed within the extra-cellular space of the intraperiod line of the myelinated sheaths, closest to the axon (i.e., between the inner loop of Schwann cell cytoplasm and the most inner dense line of the myelinated sheaths) (Bouldin and Cavanagh, 1979b). The deterioration of the myelin sheaths and axons form ovoids that are phagocytized by Schwann cells (Bishoff, 1985). With further progression of these lesions, granular degeneration develops associated with complete collapse of axons (Jortner *et al.*, 1984, 1987; Bouldin and Cavanagh, 1979b). Subsequently, Wallerian degeneration occurs with complete loss of the axon and myelin sheath distal to the presumed site of injuries. These are replaced by compact bands of proliferative Schwann cells, the so-called Buengner's bands.

The ultrastructure of axon terminals in degenerating nerve fibers have been studied in the central and peripheral nervous systems (Bischoff, 1967; Bouldin and Cavanagh, 1979a,b; Drakontides *et al.*, 1982; Prineas, 1969). OP compounds causing delayed neuropathy induce the formation of membranous structures and vacuoles, as distal focal axonal alterations, preceding myelinated nerve fiber degeneration. Lesions in the presynaptic endings of the anterior horn of the spinal cord was also described, and consisted of swollen motor terminals and spherical synaptic vesicles (Bischoff, 1970; Prineas, 1969). Accumulation and agglutination of proliferated vesicular elements are common feature in presynaptic endings. These are mingled with crowded circular membrane complexes and myelin figures. In addition, dark presynaptic terminals rich with condensed organelles and tangled filamentous structures are seen (Bishoff, 1970).

The work of Bouldin and Cavanagh (1979a,b) deserves special mention. Their electron microscopy confirms that nerve fiber varicosities precede the degeneration of axons, and the lesions are initially focal, and non-terminal. The ultrastructural modification of the teased-fiber technique, also useful in light microscopy, has greatly improved the quality of information obtained from electron microscopic evaluation of nervous tissue, giving more precise information in regard to the spatio-temporal progression of organophosphorus (DFP) induced axonal degeneration in recurrent laryngeal nerves of cats. In this study, the initial lesions consisted of focal, non-terminal midinternodal and paranodal demyelination. The axons continued to further degenerate with time. Twenty days after OP administration, marked focal axonal non-terminal, mid internodal vacuoles gave rise to swellings (varicosities), and degeneration associated with paranodal demyelination. More details on ultrastructural descriptions of the varicosities observed in that OP induced axonal degeneration could be appreciated using this technique. The importance of these varicosities resides in the fact they may play a role in the pathogenesis of OPIDN. The focal axonal degeneration leads eventually to Wallerian degeneration

distally to the initial and focal site of injuries. Therefore, the focal nature of axonal damage seems to play a significant role in OPIDN (Bouldin and Cavanagh, 1979 a, b). The pathophysiology of the formation of intra-axonal and intra-myelin vacuoles, as well as the association between these vacuoles is unknown, but may be related to altered fluid balance in affected fibers. It has been postulated that OP compounds bind to unknown proteins of the myelin sheath or axonal membrane, causing membrane damage, altering directly or indirectly the regulation of the transmembrane ionic gradient. Passive influx of water accumulates within the area of intra-period gaps, forming vacuoles into the intracellular space. Water would eventually accumulate in the dilated agranular endoplasmic reticulum.

4. Effects of organophosphorus compounds on energy metabolism.

Alterations of ATP concentrations have been previously measured in peripheral nerves of hens treated with the neuropathy-inducing OP compounds phenylsaligenin phosphate (Massicotte *et al*., 2000). In the former study, modifications in ATP concentrations were compared to the occurrence of clinical signs, electrophysiological alterations of compound action potentials (conduction velocities and amplitudes), and morphological changes observed in OPIDN. A statistical linear relationship between clinical signs and ATP concentrations in specific segments of hen sciatic nerves affected with OPIDN was found ($r^2 = 0.97$, $p = 0.01$). The most severe variations in ATP concentrations were observed 14 days after PSP exposure, when the neuropathy was most fully developed. In addition to these late changes, ATP concentrations were also altered in the distal segment of sciatic nerves early in the course if this neuropathy. A significant increase in ATP concentrations was present in the most distal segment of the sciatic nerve 2 days after exposure to PSP compound, even though clinical signs of OPIDN were not yet detected. Therefore, this author concluded that ATP changes observed in sciatic nerves could represent early events in the development of OPIDN. These latter changes in neuronal

ATP levels could be due to an increment in free energy requirements or a more active metabolic state within neuronal cell in early stages of OPIDN (Massicotte *et al*., 2000).

Because the hydrolysis of ATP is coupled to several energetically unfavorable reactions, we suspect the ATP concentration alterations to be a relevant part of mechanisms involved in OPIDN. Pertinent to axonal mechanisms of injury could be OP-induced changes in the biosynthesis of macromolecules, and the formation of reactive phosphorylated intermediates. Alterations of ion transport/gradients (Na^+-K^+ ATPase, and Ca^{2+} ATPase pumps) responsible for maintenance of the electrochemical ionic gradients across the axonoplasmic membrane could also be involved, and explain variation in ATP concentrations previously observed (Augustine *et al.*, 1990; Lingrel *et al.*, 1994; Tanford, 1983). In addition, ATP has been proposed to fulfill an important part of the metabolic and energetic demands required in all phases of axonal transport (Goodrum and Morell, 1992). Several neurotoxicants can cause progressive neuropathy by disrupting axonal transport (Griffin and Watson, 1988). For example, slower retrograde transport has been reported in animals treated with acrylamide and with a neuropathy-inducing OP (Moretto *et al*., 1987, 1988). In neuropathy caused by hexacarbons, inhibition of local energy production and shortage of axonal ATP were hypothesized to impair rapid retrograde and anterograde axonal transports (Sabri *et al.*, 1979 a, b). Even though axonal transport has been rarely studied in OPIDN, it is possible that alterations of axonal transport secondary to local ATP depletion could explain part of the mechanisms involved in OPIDN.

Moreover, other studies showed alteration in mitochondrial energy metabolism in cells exposed to OP compounds. Mitochondrial membrane depolarization (Holmuhamedov *et al*., 1996; Carlson and Ehrich, 1999), inhibition of mitochondrial oxygen consumption and respiration, and reduction of oxidative phosphorylation have been documented following OP exposure (Spetale *et al*., 1976; Sitkiewick *et al*., 1980; Skonieczna *et al*.,

1980). Other metabolic pathways affected by OP compounds include oxidation of succinate, α-glycerophosphate, and pyruvate/malate substrates (Holmuhamedov *et al*., 1996). In addition, OP-induced changes in enzymes responsible for energetic metabolism processes, including creatinine kinase and succinate dehydrogenase (Knoth-Anderson *et al*., 1992), cytochrome oxidase and cytochrome c reductase (Sitkiewick *et al*., 1980), and 6-phosphofructokinase have also been reported.

5. *In vitro* models for toxicity testing of OP compounds.

Neuroblastoma and other immortal cell lines have been used to assess potential for OP neurotoxicity (Mochida *et al*., 1988; Veronesi and Ehrich, 1993a, Ehrich *et al*., 1994, 1997; Greenman *et al*., 1997, Carlson and Ehrich, 1999; Barber *et al*., 1999a, b; Carlson *et al*., 2000). Subcellular targets responsible for toxicity in these cell cultures remain unknown, even though nuclear (Mentzschel *et al*., 1993), enzymatic (Ehrich *et al*., 1994, 1997; Barber *et al*., 1999a), cytoskeletal (Tuler and Bowen, 1989), plasma membrane (Antunes-Madeira *et al*., 1994), and transmembrane potential (Carlson and Ehrich, 1999) modifications have been demonstrated. Involvement of apoptotic processes have also been implicated in OP-induced cell death (Akbarsha and Sivasamy, 1998; Hamm *et al*., 1998; Carlson *et al*., 2000).

Organophosphate-induced *in vitro* cytotoxicity has been demonstrated using a variety of techniques, mainly testing neuroblastoma cell cultures and chromaffin cells. Among the methods used for evaluation were figure fragmentation of DNA and apoptotic mechanisms (Cai *et al*., 1998; Carlson and Ehrich, 1999; Carlson *et al*., 2000), inclusion of trypan blue in degrading cells (Nostrandt *et al*., 1992), and morphologic changes (Harvey and Sharma, 1980; Tuler and Bowen, 1989; Knoth-Anderson *et al*., 1992). *In vitro* alterations of metabolic processes and energy production have also been evaluated, and

results showed inhibition of glucose metabolism (Harvey and Sharma, 1980), and decreased incorporation rate of [^{3}H] adenosine into ATP (Knoth-Anderson *et al*., 1992). The effect of OP compound exposure on primary neuronal cell cultures have, however, been poorly studied, and few information is available in the literature at the present time (Mochida *et al*., 1988; Marinovich *et al*., 1996). Studies in primary cultures are valuable because normal cells removed from animal are used. Immortal cell lines are cancer cells, and although easier to obtain and use, they are not necessarily the best representatives of the tissues to be studied *in vitro* (Kleitman *et al.,* 1995; Varon *et al.,* 1981; Wood, 1976).

Toxicant-induced effects on mitochondrial respiration have been evaluated *in vitro*, using neuroblastoma n-2α cell lines exposed to neurotoxic compounds such as 1-methyl-4-phenyl-1, 2,3,6-tetrahydropyridine (MPTP) and 1-methyl-4-phenylpyridinium ions (MPP^+) (Steyn *et al*., 2000), as well as in lymphoblast and fibroblast cell cultures (Wanders *et al*., 1993; Robinson, 1996). The amount of ATP produced and the uncoupling of oxidative phosphorylation secondary to opening of MPT have been studied. One study used neuroblastoma SH-SY5Y cells exposed to OP compounds (Carlson and Ehrich 1999). Another used confocal microscopy in living hepatocytes challenged with either *t*-butylhydroperoxide or the Ca2+ ionophore A23187 (Niemienen *et al*., 1995; Lemasters *et al*., 1998). In these *in vitro* models, alterations of mitochondrial respiration and MPT modification were detected with the aforementioned toxic compounds. However, the cytotoxic effects of OP compounds on ATP production, MPT, and energy metabolism within primary neuronal cell cultures have not been reported. The proposed chick primary *in vitro* DRG cell model is unique because it allows investigation of OP compounds in a target species, which represent the closest *in vitro* system to evaluate neuronal effects of OP compounds occurring *in vivo*. This primary cell culture preparation has potential usefulness for studies of pathogenic mechanisms at the cellular level, and the effects of OP compounds

on neuronal cell populations can be delineated from effects on non-neuronal cell populations.

1.4. Dorsal root ganglia cell culture and preparation.

The use of myelinating cells and neuronal populations as primary tissue cultures has been essential for studying myelinating processes (Kleitman *et al*., 1995). Using a variety of techniques, isolation of pure neuronal or Schwann cell population can be achieved by dissecting dorsal root ganglia (DRG) of 15-16 day old embryonic rats or 8-11 day old chick embryos (Blood, 1975; Wood, 1976; Varon *et al*., 1981; Kleitman *et al*., 1995).

For the preparation of pure neuronal population, DRG from cervical or lumbar intumescences are initially plated as a mixed population of dissociated cells. The non-neuronal cells subsequently are eliminated by the use of antimitotic agents such as uridine and fluorodeoxyuridine (FdU). The dissociated culture prepared in this way develops in a predictable pattern (Kleitman *et al*., 1995). After the cultures are flooded with antimitotic medium on the second day *in vitro*, the non-neuronal cells (fibroblasts and Schwann cells) are destroyed rapidly. By the fourth day, a network of neuritic process should have formed. Thereafter axons begin to cross the site of initial deposition, toward the edge of the culture dish. By the third week in vitro, the culture should be mostly free of non-neuronal cells and should consist of a central network of neurons and interconnecting neurites, surrounded by a halo of radially extending bare axons. The axons should be firmly adherent to the substratum and show only a few abnormalities. The neuronal somata should exhibit homogenous cytoplasm containing few or no large granules and a centrally located nucleus with prominent nucleoli. Some neurons may contain large vacuoles, but exhibit otherwise healthy structures. This is considered within the norm of this preparation. The formation of vacuoles may be correlated with maintenance of pure neuronal cells in the absence of

their supporting cells. These purified neuronal cultures can be maintained for 21 days with minimal deterioration. These neuronal cultures often degenerate with fetal bovine serum when they are kept longer than 21 days; therefore the use of human placental serum has been advocated for this purpose, or the culture can be simply refed with Schwann cells (Kleitman *et al*., 1995).

The technique for preparation of pure Schwann cells differs from the one described for preparing neuronal cultures, since it uses whole ganglion explants from slightly older embryos (10 days for Schwann cells versus 9 days for neuronal cells) (Wood, 1976; Kleitman *et al*., 1995). Whole ganglia explants are placed on a cell culture dish and are then treated with antimitotic agents. Although the initial antimitotic treatment done immediately after culturing DRG explants, kills many Schwann cells, many survive and proliferate after transplantation, eventually repopulating the newly forming neuritic outgrowth. New neurites are required to stimulate division of the surviving Schwann cells because fibroblasts are never completely eliminated from the original culture dish, despite a series of antimitotic treatments. Therefore, transplantation of the initial explant into a new dish is performed twice prior to final harvesting of purified Schwann cells. The two major problems encountered with the Wood method are poor proliferation of Schwann cells following transplantation of explants due to the antimitotic treatments and fibroblast contamination of the outgrowth zone (Wood, 1976). This issue can be partly resolved by using only the largest lumbar ganglia (Kleitman *et al*., 1995).

Myelination of the neuronal population can be achieved by adding purified Schwann cells to the culture, in the presence of ascorbate (Kleitman *et al*., 1995). With this method, myelination is obtained within 7 days, and these myelinated cultures can be held indefinitely. These cell models are a close representation of peripheral nerves *in vivo*, and could be used for toxicity testing *in vitro*. The literature does not contain references to

toxicity-induced by OP compounds in myelinated primary dorsal root ganglia cell cultures. Morphological changes have been studied in our laboratory, however, after exposure of chick DRG to physiological concentrations of TOTP and PSP (Massicotte and Jortner, unpublished).

MATERIALS AND METHODS

PART III: CHAPTER 2

MATERIALS AND METHODS

2.1. Experimental Design.

Dorsal root ganglia were extracted from 9-day old chick embryos (n=30 embryos, 6 ganglia/embryo, 36 dissociated ganglia/dish) for differentiation of neuronal cell cultures, and from 10-day old chick embryos for mixed Schwann cell and neuronal cocultures (n=6-10 ganglia/dish). Neuronal and non-neuronal cells contained in these chicks DRG were allowed to mature for 14 days prior to OP challenge. Then, the neuronal and non-neuronal cell cultures from DRG were treated with physiological concentrations of neuropathy-inducing OP compounds (PSP and mipafox; 1 μM), and a non-neuropathy inducing OP compound (paraoxon; 1 μM). Myelinated neuronal cells from DRG were used instead of separate populations of neurons and Schwann cells for morphological studies. These cocultures were also be allowed to mature for 14 days prior to OP exposure. All OP compounds were diluted from 0.1 M concentrations dissolved in dimethyl sulfoxide (DMSO). Negative controls received DMSO vehicle only.

Neurotoxic esterase (NTE) determination, measured to characterize the DRG cells, was done using the micromethod of Correll and Ehrich (1991). Neuronal cell cultures (10^5 cells/ ml) were exposed to PSP, mipafox or paraoxon (1 μM), for one hour at 37°C, and 50 μl of the suspended cells were added to wells of microtiter plates for esterase assays (Correll and Ehrich, 1991). For this study, esterase activities were determined on duplicate cultures, and replicated 3 times. NTE activities were inhibited by PSP and mipafox compared to controls (Appendix 1).

For the studies evaluating quantification of ATP concentrations and MTP opening, each experiment was performed at 12 hours post OP exposure, and replicated 3 times with

duplicate cultures exposed each time. Phenyl saligenin phosphate, mipafox, and paraoxon were used at a physiological concentration of 1 μM. Vehicle controls were also evaluated. For morphological studies, the myelinated neuronal cells were exposed for 48 hours to PSP and paraoxon at 1 μM, then the media was washed at 48 hours, and the culture maintained for an additional 2 or 5 days for a total of 4 and 7 days after the initial exposure to OP compounds. This exposure time of 48 hr was chosen rather than the 12 hr used for ATP concentration determinations and confocal microscopic studies to minimized manipulation of these sensitive cultures that needed to be kept longer than the cultures for other endpoint determinations. The cell cultures were then embedded in plastic. Descriptions of neuronal structures in these treated myelinated neuronal cell cultures were provided following exposure to OP compounds and compared to their negative controls.

2.1.2. Organophosphorus compound preparations and dosages.

Phenyl saligenin phosphate (PSP) synthesized by Lark Enterprises (Webster, PA), and mipafox purchased from Chem Service Inc. (West Chester, PA), were chosen because of their potential for inducing delayed neuropathy *in vivo*. Stock solutions containing PSP, mipafox, and paraoxon at 100 mM were prepared by dissolving these OP compounds in dimethyl sulfoxide (DMSO). Previous studies demonstrated that PSP at concentrations 10^{-7} M could inhibit esterases in SH-SY5Y human neuroblastoma cell lines (Ehrich *et al*., 1994, 1997). Transmembrane potential modifications and DNA fragmentation in SH-SY5Y cell cultures have been reported following PSP exposures, in concentrations from 10μM to 1 mM (Carlson and Ehrich, 1999). In this proposed study, cytotoxic effects of these OP compounds were determined by using a primary neuronal cell culture and a culture of Schwann cells exposed to physiological concentrations of the OP compounds PSP, mipafox and paraoxon (1 μM). Concentrations of OP compounds proposed to treat these primary cell cultures were lower compared to the ones used to cause cytotoxicity in the

immortal cell line used by Carlson and Ehrich (1999), because primary cultures can respond to physiological concentrations of toxicants. The concentrations of 1 μM of OP compounds used on DRG were a close representation of *in vivo* exposures, especially when compared to the concentrations needed to produce cytotoxicity in immortal cell lines (Carlson and Ehrich, 1999).

2.1.3. Dorsal root ganglia cell culture, preparation and characterization.

a. Purified sensory neuronal population .

Dorsal root ganglia of 9-day old chick embryos were dissected under sterile conditions from the lumbar intumescence (Blood, 1975; Wood, 1976; Varon *et al*., 1981; Kleitman *et al*., 1995). Under a dissecting microscope, the embryo was laid on its back and the abdominal viscera were removed with care to prevent damage of the DRG underneath. The lumbar DRG were collected using microdissecting forceps, and transferred to a solution containing L-15 media. Strict sterile procedures were observed during dissections and in all subsequent steps of the purifying processes.

Following DRG collection from approximately 30 embryos, the pooled ganglia were incubated with 0.25% trypsin for 45 min at 37°C on a rotatory shaker. Trypsin inactivation was achieved by the addition of L-15 media supplemented with 15-20% fetal bovine serum (FBS). Then, the sample was centrifuged at 10000 rpm for 5 min, and the pellets resuspended and triturated in 1 ml of serum-containing medium. The volume of this suspension was increased to 5 ml, recentrifuged as before, and resuspended in the desired volume of a solution containing Eagle's minimum essential medium, supplemented with 5% human placental serum and 50 ng/ml of nerve growth factor (E-MEM + 5% HPS + 50ng/ml NGF, or C_H maintenance feed). One drop of this suspension was plated in the

center of 35 mm collagen-coated dishes for ATP determination. This method described is expected to yield 5000 to 7000 neurons per culture.

After the cells were allowed to attach to collagen for 12 hours, the dishes were flooded with L-15 media containing 15% FBS to wet the remaining collagen surface, and the purification procedure was initiated by refeeding the cell culture with a solution containing antimitotic agents contained in C_F medium (E-MEM, 5% HPS, 498 mg/dl glucose, 10 μM uridine, 10 μM FdU). The antimitotic protocol was accomplished by alternating antimitotic feedings with maintenance feedings according to the following schedule: C_H maintenance feeding on days 1, 4-6, 8-10 and day 12 onward, and C_F antimitotic feeding on days 2-4, 6-8, and 10-12. Prior to performing experiments, these purified neuronal cultures were allowed to rest in C_H media for one week to ensure that no residual FdU remains in the media, especially if Schwann cells were to be added for subsequent myelination of neuronal processes. These neuronal cultures often degenerate with FBS when they are kept longer than 21 days; therefore, since less neuronal degeneration occurs with the use of HPS, this supplement was used to maintain the purified neuronal cell cultures (Kleitman *et al*., 1995). It was believed that the survival of these neuronal cell cultures would be greatly increased with the addition of HPS to the maintenance media (Kleitman *et al.*, 1995).

b. <u>Dorsal root ganglia explants for the study of Schwann cells</u>.

The technique for preparation of neuron-Schwann cells coculture differed from the one described for preparing neuronal culture, since it uses whole ganglion explants from slightly older embryos (Wood, 1976; Kleitman *et al*., 1995). For this purpose, 10-day old chick embryos were dissected as described above for neuronal preparations.

Following the collection of 4 to 6 lumbar DRG, the ganglia explants were distributed in collagen-coated 60-mm plastic dishes and allowed to attach to the surface in C_H media. Schwann cell purification was achieved by refeeding the cell culture with a solution containing antimitotic agents, called C_F medium (E-MEM, 5% HPS, 498 mg/dl glucose, 10 μM uridine, 10 μM FdU). The antimitotic protocol was accomplished by alternating antimitotic feedings with maintenance feedings according to the following schedule: C_H maintenance feeding on days 3-6, 8-10, and day 12 onward, and C_F antimitotic feeding on days 1-3, 6-8, 10-12. Yields of up to 250,000 Schwann cells per ganglion were expected with this method (Wood, 1976; Kleitman *et al.,* 1995).

At the end of the antimitotic protocol, the explants were transplanted twice onto new wet collagen-coated dishes to ensure proper elimination of fibroblasts. The neurites were cut at the edge of the explants with a sterile razor blade. The explants were separated carefully from the collagen surface using microdissecting forceps, and moved to a new collagen-coated dish. Because newly outgrowths of neurites are required to stimulate division of the surviving Schwann cells, the explants were allowed to rest for 2 to 3 weeks in C_B media (E-MEM, 5% FBS, 20 ng/ml NGF). A second transplantation of explants was sometimes needed prior to harvesting the purified Schwann cell (Kleitman *et al.,* 1995).

Harvesting and replating Schwann cells prepared using the Wood method described above requires removal of the neuronal cells, digestion of the collagen substratum and desegregation of Schwann cells. After rinsing the culture cells with EBSS, the neuronal cell bodies were cut from their axons, and Schwann cells were dissociated from their axon using 0.05% collagenase. Then, the cultures were incubated in 5% CO_2 for 30 min at 37°C. The resulting Schwann cell aggregates were transferred and triturated in 10 ml of L-15 media, and centrifuged at 1500 rpm. Subsequently, the pellets were resuspended in 0.25% trypsin in Hank's-CMF and incubated at 37° C for 30 min. The trypsin digestion was then

stopped with L-15 media, and the cell suspension recentrifuged. Finally, after two additional rinsing of the Schwann cell pellet, the cells were resuspended in 1 ml of C_B. Drops of this final Schwann cell suspension were used for experimentation or fed onto purified neuronal populations for subsequent myelination (neuron-Schwann cell coculture). The most difficult part of this experiment was to extract the DRG explants, without the underlying collagen containing fibroblasts. Fibroblast contamination was a problem in Schwann cell cultures from DRG of 11-day old chick embryos, and the separation of Schwann cell from fibroblast populations was not possible.

c. Myelinated dissociated neuronal cell cultures.

Preparation of the neuron-Schwann cell coculture was done as described by Kleitman *et al* (1995). The coculture was maintained routinely in DM after reseeding for a period of 10 to 14 days to allow adequate neurite-driven proliferation of Schwann cells. In this serum-free medium, Schwann cells are unable to myelinate the neurites. After this resting period, the coculture was transferred to a medium (myelinating feed or MF) containing both ascorbate and bovine serum albumin (E-MEM, 15% FBS, 50 ng/ml of NGF, 498 mg/dl of glucose, and 5 mg/ml of L-ascorbic acid). The coculture was refed every 2 or 3 days. Using this technique (Kleitman *et al*., 1995), myelin formation should occur in 5-7 days. These myelinated cell cultures can be maintained on MF indefinitely, allowing long term studies to be conducted in peripheral nerve cell cultures. Myelination of neurites does not usually present problems if the appropriate substrates are provided to the media used for coculture. The success of myelinated neuronal cell culture resides in the isolation of pure Schwann cells, without fibroblast contamination. Fibroblast contamination of Schwann cells added to purified neuronal population can cause great difficulties in some experiments when the coculture needs to be maintained for a long time. Consequently, separation of Schwann cells from fibroblasts was critical for the studies proposed on myelinated neurites.

d. Esterase activities in neuronal cell cultures.

Neurotoxic esterase (NTE) determination was done using the micromethod of Correll and Ehrich (1991). NTE activity was measured to characterize the DRG cells. Inhibition of this biochemical marker has been used in animals as an indicator that OPIDN will occur. Inhibition of NTE in OP-exposed cell cultures has been used to relate *in vitro* and *in vivo* effects (Ehrich *et al.,* 1997). As done with other culture systems, neuronal cell cultures (10^5 cells/ ml) were exposed to PSP, mipafox or paraoxon (1 μM), for one hour at 37°C, and 50 μl of the suspended cells were added to wells of microtiter plates for esterase assays (Correll and Ehrich, 1991). A preincubation period of 20 min at 37°C with 0.064 mM mipafox and/or 0.5 mM paraoxon was followed by a 30-min incubation with phenyl valerate substrate in a total volume of 200 μL. The NTE activity was determined as the difference between the hydrolysis of this substrate in incubates containing mipafox + paraoxon (which inhibit all esterases) and incubates containing paraoxon (to inhibit esterases other than NTE), with absorbencies at 510 nm compared to a phenol standard curve (Johnson, 1982; Correll and Ehrich 1991). For this study, esterase activities were determined on duplicate cultures (n=2) using triplicate readings for each concentration.

2.1.4. Evaluation of mitochondrial respiration.

a. Generalities.

Eukaryotic cell culture can be used to quantify mitochondrial respiration (Wanders *et al.,* 1994; Robinson *et al.,* 1996). Mitochondrial respiration can be measured as the amount of ATP produced over time in digitonin-permeabilized cells (Wanders *et al.,* 1993; Bates *et al.,* 1994, Robinson *et al.,* 1996), or as a function of the amount of oxygen consumed by polarography (Rustin *et al.,* 1994; Hofhaus *et al.,* 1996). In the former

approach, the inner mitochondrial membrane remains intact, and the electron transport chain can be evaluated at specific complex levels. For this reason, quantifications of ATP concentrations over time were performed in these studies, in order to monitor the activity of the electron transport chain following exposure to OP compounds. This method has been performed previously in N-2α and SH-SY5Y neuroblastoma cells, and provided consistent results (Steyn *et al.*, 2000; Massicotte, unpublished).

b. Preparation of purified neuronal cell culture.

Purified neuronal cell derived from 9-day old chick DRG embryos were used to determine the effects of OP compounds. They were treated with PSP, mipafox and paroxon at a physiological concentration of 1 μM, or with diluted DMSO vehicle alone (negative controls) for 12 hours. This time-point was chosen because mitochondrial Ψm alterations were detected in previous studies at 12 hours using SH-SY5Y cells exposed to PSP and paraoxon (Carlson et al., 1999). These treated and negative control cells were harvested with 0.25% trypsin and 0.05% (w/v) EDTA, and centrifuged for 5 min at 1000 rpm (Blood, 1975; Wood, 1976; Varon *et al*., 1981; Kleitman *et al*., 1995). The cells were resuspended for 30 min in E-MEM supplemented with 15% FBS, allowing recovering of the cell from the harvesting procedure. Following this recuperation time, the cells were resuspended and washed multiple time (3X) at 1000 rpm (20°C) in a phosphate buffered-saline (PBS, 150 mM NaCl, 10 mM potassium phosphate, pH 7.4). Cell concentration contained in the final cell suspension were determined using a cytometer. The neurons were then diluted to a final cell concentration of 1 X 10^5 /ml with PBS and kept at 4° C during incubation time (Steyn *et al*., 2000).

c. Incubation of mitochondria with complex-specific substrate.

Purified neuronal or Schwann cells were added to complex-specific substrates, to reach a final concentration of 0.2 mg/ml (Wanders *et al*., 1993). Then, specific substrates were introduced into a basic isotonic solution containing 150 mM KCl, 75 mM Tris•HCl, 2 mM EDTA, 10 mM potassium dihydrogen phosphate, 0.1% (v/w) fraction V fatty-acid free bovine albumin, 40 μg/ml digitonin, and 1 mM ADP (Wanders *et al*., 1993; Ventura *et al*., 1995; Hofhaus *et al*., 1996; Robinson, 1996). The resulting mitochondrial respiration mixtures were incubated at 37° C for 30 min. For measurements of ATP production in the presence of complex-specific substrates, three different reaction mixtures were used. For complex I driven ATP production, 10 mM of malate and 10 mM of glutamate served as substrates. For quantification of ATP production through complex III, 10 mM of L-α-glycerol-3-phosphate were included in the reaction mixture. For evaluation of complex IV driven ATP production, the solution contained 200 μM of N,N,N',N'-tetraethyl-p-phenylenediamine dihydrochloride (TMDP), as well as 10 mM of ascorbic acid. The use of complex-specific substrates is important to determine that complex I, III and IV were functional prior to the addition of complex-specific xenobiotics (e.g., rotenone).

d. Complex-specific xenobiotics acting on mitochondrial respiration.

ATP production in the presence of xenobiotics specific for complexes I, III, and IV was determined after subtraction of ATP production in the presence of substrates alone. In previous studies on complex-specific inhibition of mitochondrial respiration, Complex I driven ATP production was inhibited by 20 μg/ml of rotenone. Inhibition of Complex III was done with10 μg/ml of antimycin. To block ATP production by Complex IV, azide was added to a final concentration of 10 mM (Wanders *et al*., 1996; Steyn *et al*., 2000). This

method of measurement had been previously performed in SH-SY5Y in this laboratory, although it needed to be adapted for neuronal and non-neuronal primary DRG cell cultures.

e. Quantification of ATP concentrations.

ATP concentrations in neuronal or Schwann cells were determined as previously reported for the NG 108-15 cell line (Shirhatti and Krishna, 1985; Kutty *et al.*, 1991). To terminate the reactions, the medium was removed and the cells extracted with 8% trichloroacetic acid (Steyn *et al.*, 2001). ATP assay mixture (firefly luciferase, luciferin, MgSO4, EDTA, DTT, and bovine serum albumin in tricin buffer - purchased from Sigma, no. FL-AAM) was added to 10 µl of the supernatant diluted 10-fold. The supernatant was placed in a 12 X 75 mm polystyrene tube (round bottom), and treated with antistatic additive (Analytical Luminescence Laboratory, tube 2050-10). ATP concentrations were measured with a semi-automatic bioluminometer (Monolight 2010 Instrument, Analytical Luminescence Laboratory, San Diego, CA). This method provided consistent readings to measure ATP produced within SH-SY5Y cells (Massicotte, unpublished; Steyn *et al.*, 2001).

2.1.5. Effects of OP compounds on the mitochondrial transition pore.

Dissociated and purified neuronal cells and mixed neuron-Schwann (ganglia explants) cell cocultures were needed to study the effects of OP compounds on mitochondria permeability transition in neuron and Schwann cells, respectively. Dissociated and purified neuronal cells derived from 9-day old chick DRG embryos. The neuron-Schwann cell coculture were established by collecting 2-3 ganglion explants per dish. The purified neurons and the neuron-Schwann cell cocultures were grown onto round 35-mm poly-d lysine coated glass bottom (no. 1.5) coverslips (P35 GC-1.5-10-C, Mat Tek

Corporation, Ashland, MA) for 14 days. These cells were treated with PSP, mipafox and paraoxon, 12 hours prior to microscopic evaluation. This end-point was chosen since mitochondrial Ψm alterations have been detected in previous studies, using SH-SY5Y cells exposed to PSP and paraoxon (Carlson et al., 1999). Using an objective heater set at 37°C, the treated living-cell cultures were loaded in culture medium containing 500 nM of tetramethylrhodamine methyl ester (TMRM) for 15 min, followed by TMRM plus 1 μM acetoxymethyl ester of calcein (calcein-AM) for 15 min at 37° C. Strict temperature control within the media during microscopic examination was essential, since the MPT functions can be altered. With this technique, MTP modifications were visualized in these treated cell models, and these changes were compared to controls.

Effects of OP compounds on the mitochondrial transition pore were monitored using an Axiovert 100 M Zeiss LSM 510 laser scanning confocal microscope, following the novel method of Nieminen *et al*. (1995). With the Zeiss software system, the 488 nm and 543 nm lines of argon and helium-neon lasers were directed to the sample by a double-dichroic mirror. Fluorescent light was passed back through a double-dichroic mirror into light greater or less than 575 nm. Green fluorescence of calcein continued through a 515 nm (25 nm band pass) barrier filter to a variable pinhole photodetector. Red fluorescence of TMRM was passed through a 590 nm (long-pass) barrier filter. Pinhole settings of 1 was used for both red and green channels. In this system, a 63X oil objective lens was used, and the laser was attenuated below 1% of its maximum intensity to minimize photobleaching. Confocal images were transferred to a Dell Dimension XPS 400 MHz, Pentium II for processing of the images.

The computerization of confocal images allowed quantification of red (TMRM, or mitochondria), green (calcein-AM, or cytoplasm), and co-localized (red & green) pixels within the neuronal or Schwann cells evaluated. For each confocal image analyzed, pixel

recording, expressed as raw intensity units (RIU) was obtained using a scatter plot representing pixels which occupy a particular location and intensity (x, y) within the cell. The x-axis represented graded intensity of red pixels (0-250 RIU), whereas the y-axis indicated the graded intensity of green pixels (0-250 RIU). The scatter plot is then divided in 4 rectangular quadrants. In the lower left quadrant, the green and red pixels with low intensities were considered background noise (0-35 RIU), and were removed from the calculations using a computer generated mask (blue) (Figure 7a). Hence, the upper left quadrant represents the image with green pixel only (calcein-AM, cytoplasmic staining), and the lower right quadrant illustrates the images with red pixels only (TMRM staining mitochondria). The regions where pixels of both red and green intensity were recorded are plotted in the upper right quadrant. The exact number of pixels can be recorded in each quadrant using a computer generated mask (blue), similar to the one used for calculation of the background (Figure 7b). Colocalization of green and red pixel intensities on a 45° line are considered perfectly colocalized within the scatter graph. Using the upper and lower right quadrant of the scatter graph, the degree of MPT opening can be calculated and the results expressed as the ratio of co-localized pixels/total red pixels. This was done for both neuronal and Schwann cell preparations (Figure 7c). The results were expressed as means ± SEM (1 degree of freedom) from duplicate experiments, with five different cell readings or subsamples. Statistical significance ($p < 0.01$) of mean values of the aforementioned ratios was determined using a simple one way analysis of variance with the PC-SAS software (version 6.1, Cary, NC).

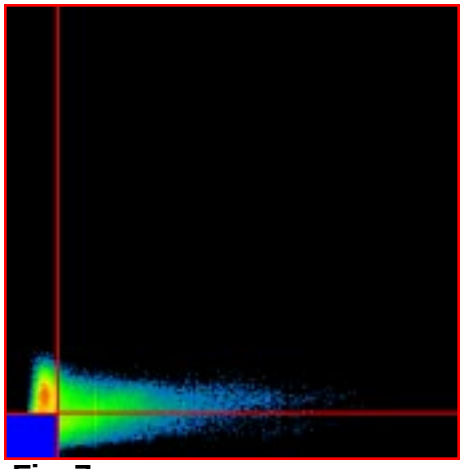

Fig. 7a

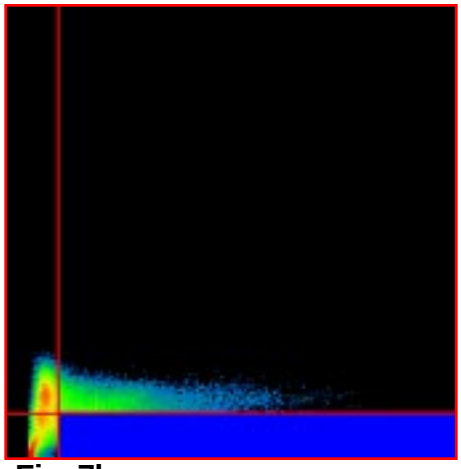

Fig. 7b

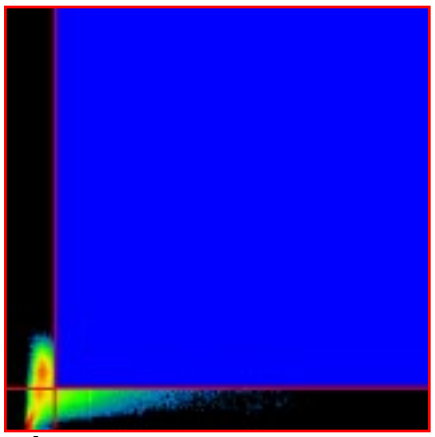

Fig. 7c

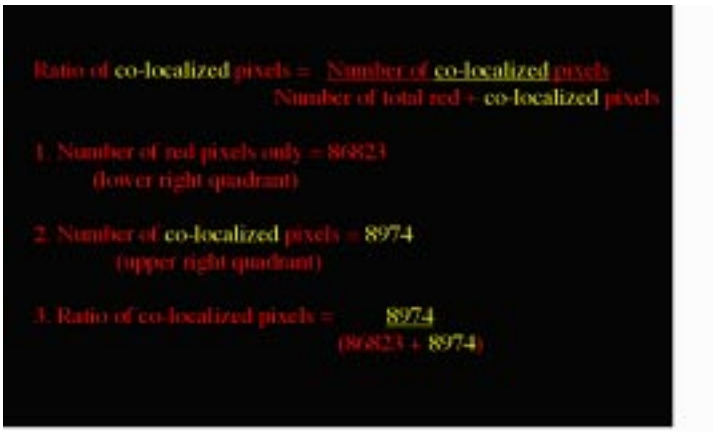

Figure 7. Confocal image of a neuron and its respective scatter graph. (a) In this scatter graph, a mask was placed in the lower left quadrant, representing background noise of green (calcein-AM), and red (TMRM) pixels with low intensities (0-35 RIU). (b). The lower right quadrant was masked (blue), illustrating recording of red (TMRM) pixels only. (c). These scatter graph shows an actual calculation of the MPT using the degree of colocalization expressed as of co-localized pixels (left image) to total red pixels (co-localized pixels/total red pixels, on the right).

2.1.6. Characterization of OP-induced morphological changes in myelinated DRG cell cultures.

Morphological changes were evaluated in neuronal cell cultures exposed to physiological dosages of PSP, mipafox, and paraoxon (1μM), at day 4 and 7 post-exposure (n=2 culture dishes per treatment). These end-points were chosen because they can be compared to lesions already described in the literature for *in vivo* studies of susceptible animal species.

For samples designated for light microscopy evaluation, inverted microscopy was used to visualized the neurons *in situ*. At least 10 micrographs were collected per plate (two plates per treatments). Morphometric data were obtained using inverted microscopy images. Randomized sampling of fibers was used to avoid bias in evaluating the parameters within DRG cell cultures. This can only be done by giving all areas of the specimen (and hence all neuronal cells) the same independent chance of being selected. This method of sampling is the present standard for sampling, and the results are expected to be accurate whether the specimen is homogenous or heterogeneous in terms of size, shape, and spatial distribution of the cell population examined (Mayhew, 1990). The cell culture area chosen were selected by dividing the round bottom dish into four quadrants. Only one of the quadrants, selected prior to cell culture purification, was evaluated for morphological study (light and electron microscopy). Therefore, by sampling randomly, the selection of interesting, typical, or average samples was avoided. Several images (n=10) were recorded using the Oncor Image software system (Gaithersburg, MD). The neurite was outlined on the computer (n=10/image) and analyzed with Adobe Photoshop software (Morphometric Analysis Tool Kit, 3.0). Parameters estimated for the evaluation of axonal integrity 4 and 7 days following OP exposures included the actual radial length, and maximum and mean diameters (Argiro *et al.,* 1985; Castellanos *et al.,* 2000; Doane *et al.,* 1992; Kawa *et al.,* 1998; Nishiyama *et*

al., 1994; Oorschot *et al.,* 1991; Saxod and Bizet, 1988; Unchern *et al.,* 1994; Ventimiglia *et al.,* 1995; Windebank *et al.,* 1985). Based on these values, length to diameter ratios (LD = total neurite length/mean diameter) and neurite swelling (s = [(maximum diameter - mean diameter)/ mean diameter] X 100) were calculated for each neuronal growth cone evaluated. Random sampling was used for estimation of all parameters (Mayhew, 1990).

For transmission electron microscopy evaluation, gluteraldehyde fixed cell cultures were post-fixed for 2 hours in 2% OsO_4 in 0.1 M phosphate buffer at pH 7.4, and washed with 0.1 M phosphate buffer solution. Following post-fixation, the cells were dehydrated in graded concentrations of ethanol (15%, 30%, 50%, 70%, 95%, 100%), and cleared in propylene oxide. The samples were then infiltrated with 50:50 propylene oxide/epoxy resin for 24 hours, followed by 100% epoxy resin for at least 24 hours, and polymerized at 60 degree Celsius oven for 24-48 hours. Then, selected blocks were cut at 80 nm, and placed on new 200 mesh grids (2-3 grids per each block). These thin sections were first stained with 2% uranyl acetate to enhance contrast of nucleic acid-containing structures and subsequent lead citrate staining. The latter staining agent was used to enhance staining of membranes of cellular components. The grids were rinsed with distilled water, dried, and placed in a grid box, with care taken to record grid identity on a grid box form. Using a JEOL JEM-100CX II transmission electron microscope, descriptive evaluation of these treated neuronal cell cultures was performed on thin sections, and was compared to untreated cell cultures for ultrastructural changes. For each treated cell culture dish (n=2), 100-125 electron micrographs were taken, and the morphological changes were determined by two different observers, with one of them being unaware of the treatment administered to the culture dishes. Then, the treated dishes were compared to controls. The electron microscopy findings were compared to neuronal cell culture pathology previously described in the literature. This morphological study provided qualitative information on *in vitro* development of OPIDN in fully differentiated neuronal populations with thin, well

developed axons. Then, the *in vitro* findings were compared to the neuropathological alterations previously observed *in vivo* with these OP compounds.

2.1.7. Data analysis.

2.1.7.1 NTE determination:

Percentage of neurotoxic esterase (NTE) activity for each assay was calculated as the mean ± SEM. Calculations of NTE inhibition were performed on duplicate cultures, and were replicated 3 times. Statistical significance ($p<0.05$) was determined by using a Macintosh Prism Software Program to perform analysis of variance (ANOVA), followed by Tukey's multiple comparison test.

2.1.7.2 ATP determination:

Concentrations of ATP produced were reported as the concentration of ATP (pmol) per neuronal cell, according to standardization with a known concentration of ATP (ATP calibration curve). The results were expressed as mean ± SEM from duplicate experiments, with three different subsamples ($n = 6$). Statistical significance ($p < 0.05$) of mean ATP concentration values was determined using a one way analysis of variance with the PC-SAS software (version 6.1). Data were graphed as the mean ± SEM.

2.1.7.3 Mitochondrial permeability transition:

Mitochondrial membrane pore opening was quantified using the ratio of co-localized pixels to total red pixels (co-localized pixels/total red pixels) for both purified neuronal and Schwann cell preparations. The results were expressed as means ± SEM (1 degree of freedom) from duplicate experiments, with five different cell readings or subsamples. Statistical significance ($p < 0.01$) of mean values of the aforementioned ratios

(co-localized pixels/total red pixels) was determined using a simple one way analysis of variance with the PC-SAS software (version 6.1, Cary, NC).

2.1.7.4 Morphological changes:

Morphometric results were expressed as mean ± SEM from duplicate experiments, with ten different subsamples (n = 50). Statistical significance ($p < 0.05$) of mean values among treatments regardless of day post-challenge were determined using a one way analysis of variance with the PC-SAS software (version 6.1). Then, a least significant difference (LSD) test was performed to compare the means among treatments within each day (4 and 7). The ultrastructural study used descriptive observations on neuronal structures treated with OP compounds compared to negative controls as describe in section 2.1.6.

RESULTS

PART IV: CHAPTER 3

NERVE CONDUCTION AND ATP CONCENTRATIONS IN SCIATIC-TIBIAL AND MEDIAL PLANTAR NERVES OF HENS GIVEN PHENYL SALIGENIN PHOSPHATE.

Christiane Massicotte

David S. Barber

Bernard S. Jortner

Marion Ehrich

Laboratory for Neurotoxicity Studies, Virginia-Maryland Regional College of Veterinary Medicine, Virginia Tech, Blacksburg, Virginia 24061-0442.

This paper contains a total of 1 table and 4 figures.

The estimated number of words is 2,900.

Please send all correspondence to:

Marion Ehrich, Ph.D., R.Ph., DABT.

Laboratory for Neurotoxicity Studies,

Virginia-Maryland Regional College of Veterinary Medicine,

Blacksburg, Virginia 24061-0442.

Phone: 540-231-4621

E-Mail: marion@vt.edu

This article was published in *Neurotoxicology* 22, 91-98, 2001.

3.1 ABSTRACT

To assess the relationship of nerve conduction and ATP status in organophosphorus-induced delayed neuropathy (OPIDN), we evaluated both in adult hen peripheral nerves following exposure to a single 2.5 mg/kg dose of phenylsaligenin phosphate (PSP). ATP concentrations were determined at days 2, 4, 7, and 14 post-dosing, from five segments (n = 5/group) representing the entire length of the sciatic-tibial and medial plantar nerve. Initial effects of PSP dosing were seen in the most distal segment at day 2, when a transient ATP concentration increase (388 ± 79 pmol/ml/mg vs. control value of 215 ± 23, $p < 0.05$) was noted. Subsequently, ATP concentration in this distal segment returned to normal. In the most proximal nerve segment, ATP concentrations were decreased on day 7, and further decreased on day 14 post-dosing ($p<0.05$). Changes in ATP concentration and nerve conduction velocity begin at post-dosing day 2, and were found prior to development of clinical neuropathy and axonopathic lesions. These results suggest that alterations in sciatic-tibial and medial plantar nerve conduction associated with sciatic-tibial and medial plantar nerve ATP concentration are early events in the development of OPIDN.

Key Words: organophosphorus ester-induced delayed neuropathy (OPIDN), hen, compound action potential, adenosine triphosphate (ATP).

3.2 INTRODUCTION

Some organophosphates (OPs) induce delayed neuropathy (OPIDN) after a single exposure in humans and other susceptible species. This neuropathy is characterized by distal, non-terminal, axonal degeneration mainly of long myelinated nerve fibers with

secondary myelin degradation (Bouldin and Cavanagh, 1979a; El-Fawal *et al.,* 1988, 1990; Jortner and Ehrich, 1987). The nerve fiber lesions progress over time (1-2 weeks) in a Wallerian-like degenerative pattern (Bouldin and Cavanagh, 1979a). The progressive morphological changes correlate with the development of neurological signs including weakness, incoordination, ataxia, and, in its most severe form, flaccid paralysis (Massicotte *et al.,* 1999; Randall *et al.,* 1997). The pathogenic mechanisms of OPIDN have not been yet determined.

Among species susceptible to OPIDN, adult domestic female chickens are considered the most reliable model (Abou-Donia, 1981). In this animal model, measurement of neurotoxic esterase (NTE), clinical signs, neuropathology, and electrophysiology have been evaluated in OPIDN. Among these end-points, neurotoxic esterase inhibition has been the earliest event, occurring prior to development of clinical signs or neuropathological changes (Johnson, 1982; Ehrich, 1996).

There are only a few electrophysiological studies of OPIDN, sometimes reporting negative or conflicting results. Needle electromyography was not useful in evaluating OPIDN in the hen (Shell *et al.,* 1988). In an electrophysiological study 21 days after dosing, when clinical signs and morphological lesions are fully developed, widening of the axonal potential complexes in the tibial nerve and faster conduction velocities in the sciatic nerve of hens treated with tri-2-cresyl phosphate were noted (Robertson *et al.,* 1987). However, in another study by the same group, conduction velocities of the sciatic and tibial nerves were unaffected following administration of di-n-butyl-2, 2-dichlorovinyl phosphate (DBCV), a compound known to produce OPIDN (Robertson *et al,* 1988), leading these investigators to conclude that conduction velocities and amplitude in compound action potential evaluation were not predictive of developing OPIDN. However, electrophysiological changes such as increased refractoriness and strength-duration

thresholds were reflective of OPIDN, as these were found to be most marked between 14 and 21 days after OP challenge, when hens already exhibited clinical signs of toxicity (Anderson *et al*., 1987; Robertson *et al.,* 1987; Robertson *et al.,* 1988). Robertson *et al.* (1988) also showed increased refractoriness and threshold excitability of hen sciatic nerves as early as 24 hours post-dosing, suggesting that these electrophysiological deficits also may precede clinical signs of OPIDN. There are no previous studies examining the relationship between electrophysiological changes and energy production in peripheral nerves.

Adenosine triphosphate (ATP) provides continual cellular input of free energy necessary for most energy requiring processes. In the nervous system, ATP plays a central role in energy exchanges for numerous biological reactions including muscle contraction, synaptic transmission, active transport of molecules and ions across the neuronal membrane and synthesis of biomolecules from simple precursors (Linden, 1998). In addition, ATP has been proposed to fulfill an important part of the metabolic and energetic demands required in all phases of axonal transport (Goodrum and Morell, 1992).

This study assessed the relationship between compound action potentials (conduction velocities and amplitudes) in peripheral nerves and ATP concentrations at specific time points following exposure to cyclic phenylsaligenin phosphate (PSP), using five different segments of hen sciatic-tibial and medial plantar nerves. Clinical signs and morphological changes were also monitored. This work provides information on early events in the development of OPIDN, which may contribute to clinical signs and lesions that develop in later stages of this neuropathy.

3.2. METHODS

To induce OPIDN, a single 2.5 mg/kg im dose of the delayed neurotoxicant phenylsaligenin phosphate (PSP, synthesized by Lark Enterprises, Webster MA) was administered im to adult hens (n = 18) (Jortner and Ehrich, 1987). The hens (4-5 per group) received a volume of 0.5 ml/kg of 5 mg/ml (2.5 mg/kg) of PSP dissolved in dimethylsulfoxide (DMSO). The control group received a similar volume of the DMSO vehicle im (n = 5).

During the course of the experiment, each chicken was clinically examined at days 2, 4, 7, and 14 post-dosing to detect the progression of neurologic deficits. The latter were graded according to an 8 point scale previously described by Cavanagh and Davies, 1961 (0=normal; 8=complete paralysis).

Electrophysiological data of the sciatic-tibial and medial plantar nerve were obtained with a Nicolet Viking II/IIe electrodiagnostic unit (V2.4, Wisconsin, Madison, 1993). For this analysis, the hens underwent general anesthesia with isoflurane (2-4%). The hen was placed in lateral recumbency in order to extend and immobilize the right limb. For the study of motor compound action potentials of the sciatic-tibial and medial plantar nerve, the recording electrode was placed between the first digit and the footpad, and the reference electrode was inserted in the distal aspect of the third digit. Stimulating electrodes were located along the sciatic-tibial and medial plantar nerve length, at the level of the ischial notch and the hock, therefore recording the compound action potential between these aforementioned points. Each site was stimulated with a 0.1 ms duration, 1.0 Hz, supramaximal intensity voltage. Temperature was monitored in all cases, and considered in the calculations of each of the neuroelectrodiagnostic parameters. For all

electrophysiological measurements the ground electrode was placed between the hock and the digits. Control hens were assessed at each electrophysiological sampling (n=2-3), and no differences noted. Therefore, the control data were pooled over all times of testing.

ATP concentrations were determined by high-performance liquid chromatography in homogenates of chicken sciatic-tibial and medial plantar nerve (Levitt *et al.,* 1984; Sedaa *et al.,* 1990; Sickles DW *et al.,* 1990). The nerve was dissected under general anesthesia. The skin was incised and blunt dissection of the underlying muscles was performed to expose the nerve trunk. The sciatic nerve was located, and followed distally until the tibial nerve was reached. The dissection was continued distally to include the plantaris medialis nerve branch, and the nerve was sectioned at the level of the hock. The nerve was further divided in five different segments of approximately 1 cm in length, from the most distal segment (A: distal medial plantar nerve branch) to the most proximal segment (E: sciatic nerve). The distal end of segment C was identified as the point where the plantar nerve is dividing into the medial plantar and the lateral plantar nerve branches. The nerve segments to be analyzed for ATP content were immediately frozen with liquid nitrogen and homogenized in ice-cold 0.4M perchloric acid containing 1.3 mM EDTA and 5.3 mM sodium metabisulfite. The homogenized nerve samples were centrifuged, and 500 µL of supernatant was transferred to a new tube and adjusted to pH = 5 with 1M potassium hydroxide (KOH). Derivatization of ATP was performed by adding 50 µL of chloracetaldehyde (1M) to each sample and incubating at 60°C for 40 minutes. When derivatization was completed, the samples were placed on ice for 10 minutes. Samples for ATP analysis were then separated by HPLC using a C18 column (250 mm X 4.6, 5µ, Phenomenex – LUNA, Torrence, CA) and fluorescence detection using 300nm excitation and 420nm emission. Mobile phase was a binary gradient. Buffer A was 0.05M phosphate buffer (pH = 6.0). Buffer B was 25% methanol and 75% buffer B. Gradient

was as follows: 0 min 95% A; 1 min 95% A; 11 min 100% B; 16 min 100% B; 21 min 95% A; 23 min 95% A. The flow rate was 1.0 ml/min. The ATP concentrations were expressed in pmol/mg wet weight nerve sample.

In order to monitor the neuropathologic changes over time, sciatic-tibial and medial plantar nerve sections were collected for light microscopy, using immersion fixation at day 2, 4, 7, and 14 post-dosing (n = 4-5). The nerve was divided in five different segments of approximately 1 cm in length, from distal (A) to proximal (E), corresponding to those taken for ATP assay. The nerve segments were then placed in a fresh 4 % paraformaldehyde solution, post-fixed in 2 % OsO_4 in 0.1 M phosphate buffer, embedded in Polybed® epoxy resin, sectioned at 1 μm thickness and stained with a combination of toluidine blue and safranin for light microscopy.

Analysis of numerical data for clinical signs, nerve conduction velocities and ATP concentrations was done using the analysis of variance (ANOVA), followed by Tukey's multiple comparison test. Significance of the relationships between clinical signs and ATP concentrations was determined by Spearman linear regression. Group data are expressed as mean ± standard error.

3.4. RESULTS

Mild transient cholinergic signs including hypersalivation, miosis and depression were observed up to 2 days post-dosing and not thereafter. Mild clinical signs of OPIDN, mainly consisting of weakness, were initially noted 4 days after PSP dosing (mean clinical score = 2.8 ± 0.6), and persisted at this level until day 7 (2.0 ± 0.1). There was clinical progression after day 7, and signs were severe on day 14 (mean clinical score = 6.6 ± 0.2).

Electrophysiological changes could be observed as early as day 2 post-dosing. Sciatic-tibial and medial plantar nerve conduction velocities were significantly decreased 2 days after the PSP dosage (treated = 57 ± 3 m/sec [n = 5], control = 76 ± 3 m/sec [n = 5], $p < 0.01$). Although the nerve conduction velocities remained significantly lower than the control values ($p < 0.01$) until the end of the study at day 14 post-dosing (Table 1), they did not continue to decrease as clinical signs increased. Although they were different from control, time from PSP administration did not make a difference in nerve conduction velocity (day 4 = 57 ± 4 m/sec; day 7 = 58 ± 5 m/sec; day 14 = 54 ± 4 m/sec) (Table 1). The mean amplitude of the action potentials, although considerably decreased, and the duration of the compound action potentials in treated animals were not always different from control values ($p > 0.05$).

Initial effects of PSP dosing were seen in the most distal segment (level A) of sciatic-tibial and medial plantar nerve at day 2, when a transient ATP concentration increase (388 ± 79 pmol ATP/mg wet wt. of tissue vs. control value of 215 ± 23, $p < 0.05$) was noted. In other more proximal nerve segments (levels B-E), ATP concentrations were significantly lower than control values on day 14 post-dosing ($p<0.05$) (Fig. 1).

Comparison between sciatic-tibial and medial plantar ATP concentration and nerve conduction velocities is presented in Figure 2. In addition, there was a linear relationship between the clinical signs and mean ATP concentration from all nerve segments (Fig. 3), in that the ATP concentration decreased when the clinical scores increased.

Cross-sections of nerve from level C had no neuropathic lesions at day 2 (Fig. 4a) and only occasional degenerating myelinated axons on day 14 (Fig. 4b). The sections from level A (Fig. 4c and 4d) also showed no morphological abnormalities on day 2 (Fig. 4c), but extensive myelinated fiber degeneration was present on day 14 (Fig. 4d).

3.5. DISCUSSION

In the present study, as demonstrated previously, the clinical signs of OPIDN observed after 2.5 mg/kg PSP administration progressed with time, and were severe at day 14 post-dosing (Jortner and Ehrich, 1987; El-Fawal *et al.,* 1988; McCain *et al.,* 1995; Massicotte *et al.,* 1999). Although PSP can inhibit acetylcholinesterase activity (up to 67% after 10 mg/kg PSP, Jortner and Ehrich, 1987), PSP has not previously been associated with cholinergic signs, but a mild, transient effect was seen in the present study.

This study is unique in that it reports significant reduction in sciatic-tibial and medial plantar nerve conduction velocities at very early stages of OPIDN, which persisted until the end of the experiment at day 14 post-dosing. Even though the nerve conduction velocity values could not be used to evaluate the progression of OPIDN, our results suggest this non-invasive technique can be helpful to detect OPIDN early in the course of the disorder. Decreased nerve conduction velocity may reflect a reduction in the axonal caliber or an indication of demyelination. Reduction in the amplitude of the compound action potential may represent axonal degeneration of the peripheral nerve fibers. These findings were consistent with previously reported elevation of excitability threshold noted

using *in vivo* preparations from PSP-treated hens 4-5 days after PSP administration (El-Fawal *et al.*, 1990).

These electrophysiological results differ from previous studies, in which nerve conduction velocities were largely unaffected by administration of OP compounds (Robertson *et al.*, 1988; 1987). The distinct electrophysiological findings noted in the present study could have been the result of a non-invasive technique, avoiding trauma to the nerve and blood supply occasionally caused by dissection. In addition, all hens were uniformly anesthetized, resulting in better muscle relaxation. This also prevented voluntary motor function, muscle contraction and complex repetitive discharges, which can appear as artifacts. The electrophysiological diagnostic unit used during this present evaluation was highly sensitive, allowing excellent detection and precise calculation of electrical events.

The present study is the first time that ATP concentrations have been measured in peripheral nerves of hens treated with neuropathy-inducing OP compounds. The nerves were carefully dissected, but it is to be recognized that nerves contain non-neuronal as well as neuronal cells and that only a small proportion of neuronal fibers are affected in OPIDN (Jortner and Ehrich, 1987). Even so, statistical linear relationship between clinical signs and ATP concentrations in specific segments of hen sciatic-tibial and medial plantar nerves affected with OPIDN was found ($r^2 = 0.97$, $p = 0.01$), with ATP concentrations most reduced 14 days after PSP exposure, when the neuropathy was most fully developed. Because the effect on ATP occurs in the proximal segments of the nerve while degeneration occurs in the most distal segments of the nerve, loss of ATP in the proximal portions of the nerve may adversely affect processes required for maintenance of the distal portion of the axon. The finding that ATP levels were not affected in distal nerve regions during active axonal degeneration probably reflects the mixed cell population evaluated (axon and Schwann cells), and multiple events that impact ATP content (compensatory Schwann cell

changes). Progressive deficit of retrograde transport could provide an explanation for the decreased ATP concentration in proximal peripheral nerve segments and the lack of decrease in most distal nerve segments (Moretto *et al.,* 1987; Goodrum and Morell, 1992). The transient elevation in ATP concentration could be also due to an increase in free energy requirements within the distal segment of sciatic-tibial and medial plantar nerve in early stages of OPIDN, which responded by creating a more active metabolic state.

Because the hydrolysis of ATP is coupled to several energetically unfavorable reactions, it is possible that ATP concentration alterations are a relevant event in the pathogenesis of OPIDN mechanisms. Direct axonal injury due to reduction of ATP in nerve may be due to events such as the formation of reactive phosphorylated intermediates, or alterations of ion transport/gradients (Na^+-K^+ ATPase, and Ca^{2+} ATPase pumps). The latter are responsible for maintenance of the electrochemical ionic gradients across the axonoplasmic membranes (Augustine *et al.,* 1990; Tanford, 1983). In addition, ATP has been proposed to have an important part of the metabolic and energetic demands required in all phases of axonal transport, as noted in studies with other neurotoxicants (Goodrum and Morell, 1992; Griffin and Watson, 1988; Moretto *et al*., 1988; Sabri *et al*., 1979a,b). It is possible that these alterations in axonal transport could be secondary to local changes in ATP concentrations, as suggested in an earlier study of OPIDN (Moretto *et al.,* 1987).

Electrophysiological studies and ATP determinations in peripheral nerve in this study revealed changes prior to the occurrence of both clinical signs and neuropathological alterations of OPIDN (Jortner and Ehrich, 1987, El-Fawal *et al.,* 1990). These early events may be interrelated as variations in sciatic-tibial and medial plantar nerve ATP concentration could contribute to disturbances in axonal transport, and the maintenance of the electronic gradient responsible for membrane conduction and permeability. These may have been reflected in the electrophysiological changes noted in this study. Further work needs to be

conducted to better understand the relationship of these types of early events that occur in OPIDN, especially using simple systems that contain only neuronal cells.

3.6. ACKNOWLEDGEMENTS

The authors gratefully acknowledge the technical assistance of Linda Correll, Kristel Fuhrman, Jason Hunt, Kristy Karas, and Jonathan Hinckley, without whom this work could not have been performed. Virginia-Maryland Regional College of Veterinary Medicine has primarily supported this work.

3.7. REFERENCES

Abou-Donia MB. Organophosphorus ester-induced delayed neurotoxicity. *Ann Rev Pharmacol Toxicol* 1981; 21: 511-548.

Anderson RJ, Robertson DG, Henderson JD, Wilson BW. DFP-induced elevation of strength-duration threshold in hen peripheral nerve. *Neurotoxicology* 1988; 9: 47-52.

Augustine CK, Bezanilla F. Phosphorylation modulates potassium conductance and gating current of perfused giant axons of squid. *J Gen Physiol* 95; 1990: 245-271.

Bouldin TW, Cavanagh JB. Organophosphorous neuropathy. 1. Teased fiber studies. *Am J Path* 1979a; 94: 241-247.

Cavanagh JB, Davies DR, Holland P, Landcaster M. Comparison of the functional effects of dyflos, tri-ortho-cresyl phosphate and tri-p-ethyl-phenyl phosphate in chickens. *Br J Pharmacol* 1961; 17: 21-27.

El-Fawal HAN, Jortner BS, Eyre P, Ehrich M. The biventer cervicis nerve-muscle preparation of adult hens: effect of phenyl saligenin phosphate administration. *Neurotoxicology* 1988; 9: 625-636.

El-Fawal HAN, Jortner BS, Ehrich M. Use of the biventer cervicis nerve-muscle preparation to detect early changes following exposure to organophosphates inducing delayed neuropathy. *Fund Appl Tox* 1990; 15: 108-120.

EL-Fawal HAN, Jortner BS, Ehrich M. Modification of phenyl saligenin phosphate-induced delayed effects by calcium channel blockers: *in vivo* and *in vitro* electrophysiological assassment. *Neurotoxicology* 1990; 11: 573-592.

Ehrich M. Neurotoxic esterase inhibition: predictor of potential for organophosphorus-induced delayed neuropathy. In*: Biomarkers for agrochemicals and toxic substances*, Blancato JN, Brown RN, Dary CC, Saleh MA, eds., Washington, DC: American Chemical Society, 1996; pp 79-93.

Goodrum JF, Morell P. Axonal transport. In: *Neurotoxicology*, Abou-donia MB, ed. CRC Press, 1992, pp 79-119.

Griffin JW, Watson DF. Axonal transport in neurological disease. *Ann Neurol* 23; 1988: 3-13.

Johnson, MK. The target for initiation of delayed neurotoxicity by organophosphorus esters. *Rev Biochem Toxicol* 1982; 8: 141-212.

Jortner BS, Ehrich M. Neuropathological effects of phenyl saligen phosphate in chickens. *Neurotoxicology* 1987; 8: 97-108.

Linden JM. Purinergic systems. In: *Basic neurochemistry*, Siegle GJ, Agranoff BW, Albers RW, Fisher SK, Uhler MD., 6th ed., Philadelphia, Lippincott-Raven Publishers, 1998, pp 347- 352.

Levitt B, Head RJ, Westfall DP. High-pressure liquid chromatographic fluorometric detection of adenosine and adenine nucleotides: application to endogenous content and electrically induced released of adenyl purines in guinea pig vas deferens. *Anal Biochem* 1984; 137: 93-100.

Massicotte C, Inzana KD, Ehrich M, Jortner BS. Neuropathologic effects of phenylmethylsulfonyl fluoride (PMSF)-induced promotion and protection in organophosphorus ester-induced delayed neuropathy (OPIDN) in hens. *Neurotoxicology* 1999; 20: 749-760.

McCain WC, Wilcke J, Ehrich M. Effect of cyclic phenyl saligenin phosphate and paraoxon treatment on vascular response to adrenergic and cholinergic agents in hens. *J Toxicol Environ Health* 1995; 44: 167-187.

Moretto A, Sabri MI. Progressive deficits in retrograde axon transport precede degeneration of motor neuron in acrylamide neuropathy. *Brain Res* 1988; 440; 18-24.

Moretto A, Lotti M, Sabri M, Spencer PS. Progressive deficit of retrograde axonal transport is associated with the pathogenesis of di-n-butyl dichlorvos axonopathy. *J Neurochem* 1987; 49: 1515-1522.

Randall JC, Yano BL, Richardson RJ. Potentiation of organophosphorus compound-induced delayed neurotoxicity (OPIDN) in the central and peripheral nervous system of the adult hen: distribution of axonal lesions. *J Toxicol Environ Health* 1997; 51: 571-590.

Robertson DG, Schwab BW, Sills RD, Richardson RJ, Anderson RJ. Electrophysiology changes following treatment with organophosphorus-induced delayed neuropathy-producing agents in the adult hen. *Toxicol Appl Pharmacol* 1987; 87: 420-429.

Robertson DG, Mattson AM, Bestervelt LL, Richardson RJ, Anderson RJ. Time course of electrophysiologic effects induced by di-*n*-butyl-2,2-dichlorovinyl phosphate (DBCV) in the adult hen. *Toxicol Env Health* 1988; 23: 283-294.

Sabri MI, Ederle K, Holdsworth CE, Spencer PS. Studies on the biochemical basis of distal axonopathies. II. Specific inhibition of fructose-6-phosphate kinase by 2, 5-hexanedione and methyl-butyl ketone. *Neurotoxicology* 1979a; 1: 1-11.

Sabri MI, Moore CL, Spencer PS. Studies on the biochemical basis of distal axonopathies. I. Inhibition of glycolysis by neurotoxic hexacarbone compounds. *J Neurochem* 1979b; 32: 683-689.

Sedaa KO, Bjur RA, Shinozuka K, Westfall DP. Nerve and drug-induces release of adenine nucleosides and nucleotides from rabbit aorta. *J Pharmacol Exp Ther* 1990; 252: 1060-1067.

Sickles DW, Fowler SR, Testino AR. Effects of neurofilamentous axonopathy-producing neurotoxicants upon production of ATP by brain mitochondria. *Brain Res* 1990; 528: 25-31.

Shell L, Jortner BS, Ehrich M. Assessment of organophosphorus-induced delayed neuropathy in chickens using needle electromyography. *Toxicol Env Health* 1988; 24: 21-33.

Tanford C. Mechanism of free energy coupling in active transport. Ann Rev Biochem 52; 1983: 379-409.

TABLE 1

Compound Action Potential Parameters [1] (CAP) for the Sciatic-Tibial and Medial Plantar Nerve of Hens Treated with PSP 2.5 mg/kg.

Groups	NCV (m/sec)	Amplitude (mV)	Duration (msec)
Controls	76 ± 3	2.6 ± 0.7	2.0 ± 0.2
Day 2	57 ± 2 *	1.0 ± 0.4 *	2.5 ± 0.4
Day 4	57 ± 4 *	1.6 ± 0.5	2.1 ± 0.3
Day 7	58 ± 5 *	0.8 ± 0.4 *	1.9 ± 0.3
Day 14	54 ± 4 *	1.3 ± 0.7	2.7 ± 0.3 *

[1] CAP values are expressed as mean ± SE (n = 5). Statistical significance is represented by asterix

[2] Values from PSP-treated hens were significantly different from controls at all times tested.

FIGURE LEGENDS

FIG.1. Mean ATP concentrations at specific sciatic-tibial and medial plantar nerve levels (A-distal; E-proximal) obtained 2, 4, 7, and 14 days after exposure to 2.5 mg/kg of PSP. Initial effects of PSP dosing was seen in the most distal segment of sciatic-tibial and medial plantar nerve at day 2, when a transient ATP concentration increase (388 ± 79 pmol/ml/mg vs. control value of 215 ± 23, $p < 0.05$) was noted. Subsequently, ATP concentration in this distal segment returned to normal. In the most proximal nerve segment, ATP concentrations were decreased, and were significantly lower than control values on day 7 and day 14 post-dosing ($p<0.05$). Significance is indicated by the asterix.

FIG.2. Sciatic-tibial and medial plantar ATP concentration compared with nerve conduction velocities of OPIDN in hens (n=4-5) after exposure to PSP (2.5 mg.kg). ATP concentrations, indicated on the y axis, tended to decrease as the nerve conduction velocities declined. The slowest nerve conduction velocities (54 ± 4) were observed at day 14 post-dosing, when the ATP concentrations were at its lowest point of the study. Individual data points were used for determination of the relationship; group data (mean ± standard error) are graphed.

FIG.3. Relationship between the mean sciatic-tibial and medial plantar nerve ATP concentrations and the clinical signs in hens treated with 2.5 mg/kg of PSP. This graph represents the last clinical scores (x) obtained prior to euthanasia, and the individual mean ATP concentrations of all nerve segments (y=A-E) determined in the sciatic-tibial and medial plantar nerve (n = 8-10) (mean ± SEM). There is a significant linear relationship, determined by simple linear regression, between the last clinical scores and the mean ATP concentrations, described by the line $y = 280 – 15.7x$ ($r^2 = 0.97$, $p=0.05$).

FIG.4. Cross-sections of the sciatic-tibial and medial plantar nerve from hens dosed with 2.5 mg/kg PSP at 2 and 14 days post-dosing. The nerve sections from level C (a) and A (c) obtained 2 days after dosing had no morphological changes. At day 14 post-dosing, level C demonstrates mild lesions of OPIDN mainly consisting of occasional axonal swelling (thin arrow, b), and profiles of myelin ovoids (thick arrow, b). In contrast, lesions in the distal nerve segment (level A) were extensive on day 14, including degenerating axons (curved arrows, d), myelin collapse (thin arrow, d), and severe myelinated fiber degeneration (thick arrow, d). Endoneurial edema is also present. Toluidine blue and safranin stains, bar = 10 µm.

Mean ATP measurements at specific sciatic levels

(Days 2-4-7-14 post-dosing)

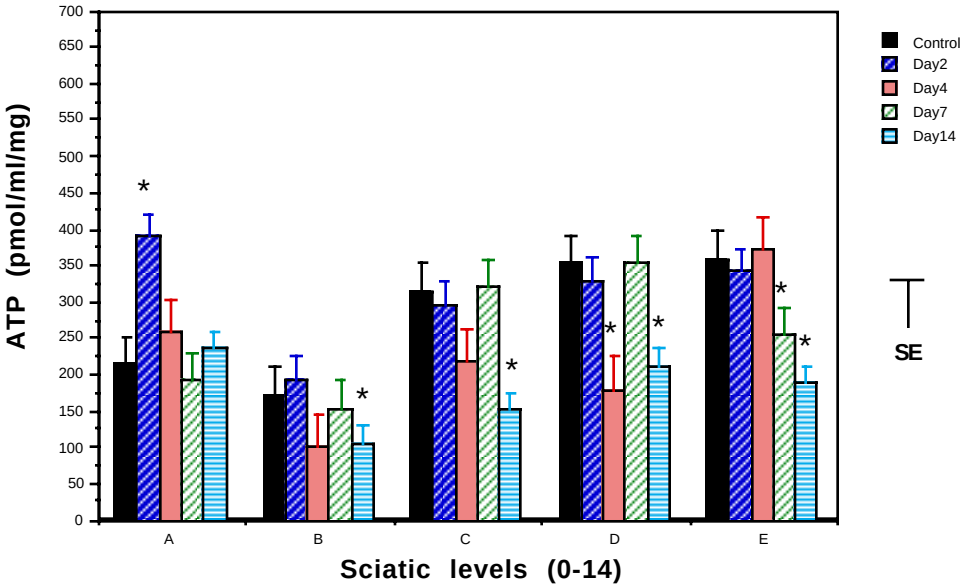

Mean ATP Concentration vs Nerve Conduction Velocity in OPIDN

(Sciatic nerve – PSP 2.5)

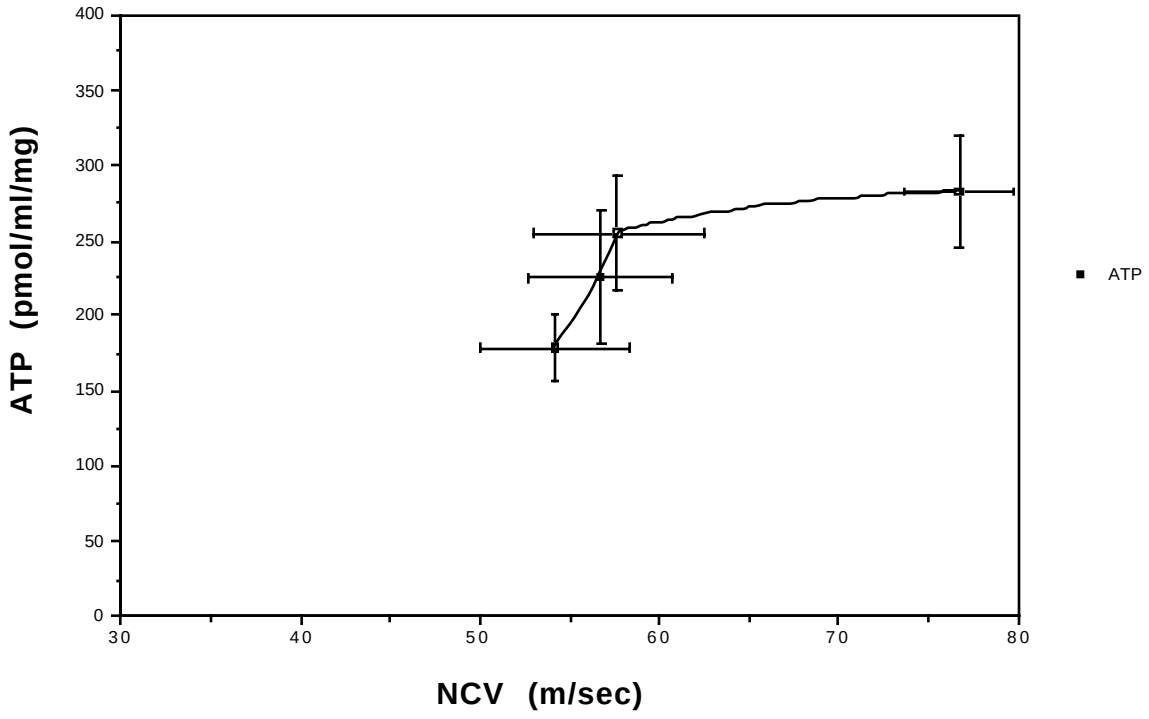

Mean ATP Variations vs Clinical Signs in OPIDN

(Sciatic-Tibial and Medial Plantar Nerve - PSP 2.5)

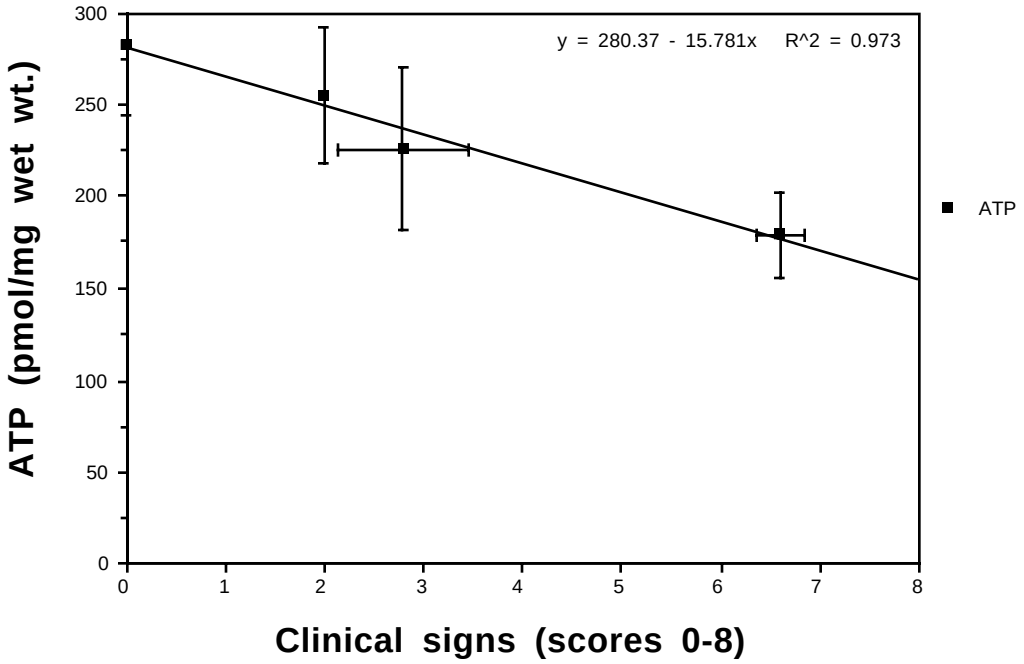

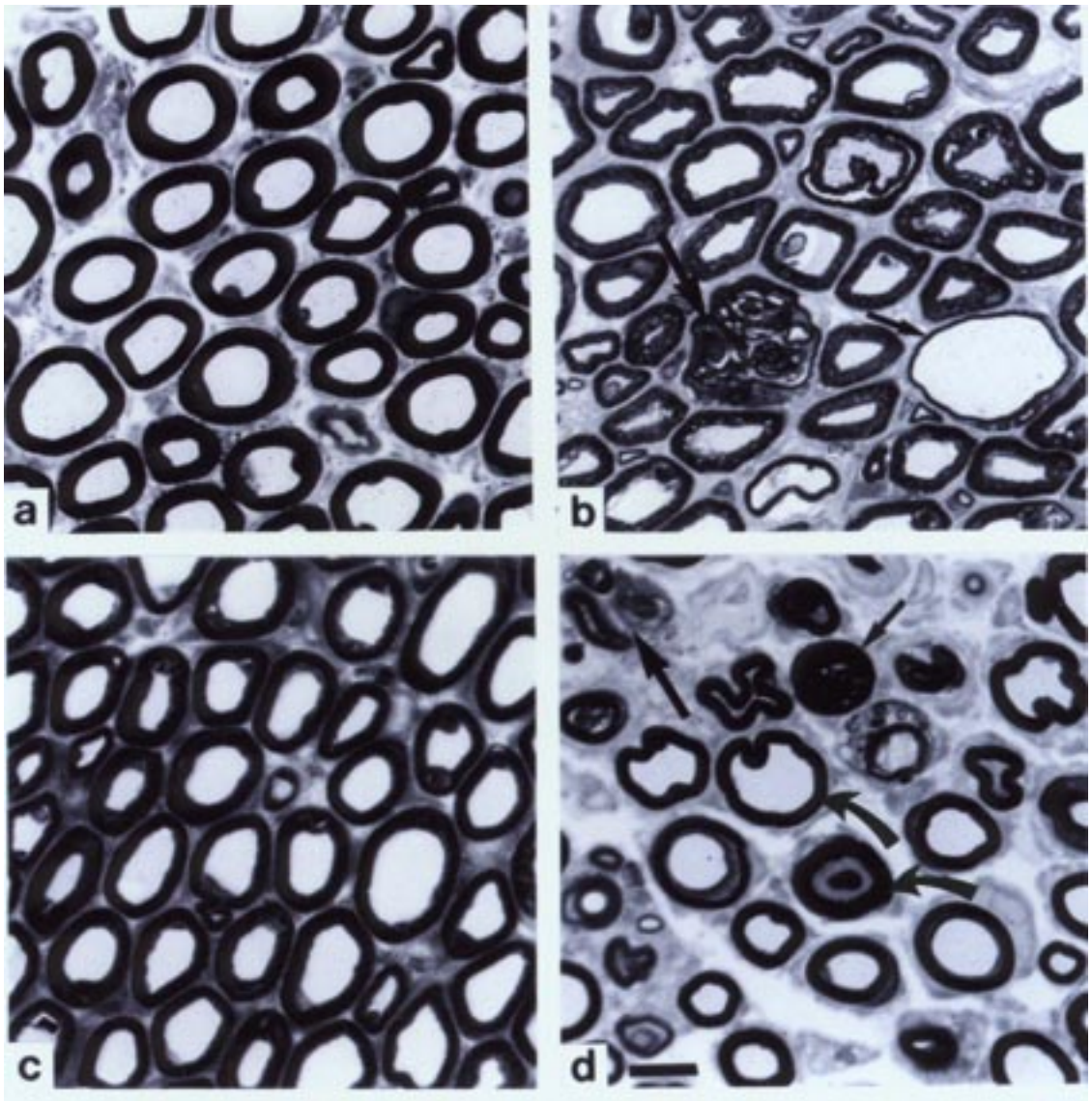

FIG. 4

RESULTS

PART IV: CHAPTER 4

Effects of Neuropathy-Inducing Organophosphorus Compounds on Mitochondrial Permeability Transition in Primary Dorsal Root Ganglia Cell Cultures.

Authors:

Christiane Massicotte

Bernard S. Jortner

Marion Ehrich

Virginia-Maryland Regional College of Veterinary Medicine

Laboratory for Neurotoxicity Studies, VA-MA Regional College of Veterinary Medicine,

1 Duckpond Drive

Blacksburg, VA 24061-0442.

Running title:

Mitochondrial permeability transition in OP-exposed DRG

4.1. ABSTRACT

Cultures of dorsal root ganglia (DRG) can achieve neuronal maturation with axons and synapses, making them useful for neurobiological studies. They have not, however, previously been used to investigate subcellular events that occur following exposure to neuropathy-inducing organophosphorus (OP) esters. Recent studies in other *in vitro* systems demonstrated alterations of ATP concentrations and changes in mitochondrial transmembrane potential ($\Delta\Psi m$) following exposure to neuropathy-inducing OP compounds, suggesting that mitochondrial dysfunction occurs. We report an investigation using chick embryo DRG cultures to explore early mechanisms associated with exposure to these toxicants. This approach uses an *in vitro* neuronal system from the species that provides the animal model for OP-induced delayed neuropathy (OPIDN). DRG were obtained from 9-10 day old chick embryos, and grown for 14 days in minimal essential media (MEM) supplemented with bovine and human placental sera and growth factors. Cultures were then treated with 1 μM OP compounds, or the DMSO vehicle control. OP compounds used were phenylsaligenin phosphate (PSP) and mipafox, which readily elicit OPIDN in hens, and paraoxon, which does not cause OPIDN. Confocal microscopic evaluation of neuronal populations treated with PSP and mipafox showed opening of mitochondrial permeability transition (MPT) pores, and significantly lower mitochondrial tetramethylrhodamine fluorescence, suggesting alteration of mitochondrial structure and function. This supports the conclusion that mitochondria are a primary target for neuropathy-inducing OP compounds by inducing mitochondrial permeability transition. This study also provides evidence that chick DRG cell cultures are an excellent model to study early structural and functional features of OPIDN.

Key words: organophosphorus; mitochondria; permeability transition; dorsal root ganglia.

4.2. INTRODUCTION

Some organophosphate (OP) compounds induce delayed neuropathy (OPIDN) after a single exposure in humans and other susceptible species. This neuropathy is characterized by distal, non-terminal, axonal degeneration mainly of long myelinated nerve fibers with secondary myelin degradation (Bouldin and Cavanagh, 1979; El-Fawal *et al.*, 1988, 1990; Jortner and Ehrich, 1987). The nerve fiber lesions progress over time (1-2 weeks) in a Wallerian-like degenerative pattern (Bouldin and Cavanagh, 1979). The progressive morphological changes correlate with the development of neurological signs that include weakness, incoordination, ataxia, and, in its most severe form, flaccid paralysis (Massicotte *et al.*, 1999; Randall *et al.*, 1997; Ehrich and Jortner, 2001). The pathogenic mechanisms of organophosphorus-induced delayed neuropathy (OPIDN) have not yet been determined.

Although many animal species are susceptible to OPIDN, adult hens (chickens) are considered the most reliable model for evaluation of neurotoxic esterase (NTE), clinical signs, neuropathology, and electrophysiology (Abou-Donia, 1981). Among these end-points, NTE inhibition is the earliest event, occurring prior to development of clinical signs or neuropathological changes (Johnson, 1982; Ehrich, 1996; Ehrich and Jortner 2001).

Neuroblastoma and other immortal cell lines have been used to assess the potential for OP neurotoxicity (Mochida *et al.*, 1988; Veronesi and Ehrich, 1993a, Ehrich *et al.*, 1994, 1997; Greenman *et al.*, 1997, Carlson and Ehrich, 1999; Barber *et al.*, 1999a, b; Carlson *et al.*, 2000). General morphological (Harvey and Sharma, 1980; Tuler and Bowen, 1989, Knoth-Anderson *et al.*, 1992), nuclear (Carlson *et al.*, 2000; Cai *et al.*, 1998; Mentzschel *et al.*, 1993; Nostrandt *et al.*, 1992), enzymatic (Ehrich *et al.*, 1994, 1997; Barber *et al.*, 1999a), cytoskeletal (Tuler and Bowen, 1989), plasma membrane (Antunes-Madeira *et al.*, 1994), and mitochondrial transmembrane potential (Carlson and Ehrich,

1999) modifications have been demonstrated. Involvement of apoptotic processes have been implicated in OP-induced cell death (Akbarsha and Sivasamy, 1998; Hamm *et al.*, 1998; Carlson *et al.*, 2000). *In vitro* alterations of metabolic processes and energy production have also been evaluated, and results showed inhibition of glucose metabolism (Harvey and Sharma, 1980), and decreased incorporation rate of [^{3}H] adenosine into ATP (Knoth-Anderson *et al.*, 1992). The effects of OP compound exposure on primary neuronal cell cultures have, however, not been studied, and little information is available in the literature at the present time (Mochida *et al.*, 1988; Marinovich *et al.*, 1996). Primary cultures are more representative of in vivo cell populations but they are difficult to obtain and maintain (Kleitman *et al.*, 1995; Varon *et al.*, 1981; Wood, 1976).

Mitochondria play an essential role in necrotic and apoptotic neuronal death by regulation of cellular energy and release of proapoptotic factors in the cytosol. In previous studies, OP compounds induced significant changes in mitochondrial transmembrane potentials ($\Delta\Psi m$) in a human neuroblastoma cell line (SH-SY5Y) (Carlson and Ehrich, 1999). Initially, OP-exposure of SH-SY5Y cell cultures induced mitochondrial hyperpolarization in concentration-dependent manner, followed by gradual depolarization shortly thereafter. These changes in $\Delta\Psi m$ were followed by DNA fragmentation, suggesting that mitochondria are a primary target in OP-induced cytotoxicity (Carlson and Ehrich, 1999; Carlson *et al.*, 2000). Studies in the hen model of OPIDN demonstrated changes in sciatic nerve ATP concentrations, also suggesting dysregulation of mitochondrial-associated cellular energy production (Massicotte *et al.*, 2001).

Rapid spontaneous fluctuations in $\Delta\Psi m$ have been associated with opening of a high-conductance channel of the mitochondrial inner membrane (Hunter and Haworth, 1979). The hypothesized structural model of the mitochondrial permeability transition (MPT) pore suggest that its core is a protein complex which includes the voltage-dependent

anion channel of the outer membrane and the adenine translocase (ANT) of the inner membrane (Halestrup and Davidson, 1990). It is generally expected that the protein complex spans the inner and outer membrane (Hackenbrock, 1968; Lemasters, 1998). Other proteins from the matrix and outer membrane are proposed to be associated with ANT in the pore complex. Among these proteins, cyclophillin D (a cyclosporin A-binding protein in the matrix) can be found in the matrix, while creatine kinase, porin, and hexokinase are present in the outer compartment of the mitochondrial membrane (Zoratti and Szabo I, 1995; Halestrap and Davidson, 1990; Beutner *et al.,* 1996; Lemasters, 1998; Hüser and Blatter, 1999). MTP opening results in mitochondrial membrane depolarization (Zoratti and Szabo, 1995; Bernadi, 1996: Niemienen *et al.,* 1995), uncoupling of oxidative phosphorylation (Zoratti and Szabo, 1995; Cassarino *et al.,* 1998), and release of intramitochondrial solutes with severe osmotic mitochondrial swelling (Lemasters, 1998). In addition, prolonged mitochondrial permeability transition causes passive cytochrome c release secondary to mitochondrial depolarization and significant matrix swelling (Poppe *et al.,* 2001 Petit *et al.,* 1997; Lemasters *et al.,* 1998; Cai *et al.,* 1998).

New techniques have been developed to study the physiological role and function of MPT, and its change in permeability following exposure to toxic compounds (Niemienen *et al.,* 1995, Lemasters *et al.,* 1993, 1998). Visualization of the MPT in living cells can be achieved by using laser scanning confocal microscopy (Niemienen *et al.,* 1995, Lemasters *et al.,* 1993, 1998; Lemasters, 1999; Qian *et al.,* 1999). This technique can create submicron thin optical slices through living cells, allowing unprecedented resolution of subcellular structures such as mitochondria, within living cell systems. This new method has been used to monitor MPT *in situ* within hepatocytes and brain tissue following exposure to toxicants, ionophores, and oxidative stress (Berman *et al.,* 2000; Hüser *et al.,* 1998; Korge *et al.,* 2001; Kowaltowski *et al.,* 2001; Kushnareva *et al.,* 2001; Lemasters *et al.,* 1993,

1997, 1998; Lemasters, 1999; Niemienen *et al.*, 1995, 1997, Petronilli *et al.*, 1994; Qian *et al.*, 1999; Sabel *et al.*, 1997; Schild *et al.*, 2001; Zahrebelski *et al.*, 1995).

In this study, confocal microscopy was adapted to evaluate *in situ* MPT in neuronal or Schwann cell cultures originating from dorsal root ganglia (DRG) of 9 or 10-day old chick embryos, respectively, during normal incubation and following OP exposure. This work demonstrated OP induced opening of the MPT pore, an event that occurred only with compounds capable of causing OPIDN.

4.3. EXPERIMENTAL METHODS

Organophosphorus compound preparations.

Phenylsaligenin phosphate (PSP), synthesized by Lark Enterprises (Webster, MA), and mipafox, purchased from Chem Services Inc. (West Chester, PA), were used because they induce delayed neuropathy *in vivo*. Paraoxon (Chem Services) was used as a non-neuropathic OP control. Stock solutions containing PSP, mipafox, and paraoxon at 100 mM were prepared by dissolving these OP compounds in dimethyl sulfoxide (DMSO). In this proposed study, cytotoxic effects of these OP compounds were determined by using a primary neuronal cell culture and culture of Schwann cells exposed to physiological concentrations of the OP compounds PSP, mipafox and paraoxon (1 μM). Vehicle controls received equivalently diluted DMSO only. The exposure time was 12 hours, based on previous studies that demonstrated OP-induced effects on mitochondria in a neuroblastoma cell line (Carlson and Ehrich, 1999).

Neuronal preparation from dorsal root ganglia cultures.

Dorsal root ganglia of 9-days old chick embryos were dissected under sterile conditions from the lumbar intumescence (Blood, 1975; Wood, 1976; Varon *et al.,* 1981; Kleitman *et al.,* 1995). Under a dissecting microscope, the embryo was laid on its back and the abdominal viscera were removed with care to prevent damage of the DRG underneath. The lumbar DRGs were collected using microdissecting forceps, and transferred to a solution containing L-15 media. Strict sterile procedures were observed during dissections and in all subsequent steps of the purifying processes.

Following DRG collection from approximately 30 embryos, the ganglia were incubated with 0.25% trypsin for 45 min at 37° C on a rotatory shaker. Trypsin inactivation was achieved by the addition of L-15 media (Sigma Cell Culture Product, L-5520, St-Louis, Mo) supplemented with 15-20% fetal bovine serum (FBS). Then, the sample was centrifuged at 1000 rpm for 5 min, and the pellets resuspended and triturated in 1 ml of serum-containing medium. The volume of this suspension was increased to 5 ml, recentrifuged as before, and resuspended in the 10 ml of a solution containing Eagle's minimum essential medium (E-MEM, Sigma Cell Culture Product, M-0643), supplemented with 5% human placental serum (Scantibodies Laboratory, Inc, Santee, California), 50 ng/ml of nerve growth factor (fraction 2.5S, murine, natural, Gibco BRL), 5 mg/L y-irradiated and lyophilized bovine insulin (Sigma, I-1882), 10 mg/L human transferrin (98% purity, Sigma, T-3309), 20 nM progesterone (Sigma, P-0130), 30 nM sodium selenite anhydrous (45% purity, Johnson Matthew Electronics, Ward Hill, MA, E-07B17), and 100 μM tetramethylenediamine dihydrochloride (98% purity, Sigma, P-7505). One drop of this suspension was plated in the center of a round 35-mm poly-d lysine coated glass bottom (no. 1.5) coverslips (P35 GC-1.5-10-C, Mat Tek Corporation, Ashland, MA).

After the cells had been allowed to attach to collagen for 12 hours, the purification procedure was initiated by refeeding the cell culture with a solution containing antimitotic agents (E-MEM, 5% HPS, 498 mg/dl glucose, 50 ng/ml NGF, 10 mg/L transferrin, 100 μM putrescine, 20 nM progesterone, 5 mg/L bovine insulin, 30 nM sodium selenite, 10 μM uridine, 10 μM fluoro-d uracil-FdU). The antimitotic protocol involved alternating antimitotic feedings with maintenance feedings according to the following schedule: maintenance feeding on days 1, 4-6, 8-10 and day 12 onward, and antimitotic feeding on days 2-4, 6-8, and 10-12. Prior to performing experiments, these purified neuronal cultures were allowed to rest in maintenance media for one week to ensure that no residual FdU remained. These neuronal cultures will often degenerate with FBS when they are kept

longer than 21 days. Since less neuronal degeneration occurs with the use of human placental serum (HPS), this supplement was used to maintain the purified neuronal cell cultures (Kleithman *et al.,* 1995).

Schwann cell preparations from dorsal root ganglia.

The technique for preparation of pure Schwann cells differed from the one described for preparing neuronal culture, since it used ganglion explants from slightly older embryos to facilitate dissection, and to provide higher concentration of Schwann cells per ganglia (Wood, 1976; Kleithman *et al.,* 1995). Chick embryos of 10 days were dissected as described above for neuronal preparations. Schwann cells were recognized on these explants based on their appearance and location in relation to the axons.

Following the collection of 4 to 6 lumbar DRGs, the ganglia explants were plated in the center of a round 35 mm poly-d lysine coated glass bottom (no. 1.5) coverslips (P35 GC-1.5-10-C, Mat Tek Corporation, Ashland, MA) using the maintenance feeding solution E-MEM supplemented with 10% FBS, 5% HPS, 498 mg/dl glucose, 50 ng/ml NGF, 10 mg/L transferrin, 100 μM putrescine, 20 nM progesterone, 5 mg/L bovine insulin, and 30 nM sodium selenite. Schwann cell purification was achieved by refeeding the cell culture with a solution containing antimitotic agents (E-MEM, 5% HPS, 498 mg/dl glucose, 10 μM uridine, 10 μM FdU). The antimitotic protocol was alternate antimitotic and maintenance feedings according to the following schedule: maintenance feeding on days 3-6, 8-10, and day 12 onward, and antimitotic feeding on days 1-3, 6-8, 10-12 (Wood, 1976; Kleithman *et al.,* 1995).

For the studies evaluating MTP opening, each experiment was performed at 12 hours post OP exposure. Vehicle controls were also evaluated. The treated living-cell

cultures were loaded in culture medium containing 500 nM of the mitochondria specific dye tetramethylrhodamine methyl ester (TMRM, Molecular Probes) for 15 min, followed by TMRM plus 1 μM acetoxymethyl ester of calcein (calcein-AM, Molecular Probes, Eugene, OR) for 15 min at 37° C. Strict temperature control within the media during microscopic examination was maintained with a Bioptics Objective Heater to avoid temperature-related alterations of the MPT function.

Effects of OP compounds on the mitochondrial transition pore were monitored using an Axiovert 100 M Zeiss LSM 510 laser scanning confocal microscope, following the method of Nieminen *et al*. (1995). With the Zeiss software system, the 488 nm and 543 nm lines of argon and helium-neon lasers were continuously directed to the sample by a double-dichroic mirror. Fluorescent light passed back through a double-dichroic mirror into light greater or less than 575 nm. Green fluorescence of calcein continued through a 515 nm (25 nm band pass) barrier filter to a variable pinhole photodetector. Red fluorescence of TMRM passed through a 590 nm (long-pass) barrier filter. Pinhole setting of 1 was used for both red and green channels. In this system, 63X oil-immersion objective lens was used, and the lasers were attenuated below 10% of maximal output intensity to minimize photobleaching. Confocal images were transferred to a Dell Dimension XPS 400 MHz, Pentium II for processing of the images.

The computerization of confocal images allowed quantification of red (TMRM, or mitochondria), green (calcein-AM, or cytoplasm), and co-localized (red & green) pixels within the neuronal or Schwann cells evaluated. For each confocal image analyzed, pixel recording, expressed as raw intensity units (RIU) was obtained using a scatter plot representing pixels which occupy a particular location and intensity (x, y) within the cell. The x-axis represented graded intensity of red pixels (0-250 RIU), whereas the y-axis indicated the graded intensity of green pixels (0-250 RIU). The green and red pixels with

low intensities were considered background noise, and were removed from the calculations. The degree of MPT opening was expressed as the ratio of co-localized pixels to total red pixels (co-localized pixels/total red pixels) for both neuronal and Schwann cell preparations. The results were expressed as means ± SEM (1 degree of freedom) from duplicate experiments, with five different cell readings or subsamples. Statistical significance ($p < 0.01$) of mean values of the aforementioned ratios (co-localized pixels/total red pixels) was determined using a simple one way analysis of variance with the PC-SAS software (version 6.1, Cary, NC).

4.4. RESULTS

Effects of OP compounds on mitochondrial integrity in chick dorsal root ganglia cell cultures.

Purified dissociated neuronal cell cultures exposed for 12 hours to OP compounds altered the degree of TMRM fluorescence within neuronal cell populations (Fig. 1a). More specifically, OP compounds capable of inducing delayed neuropathy, represented by 1 µM mipafox and 1 µM PSP, induced decreased intensities of TMRM fluorescence recorded from the confocal images (RIU = 11660 ± 2572 and 7406 ± 2446 respectively; mean ± SEM; $p < 0.05$) compared to neuronal cells exposed to DMSO vehicle only (RIU = 28510 ± 5140). There were no differences noted between 1 µM paraoxon-challenged neuronal cell cultures (RIU = 23820 ± 5546) and the control cell populations (n=2).

Schwann cells exposed to OP-compounds responded differently from purified neurons when the same concentrations of OP compounds were used (Fig 1b). Total TMRM fluorescence intensities were not significantly different when they were challenged with any of the OP-compounds used in this study. Moreover, there were no significant changes in TMRM intensities between the OP-treated Schwann cell populations and the cultures exposed to DMSO vehicle only.

Effects of OP compounds on mitochondrial permeability transition in chick dorsal root ganglia cell cultures.

Mitochondrial function of purified neuronal and Schwann cell populations were also evaluated 12 hours post-exposure to OP-compounds. Co-localization of pixels produced by TMRM and calcein-AM were used to determine mitochondrial permeability transition

caused by challenge with paraoxon (1 μM), mipafox (1 μM), and PSP (1 μM). The degree of MPT was expressed as the ratio of co-localized pixels to total red pixels (co-localized pixels/total red pixels) for both neuronal and Schwann cell preparations.

Purified neuronal cell populations treated with neuropathy-inducing OP-compounds showed a significantly higher degree of co-localization of calcein-AM and TMRM fluorescence dyes in axons and neuronal cell bodies (Fig. 2a). In these cultures, calcein-AM (green fluorescence) shifted from the cytoplasmic compartment to the mitochondrial matrix (Fig. 3), and these latter pixels were recorded along TMRM fluorescence concomitantly present within the mitochondria (Fig. 4). The co-localization ratios of red and green pixels within the mitochondrial matrix were significantly higher for mipafox (0.86 ± 0.04) and PSP (0.83 ± 0.04) when compared to neuronal cell cultures treated with DMSO vehicle or paraoxon (mean ± SEM, $p < 0.05$). Moreover, there were no statistical differences noted between cultures exposed to paraoxon (0.64 ± 0.08) and the ones treated with DMSO vehicle only (0.52 ± 0.08).

Schwann cell cultures reacted differently to OP challenge. The ratio of co-localization pixels did not differ among any of the OP-treated Schwann cell preparations, and the results were comparable to the DMSO-vehicle control cells (Fig. 2b). Calcein-AM and TMRM fluorescence was distinct, and calcium-AM remained within the cytosol, outside the mitochondrial matrix (Fig. 5).

4.5. DISCUSSION

The present study is the first report that evaluates and quantifies the effects of organophosphorus compounds in primary cell culture preparations. Among animal susceptible to OPIDN, adult domestic chickens are considered the most reliable model (Abou-Donia, 1981). Therefore, primary neuronal and Schwann cell cultures from 9-10 day-old chick dorsal root ganglia were used as the closest *in vitro* model to study and extrapolate mechanisms occurring *in vivo* in a species highly sensitive to OPIDN.

Results reported in this study support other *in vitro* and *in vivo* models that demonstrated the toxic effects of OP-compounds on mitochondria. This study is unique in that it evaluates mitochondria as intracellular targets for OP-compound-induced cytotoxicity in living cells exposed to physiological concentrations of neuropathy-inducing OP compounds. This study shows that purified dissociated neuronal cell cultures exposed to OP compounds altered the degree of TMRM fluorescence within neuronal cell populations. Since TMRM fluorescence is directly related to the presence of intact mitochondrial structures, the intensity decrement can be explained by lower numbers of mitochondria or mitochondrial alteration following exposure to OP-compounds that are capable of inducing delayed neuropathy. Moreover, similar changes in TMRM intensities were not detected in Schwann cell populations, suggesting that OP compounds have no effects on number of mitochondria in these cells. In addition, the findings reported in this study confirm that OP compounds causing delayed neuropathy induced mitochondrial permeability transition (MPT), which can result in subsequent depolarization of the mitochondrial membrane (Carlson and Ehrich, 1999). Calcein-AM, a large molecule normally impermeable to intracytoplasmic membranes, was able to penetrate the mitochondrial matrix of neurons through the MPT pore following exposure to neuropathy-inducing OP compounds. The changes in MPT occurred as early as 12 hours post-exposure to OP-compounds, which is

considerably earlier than morphological alterations (Massicotte et al., 2001). Abrupt depolarization of the mitochondria caused by MPT, and mitochondrial swelling have been reported to result in the release of calcium and apoptotic factors into the cytosol (Halestrup and Davidson, 1990; Minamikawa *et al.,* 1999; Zahrebelski *et al.,* 1995). This could contribute to the subsequent neuronal damage observed later in the course of OPIDN.

More specifically, initiation of mitochondrial permeability transition by neuropathy-inducing OP compounds, as demonstrated in our investigation, could explain the altered mitochondrial oxygen consumption and respiration, and reduction of oxidative phosphorylation documented in previous studies (Carlson and Ehrich, 1999; Holmuhamedov *et al.,* 1996; Sitkiewick *et al.,* 1980; Skonieczna *et al.,* 1980; Spetale *et al.,* 1976). In addition, several studies have suggested that the mitochondrial permeability transition is a potential modulator of mitochondrial membrane potentials in neuroblastoma cell lines, brain, and liver mitochondria (Cassarino *et al.,* 1998, Carlson and Ehrich, 1999; Trecidi *et al.,* 1995; Bernadi *et al.,* 1996, 1999; Bradham *et al.,* 1998; Crompton, 1999; Hirsch *et al.,* 1998; Lemasters, 1999; Lemasters *et al.,* 1998; Qian *et al.,* 1997, 1999; Sugrue and Tatton, 2001). These previous studies strongly support similar changes occurring in the primary neuronal DRG used in this study.

Several mechanisms of necrosis, apoptosis, and autophagy have been associated with MPT. These include release of apoptotic factors within the cytoplasm (Aguilar *et al.,* 1996; Andreyev *et al.,* 1999; Feldmann *et al.,* 2000; Higuichi *et al.,* 1998; Kushnareva *et al.,* 2001; Tafani *et al.,* 2000; Yang et Cortopassi, 1998), and alteration in Ca^{2+} flux across the inner mitochondrial membrane (Holmuhamedov *et al.,* 1999; Schild *et al.,* 2001; Xu et al; 2001). The release of cytochrome c and initiation of apoptosis reported in a neuroblastoma cell line exposed to OP compounds following collapse of $\Delta\Psi m$ (Carlson *et al.,* 2000) suggest MPT induced by neuropathy-inducing OP compounds could lead to

some degree of apoptosis in the neuronal DRG cultures model evaluated in this current study.

The high degree of resolution obtained with confocal microscopy permitted visualization of cellular structures and mitochondrial function, including MPT. Confocal microscopic evaluation of neuronal populations treated with PSP and mipafox, which readily elicit OPIDN in hens, showed opening of mitochondrial permeability transition (MPT) pores, and significant lower mitochondrial TMRM fluorescence when compared to the negative controls. PSP, mipafox, and paraoxon are all esterase inhibitors, but paraoxon did not decrease TMRM fluorescence, indicating hydrolysis of the ester derivative of the dye incubated with the cultures. Therefore, results indicate MPT was unique to neuropathy-inducing OP-compounds since exposure of neuronal cells to paraoxon, an OP that does not cause OPIDN, failed to alter MPT. In Schwann cells, OP compounds used in this study failed to produce MPT, and TMRM-induced mitochondrial fluorescence was similar to the control. Therefore, these findings demonstrate that mitochondrial structural change are significant in neuronal populations but minimal in Schwann cell cultures, as can be expected for neuropathy inducing OP compounds. These findings demonstrate that MPT was also unique to neurons. According to these results, mitochondria were a primary target in neurons affected by OPIDN, which provides new insight on the early mechanistic events involved in OPIDN.

This study verifies that mitochondria are one of the earliest primary targets involved when neurons are exposed to neuropathy inducing OP compounds. Damage to mitochondria is likely to serve as a precursor of a cascade events resulting in necrosis and apoptosis. We suggest that the induction MPT causes rapid collapse of $\Delta\Psi m$, redistribution of soluble calcium within the mitochondrial matrix, mitochondrial swelling and release of apoptotic factors and proteases within the cytoplasm. Since MPT induces

depolarization of $\Delta\Psi m$, uncoupling of the respiratory chain can occur at any of the complex levels, resulting in alteration of mitochondrial ATP production, as reported in another study (Massicotte *et al.*, 2001). This could eventually lead to the neuronal degeneration observed in OPIDN.

4.6. ACKNOWLEDGEMENTS

The authors gratefully acknowledge the technical assistance of Wen Li, Kristy Decourcy, Dan Ward, Sandy Handcock and Jonathan Hinckley, without whom this work could not have been performed. Virginia-Maryland Regional College of Veterinary Medicine has primarily supported this work.

REFERENCES

Abou-Donia, M.B. (1981). Organophosphorus ester-induced delayed neurotoxicity. *Ann Rev. Pharmacol. Toxicol.* **21**, 511-548.

Aguilar, H.I., Bolta, R., Arora, A.S., Bronk, S.F., Gores, G.J. (1996). Induction of the mitochondrial permeability transition by protease activity in rats: a mechanism of hepatocyte necrosis. *Gastroenterology* **110**, 558-566.

Akbarsha, M.A., Sivasamy, P. (1998). Male reproductive toxicity of phosphamidon: Histopathological changes in epididymitis. *Indian J. Exp. Biol.* **36**, 34-38

Antunes-Madeira, M.C., Videira, R.A., Madeira, V.M.C. (1994). Effects of parathion on membrane organization and its implications for the machanisms of toxicity. *Biochim. Biophys. Acta* **1190**, 149-154.

Andreyev, A., Fiskum, G. (1999). Calcium induced release of mitochondrial cytochrome *c* by different mechanisms selective for brain versus liver. *Cell. Death. Differ.* **6**, 825-832.

Barber, D.S., Correll, L., Ehrich, M. (1999a). Comparison of two *in vitro* activation systems for prototoxicant activating organophosphorus esterase inhibitors. *Toxicol. Sci.* **47**, 16-23.

Barber, D.S., Correll, L., Ehrich, M. (1999b). Comparative effectiveness of organophosphorus protoxicant activating systems in neuroblastoma cells and brain homogenates. *J. Toxicol. Environ. Health* **57**, 63-74.

Berman, S.B., Watkins, S.C., Hastings, T.G. (2000). Quantitative biochemical and ultrastructural comparison of mitochondrial permeability transition in isolated brain and liver mitochondria: evidence for reduced sensitivity of brain mitochondria. *Exp. Neurol.* **164**, 415-425.

Berman, S.B., Hastings, T.G. (1999). Dopamine oxidation alters mitochondrial respiration and induces permeability transition in brain mitochondria: implications for Parkinson's disease. *J. Neurochem.* **73**, 1127-1137.

Bernardi, P., Scorrano, L., Colonna, R., Petronilli, V., Di Lisa, F. (1999). Mitochondria and cell death. Mechanistic and methodological issues. *Eur. J. Biochem.* **264**, 687-701.

Bernardi, P. (1996). The permeability transition pore. Control points of a cyclosporin A-sensitive mitochondrial channel involved in cell death. *Biochim. Biophys. Acta.* **1275**, 5-9.

Beutner, G., Ruck, A., Riede, B., Welte, W., Brdiczka, D. (1996). Complexes between kinases, mitochondrial porin and adenylate translocator in rat brain resemble the permeability transition pore. *FEBS. Lett.* **396**, 189-195.

Blood, L.A. (1975). Scanning electron microscope observations of the outgrowth from embryonic chick dorsal root ganglia in culture. *Neurobiology* **5**, 75-83.

Bouldin, T.W., Cavanagh, J.B. (1979). Organophosphorous neuropathy. 1. Teased fiber studies. *Am. J. Path.* **94**, 241-247.

Bradham, C.A, Qian, T., Streetz, K., Trautwein, C., Brenner, D.A., Lemasters, J.J. (1998). The mitochondrial permeability transition is required for tumor necrosis factor alpha-mediated apoptosis and cytochrome *c* release. *Mol. Cell. Biol.* **18**, 6353-6364.

Byrne, A.M., Lemasters, J.J., Nieminen, A.L. (1999). Contribution of increased mitochondrial free Ca^{2+} to the mitochondrial permeability transition induced by tetra-butylhydroperoxide in rat hepatocytes. *Hepatology* **29**, 1523-1531.

Cai, J., Yang, J., Jones, D.P. (1998). Mitochondrial control of apoptosis: the role of cytochrome *c*. *Biochem. Biophys. Acta.* **1366**, 139-149.

Carlson, K., Ehrich, M. (1999). Organophosphorus compound-induced modification of SH-SY5Y human neuroblastoma mitochondrial transmembrane potential. *Toxicol. Appl. Pharmacol.* **160**, 33-42.

Carlson, K., Jortner, B.S., Ehrich, M. (2000). Organophosphorus compound-induced apoptosis in SH-SY5Y human neuroblastoma cells. *Toxicol. Appl. Pharmacol.* **168**, 102-113.

Cassarino, D.S., Swerdlow, R.H., Parks, J.K., Parker, W.D. Jr., Bennett, J.P. Jr. (1998). Cyclosporin A increases resting mitochondrial membrane potential in SY5Y cells and reverses the depressed mitochondrial membrane potential for Alzheimer's disease cybrids. *Biochem. Biophys. Res. Commun.* **248**, 168-173.

Castedo, M. (1997). Implication of mitochondria in apoptosis. *Mol. Cell. Biochem.* **174**, 185-188.

Crompton, M. (1999). The mitochondrial permeability transition pore and its role in cell death. *Biochem. J.* **341**, 233-249.

Dolder, M., Wendt, S., Wallimann, T. (2001). Mitochondrial creatine kinase in contact sites: interaction with porin and adenine nucleotide translocase, role in permeability transition and sensitivity to oxidative damage. *Biol. Signals. Recept.* **10**, 93-111.

Dubinsky, J.M., Levi, Y. (1998). Calcium-induced activation of the mitochondrial permeability transition in hippocampal neurons. *J. Neurosci. Res.* **53**, 728-741.

Ehrich, M., Correll, L., Veronesi, B. (1997). Acetylcholinesterase and neuropathy target esterase inhibitions in neuroblastoma cells to distinguish organophosphorus compounds causing acute and delayed neurotoxicity. *Fundam. Appl. Toxicol.* **38**, 1-9.

Ehrich, M., Jortner, B.J. (2001). Organophosphorus-induced delayed neuropathy. In: *Neurotoxicology Handbook*, Massaro, E.J., ed., Totowa, NJ: Humana Press, pp. 17-27.

Ehrich, M. (1996). Neurotoxic esterase inhibition: predictor of potential for organophosphorus-induced delayed neuropathy. In*: Biomarkers for agrochemicals and toxic substances*, Blancato, J.N., Brown, R.N., Dary, C.C., Saleh, M.A., eds., Washington, DC: American Chemical Society, pp 79-93.

Eldrige, C.F., Bunge, M.B., Bunge, R. (1989). Differentiation of axon-related Schwann cells in vitro: II. Control of myelin formation by basal lamina. *J. Neurosci.* **9**, 625-638.

El-Fawal, H.A.N., Jortner, B.S., Eyre, P., Ehrich, M. (1988). The biventer cervicis nerve-muscle preparation of adult hens: effect of phenylsaligenin phosphate administration. *Neurotoxicology* **9**, 625-636.

El-Fawal, H.A.N, Jortner, B.S., Ehrich, M. (1990). Use of the biventer cervicis nerve-muscle preparation to detect early changes following exposure to organophosphates inducing delayed neuropathy. *Fund. Appl. Toxicol.* **15**, 108-120.

Feldmann, G., Haouzi, D., Morean, A., Durand-Schneider, A.M., Bringuier, A., Berson, A., Mansouri, A., Fau, D., Pessayre, D. (2000). Opening of the mitochondrial permeability transition pore causes matrix expansion and outer membrane rupture in Fas-mediated hepatic apoptosis in mice. *Hepatology* **31**, 674-683.

Fontaine, E., Aichas, F., Bernardi, P. (1998). A ubiquinone-binding site regulates the mitochondrial permeability transition pore. *J. Biol. Chem.* **273**, 25734-25740.

Greenman, S.B., Rutten, M.J., Fowler, W.M., Scheffler, L., Shortridge, L.A., Brown, B., Sheppard, B.C., Deveney, K.E., Deveney, C.W., Trunkey, D.D. (1997). Herbicide/pesticide effects on intestinal epithelium growth. *Environ. Res.* **75**, 85-93

Hackenbrock, C.R. (1968). Chemical and physical fixation of isolated mitochondria in low-energy and high-energy states. *Proc. Nat. Acad. Sci. USA.* **61**, 598-605

Halestrap, A.P., Davidson, A.M. (1990). Inhibition of Ca^{2+} -induced large amplitude swelling of liver and heart mitochondria by cyclosporine is probably caused by the inhibitor binding to mitochondrial-matrix peptidylprolyl cis-trans isomerase and preventing it interacting with the adenine nucleotide translocase. *Biochem. J.* **268**, 153-160.

Hamm, J.T., Wilson, B.W., Hinton, D.E. (1998). Organophosphate-induced acetylcholinesterase inhibition and embryonic retinal cell necrosis *in vivo* in the teleost (Oryzias Latipes). *Neurotoxicology* **19**, 853-870.

Harvey, M.J., Sharma, R.P. (1980). Organophosphate cytotoxicity: The effects on protein metabolism in cultured neuroblastom cells. *J. Environ. Pathol. Toxicol.* **3**, 423-436.

Higuichi, M., Proske, R.J., Yeh, E.T. (1998). Inhibition of mitochondrial respiratory chain complex I by TNF results in cytochrom *c* release, membrane permeability transition, and apoptosis. *Oncogene* **17**, 2515-2524.

Hirsch, T., Susin, S.A., Marzo, I., Marchetti, P., Zamzami, N., Kroemer, G. (1998). Mitochondrial permeability transition in apoptosis and necrosis. *Cell. Biol. Toxiol.* **14**, 141-145.

Holmuhamedov, E.L., Kholmoukhamedova, G.L., Baimuradov, T.B. (1996). Non-cholinergic toxicity of organophosphates in mammals: interaction of ethaphos with mitochondrial functions. *J. Appl. Toxicol.* **16,** 475-481.

Hunter, D.R., Haworth, R.A. (1979). The Ca^{2+}-induced membrane transition in mitochondria. I. The protective mechanisms. *Arch. Biochem. Biophys.* **195**, 453-459.

Hunter, D.R., Haworth, R.A. (1979). The Ca^{2+}-induced membrane transition in mitochondria. II. Nature of the Ca^{2+} trigger site. *Arch. Biochem. Biophys.* **195**, 460-467.

Hüser, J., Rechenmacher, C.E., Blatter, L.A. (1998). Imaging the permeability pore transition in single mitochondria. *Biophys. J.* **74**, 2129-2137.

Hüser, J., Blatter, L.A. (1999). Fluctuations in mitochondrial membrane potential caused by repetitive gating of the permeability transition pore. *Biochem. J.* **343**, 311-317.

Johnson, M.K. (1982). The target for initiation of delayed neurotoxicity by organophosphorus esters. *Rev. Biochem. Toxicol.* **8**, 141-212

Jortner, B.S., Ehrich, M. (1987). Neuropathological effects of phenylsaligenin phosphate in chickens. *Neurotoxicology* **8**, 97-108.

Kleitman, N., Wood, P.M., Bunge, R.P. (1995). Tissue culture methods for the study of myelination. In: *Culturing Nerve Cells*, Banker G, Goselin K (eds)., Cambridge, Massachussetts Institute of Technology, pp 545-594.

Korge, P., Honda, H.M., Weiss, J.N. (2001). Regulation of the mitochondrial permeability transition by matrix Ca^{2+} and voltage during anoxia/reoxygenation. *Am. J. Physiol.* **280**, C517-C536.

Kowaltowski, A.J., Castilho, R.F., Vercesi, A.E. (2001). Mitochondrial permeability transition and oxidative stress. *FEBS Lett.* **495**, 12-15.

Knoth-Anderson, J., Veronesi, B., Jones, K., Lapadula, D.M., Abou-Donia, M.B. (1992). Triphenyl phosphite-induced ultrastructural changes in bovine adrenomedullary chromaffin cells. *Toxicol. Appl. Pharmacol.* 112, 110-119.

Kushnareva, Y.E., Polster, B.M., Sokolove, P.M., Kinnaly, K.W., Fiskum, G. (2001). Mitochondrial precursor signal peptide induces a unique permeability transition release of cytochrome *c* from liver and brain mitochondria. *Arch. Biochem. Biophys.* **386**, 251-260.

Lemasters, J.J., Nieminen, A.L., Qian, T., Trost, L.C., Elmore, S.P., Nishimura, Y., Crowe, R.A., Cascio, W.E., Bradham, C.A., Brenner, D.A,. Herman, B. 1998; The mitochondrial permeability transition in cell death: A common mechanism in necrosis, apoptosis and autophagy. *Biochim. Biophys. Acta.* **1366**, 177-196.

Lemasters, J.J., Qian, T., Bradham, C.A., Brenner, D.A., Casico, W.E., Trost, L.C., Nishimura, Y., Nieminen, A.L., Herman, B. (1999). Mitochondrial dysfunction in the pathogenesis of necrotic and apoptotic cell death. *J. Bioenerg. Biomembr.* **31**, 305-319.

Lemasters, J.J. (1998). The mitochondrial permeability transition: from biochemical curiosity to pathophysiological mechanism. *Gastroenterology* **115**, 783-786.

Lemasters, J.J. (1999). Mechanisms of hepatic toxicity V. Necrapoptosis and the mitochondrial permeability transition: shared pathways to necrosis and apoptosis. *Am. J. Physiol.* **276**, G1-11.

Lemasters, J.J, Qian, T., Trost, L.C., Herman, B., Casico, W.E., Bradham, C.A., Brenner, D.A., Nieminen, A.L. (1999). Confocal microscopy of the mitochondrial permeability transition in necrotic and apoptotic cell death. *Biochem. Soc. Symp.* **66**, 205-222.

Lemasters, J.J., Qian, T., Elmore, S.P., Trost, L.C., Nishimura, Y., Herman, B., Bradham, C.A., Brenner, D.A., Nieminen, A.L. (1998). Confocal microscopy of the mitochondrial permeability transition in necrotic cell killing, apoptosis and autophagy. *Biofactors* **8**, 283-285.

Lemasters, J.J., Nieminen, A.L., Qian, T., Trost, L.C., Herman, B. (1997). The mitochondrial permeability transition in toxic hypoxic and reperfusion injury. *Mol. Cell. Biochem.* **174**, 159-165.

Lofrumento, N.E., Marzulli, D., Cafagno, L., La Piana, G., Cipriani, T. 1991; Oxidation and reduction of exogenous cytochrome c by the activity of the respiratory chain. *Arch. Biochem. Biophys.* **288**, 293-301.

Martinou, J.C., Desagher, S., Antonsson, B. (2000). Cytochrome c release form mitochondria: all or nothing. *Nat. Cell. Biol.* **2**, E41-43.

Massicotte, C., Inzana, K.D., Ehrich, M., Jortner, B.S. (1999). Neuropathologic effects of phenylmethylsulfonyl fluoride (PMSF)-induced promotion and protection in organophosphorus ester-induced delayed neuropathy (OPIDN) in hens. *Neurotoxicology* **20**, 749-760.

Massicotte, C., Barber, D.S., Jortner, B.S., Ehrich, M. (2001). Nerve conduction and ATP concentrations in sciatic-tibial and medial plantar nerves of hens given phenylsaligenin phosphate. *Neurotoxicology* **22**, 91-98.

Mentzschel, A., Schmuck, G., DeKant, W., Henschler, D. (1993). Genotoxicity of neurotoxic triaryl phosphatesL identification of DNA adducts of the ultimate metabolites, saligene phosphate. *Chem. Res. Toxicol*. **6**, 294-301.

Minamikawa, T., Williams, D.A., Bowser, D.N., Nagley, P. (1999). Mitochondrial permeability transition and swelling can occur reversibly without inducing cell death in intact human cells. *Exp. Cell. Res.* **246**, 26-37.

Marinovich, M., Ghilardi, F., Galli, C.L. (1996). Effect of pesticide mixtures on *in vitro* nervous cells: Comparison with single pesticides. *Toxicology* **108**, 201-206.

Mochida, K., Gomyoda, M., Fujita, T., Yamagata, K. (1988). Tricresyl phosphate and triphenyl phosphate are toxic to culture human, monkey and dog cells. *Zbl. Batk. Hyg. B.* **185**, 427-429.

Nemienen, A.L., Saylor, A.K., Tesfai, S.A., Herman, B., Lemasters, J.J. (1995). Contribution of the mitochondrial permeability transition to lethal injury after exposure of hepatocytes to t-butylhydroxyperoxide. *Biochem. J.* **307**, 99-106

Nieminen, A.L., Byrne, A.M., Herman, B., Lemasters, J.J. (1997). Mitochondrial permeability transition in hepatocytes induced by t-BuOOH: NAD(P)H and reactive oxygen species. *Am. J. Physiol.* **272**, C1286-C1294.

Nostrandt, A.C., Ehrich, M. (1992). Developement of a model cell culture system in which to study early effects of neuropathy-including organophosphorus esters. *Toxicol. Lett.* **60**, 107-114.

Parks, J.K., Smith, T.S., Trimmer, P.A., Bennett, J.P., Parker, W.D. Jr. (2001). Neurotoxic Abeta peptides increase oxidative stress *in vivo* through NMDA-receptor and nitric-oxide-synthase mechanisms, and inhibit complex IV activity and induce a mitochondrial permeability transition *in vitro*. *J. Neurochem.* **76**, 1050-1056.

Petit, P.X., Zamzami, N., Vayssiere, J.L., Mignotte, B., Kroemer, G., Castedo, M. (1997). Implication of mitochondria in apoptosis. *Mol. Cell. Biochem.* **174,** 185-188.

Petronilli, V., Cola, C., Massari, S., Colonna, R., Bernadi, P. (1993). Physiological effectors modify voltage sensing by the cyclosporin A-sensitive permeability transition pore of mitochondria. *J. Biol. Chem.* **268**, 21939-21945.

Petronilli, V., Costantini, P., Scorrano, L., Colonna, R., Passamonti, S., Bernardi, P. (1994). The voltage sensor of the mitochondrial permeability transition pore is tuned by the oxidation-reduction state of vicinal thiols. *J. Biol. Chem.* **269**, 16638-16642.

Petronilli, V., Penzo, D., Scorrano, L., Bernadi, P., Di Lisa, F. (2001). The mitochondrial permeability transition, release of cytochrome *c* and cell death. *J. Biol. Chem.* **276**, 12030-12034.

Poppe, M., Reimertz, C., Düßmbann, H., Krohn, A.J., Luetjens, C.M., Böckelmann, D., Nieminen, A.L., Kögel, D., Prehn, J.H.M. (2001). Dissipation of potassium and proton gradients inhibits mitochondrial hyperpolarization and cytochrome *c* release during neural apoptosis. *J. Neurosci.* **21**, 4551-4563.

Qian, T., Nieminen, A.L., Herman, B., Lemasters, J.J. (1997). Mitochondrial permeability transition in pH-dependent reperfusion injury to rat hepatocytes. *Am. J. Physiol.* **273**, C1783-C1792.

Qian, T., Herman, B., Lemasters, J.J. (1999). The mitochondrial permeability transition mediates both necrotic and apoptotic death of hepatocytes exposed to Br-A23187. *Toxicol. Appl. Pharmacol.* **154**, 117-125.

Randall, J.C., Yano, B.L., Richardson, R.J. (1997). Potentiation of organophosphorus compound-induced delayed neurotoxicity (OPIDN) in the central and peripheral nervous system of the adult hen: distribution of axonal lesions. *J. Toxicol. Environ. Health.* **51**, 571-590.

Sabel, B.A., Engelmann, R., Humphrey, M.F. (1997). *In vivo* confocal imaging (ICON) of CNS neurons. *Nature Medicine* **3**, 244-246.

Schild, L., Keilhoff, G., Augustin, W.E., Reiser, G., Striggow, F. (2001). Distinct Ca^{2+} thresholds determine cytochrome *c* release or permeability transition pore opening in brain mitochondria. *FASEB J.* **15**, 565-567.

Scoranno, L., Petronilli, V., Bernadi, P. (1997). On the voltage dependence of the mitochondrial permeability transition pore: a critical appraisal. *J. Biol. Chem.* **272**, 12295-12299.

Skonieczna, D., Sitkiewick, D., Bicz, W. (1980). Modification of oxidative phosphorylation in brain mitochondria during development and aging by the oxygen analog of Ronnel. *Pest. Biochem. Physiol.* **14**, 314-318.

Smith, M.L., Elvove, E., Valaer, P.J., Frazier, W.H., Mallory, G.E. (1930). Pharmacological and chemical studies of the cause of so-called ginger paralysis. *U.S. Public Health Rep.* **45**, 1703-1716.

Sugrue, M.M., Tatton, W.G. (2001). Mitochondrial membrane potential in aging cells. *Biol. Signals. Recept.* **10**, 176-188.

Tafani, M., Schneider, T.G., Pastorino, J.G., Farber, J.L. (2000). Cytochromed *c*-dependent activation of caspase-3 by tumor necrosis factor requires induction of the mitochondrial permeability transition. *Am. J. Path.* **156**, 2111-2121

Tredici, G., Petruccioli, M.G., Tarelli, L.T., Cece, R., Pizzini, G. (1995). Ultrastructural and confocal laser scanning microscopical aspects of apoptosis in cultured human neuroblastoma SH-SY5Y cells. *J. Anat. Embryol.* **100**, 47-53.

Tuler, S.M., Bowen, J.M. (1989). Toxic effect of organophosphates on nerve cell growth and ultrastructure in culture. *J. Toxicol. Environ. Health* **27**, 209-223.

Varon, S., Skaper, S.D., Manthorpe, M. (1981). Trophic activities for dorsal root and sympathetic ganglionic neurons in media conditioned by Schwann and other peripheral cells. *Dev. Brain Res.* **1**, 73-87.

Veronesi, B., Ehrich, M. (1993). Using neuroblastoma cell lines to examine organophosphate neurotoxicity. *In Vitro* **6**, 57-65.

Wood, P. (1976) Separation of functional Schwann cells and neurons from normal peripheral nerve tissue. *Brain Res.* **155**, 361-375

Xu, M., Wang, Y., Hirai, K., Ayub, A., Ashraf, M. (2001). Calcium preconditioning inhibits mitochondrial transition and apoptosis. *Am. J. Physiol.* **280**: H899-H908.

Yang, J.C., Cortopassi, G.A. (1998). Induction of the mitochondrial permeability transition causes release of the apoptotic factor cytochrome *c*. *Free Radic. Biol. Med.* **24**, 624-631.

Zahrebelski, G., Nieminen, A.L., al-Ghoul, K., Qian, T., Herman, B., Lemasters, J.J. (1995). Progression of subcellular changes during chemical hypoxia to cultured rat hepatocytes: a laser confocal microscopic study. *Hepatology* **21**, 1361-1372.

Zoratti, M., Szabo, I. (1995). The mitochondrial permeability transition. *Biochem. Biophys. Acta* **1241**, 139-176.

LEGENDS

FIG 1. Graph illustrating number of red pixels representing total amount of fluorescence created by TMRM in mitochondria within different treatment groups, including vehicle controls (DMSO), paraoxon (1 µM), mipafox (1 µM) and PSP (1 µM) in neuronal and Schwann cell populations. (A) Neurons treated with mipafox and PSP showed statistically significant lower TMRM intensities ($p < 0.05$) compared to cells exposed to DMSO vehicle only. Differences between 1 µM paraoxon-challenged neuronal cell cultures and the control cell populations were not significant. Neurons treated with mipafox and PSP showed statistically significant lower TMRM intensities ($p < 0.05$) compared to the control neuronal cells exposed to DMSO vehicle only. Therefore, only the OP-compounds capable of causing delayed neuropathy induced decreased intensities of TMRM mitochondrial staining. (B). No statistical alterations in the degree of mitochondrial TMRM staining were detected among the different type of OP compounds used to treat Schwann cell cultures.

FIG. 2. Co-localization ratios of the fluorescent dyes in the green (calcein-AM) and the red (TMRM) channels in neuronal and Schwann cell populations 12 hours post-exposure to OP-compounds. (A) In the neuronal cell populations, co-localization ratios recorded from the neurons challenged with 1 µM mipafox and 1 µM PSP were statistically different from negative controls (DMSO vehicle) (mean ± SEM, $p < 0.05$ indicated by *). Paraoxon (1 µM) exposed cells were not different from the negative control group. (B) In Schwann cell cultures, no statistical differences in the degree of co-localization were observed among the different treatment groups, including the negative controls.

FIG. 3. Confocal microscopy of a neuronal cell body from a purified and dissociated neuronal DRG cell culture of a day-9 old chick embryo 12 hours post-exposure DMSO-treated cells (negative control). (A) This image showed normal mitochondrial structure and function. Mitochondria transition pores were closed as demonstrated by its respective

scatter graph. Bar = 10 µm. (B) Scatter graph representing degree of co-localization of the dyes in the green (calcein-AM, cytoplasm) and the red (x =TMRM, mitochondria) channels within the neuronal cell body previously illustrated in (A). Bar = 5 µm.

FIG. 4. Confocal microscopy of a neuronal cell body from purified and dissociated neuronal DRG cell culture of a 9-day old chick embryo 12 hours post exposure to PSP (1 µM), showing altered mitochondrial structure and function. (A). Mitochondrial permeability transition induced by PSP was demonstrated by the high degree of co-localized pixels in its respective scatter graph. (B) Scatter graph representing degree of co-localization of the dyes in the green (calcein-AM) and the red (TMRM) channels within the neuronal cell body seen in A. There was a high degree of co-localization of both fluorescent dyes, illustrating altered mitochondrial function and opening of MPT pores. Calcein-AM was capable to penetrate the mitochondrial matrix through the MPT pores. With neuronal exposure to neuropathy-inducing OP compounds, calcein-AM (green fluorescence) shifted from the cytoplasmic compartment to the mitochondrial matrix, and this dye was concomitantly recorded with TMRM mitochondrial staining.

FIG. 5. Confocal microscopy of a Schwann cell from a DRG explant of a 10-day old chick embryo, 12 hours post exposure to mipafox (1µM). The arrow shows a normal Schwann cell attached to a differentiated axon with minimal degree of co-localization of the fluorescent dyes, demonstrating mitochondrial integrity in this cell system. Mitochondrial permeability transition was not initiated by this toxicant. Bar = 5 µM.

Mitochondrial fluorescence in neuronal cells exposed to OP-compounds

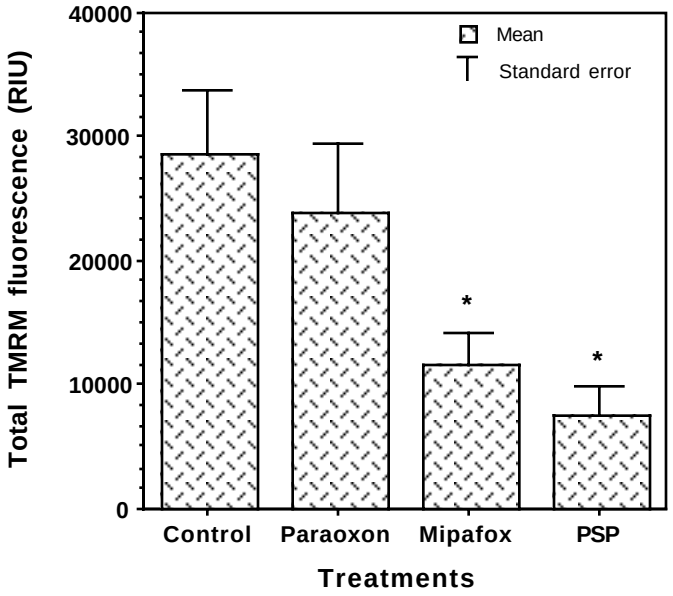

Fig. 1A.

Mitochondrial fluorescence in Schwann cells exposed to OP-compounds

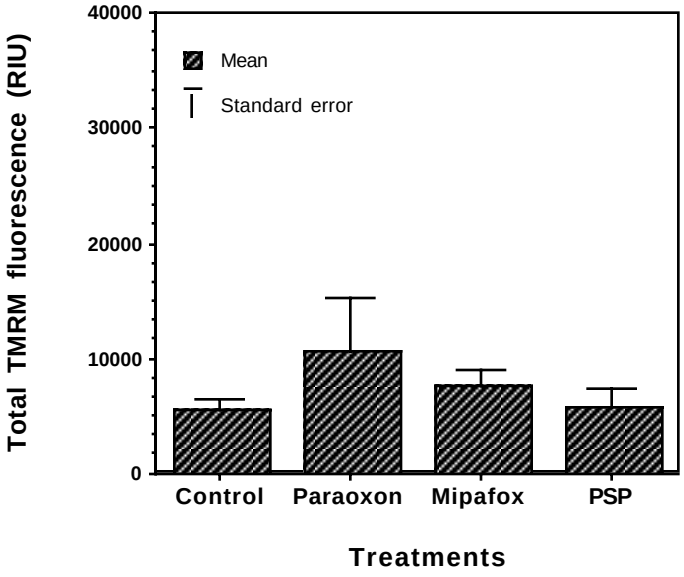

Fig. 1B.

MPT in neuronal cell cultures following OP-exposure.

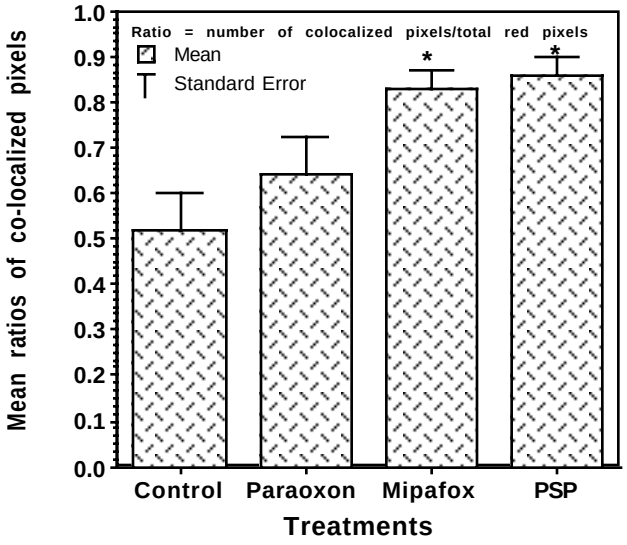

Fig. 2A.

MPT in Schwann cell cultures following OP-exposures.

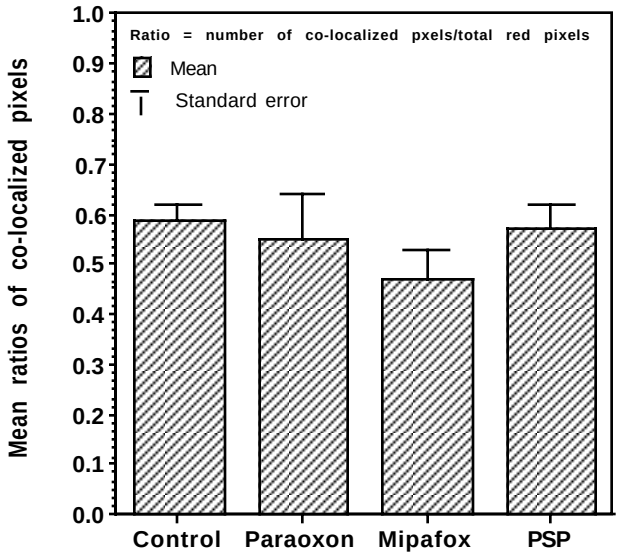

Fig. 2B.

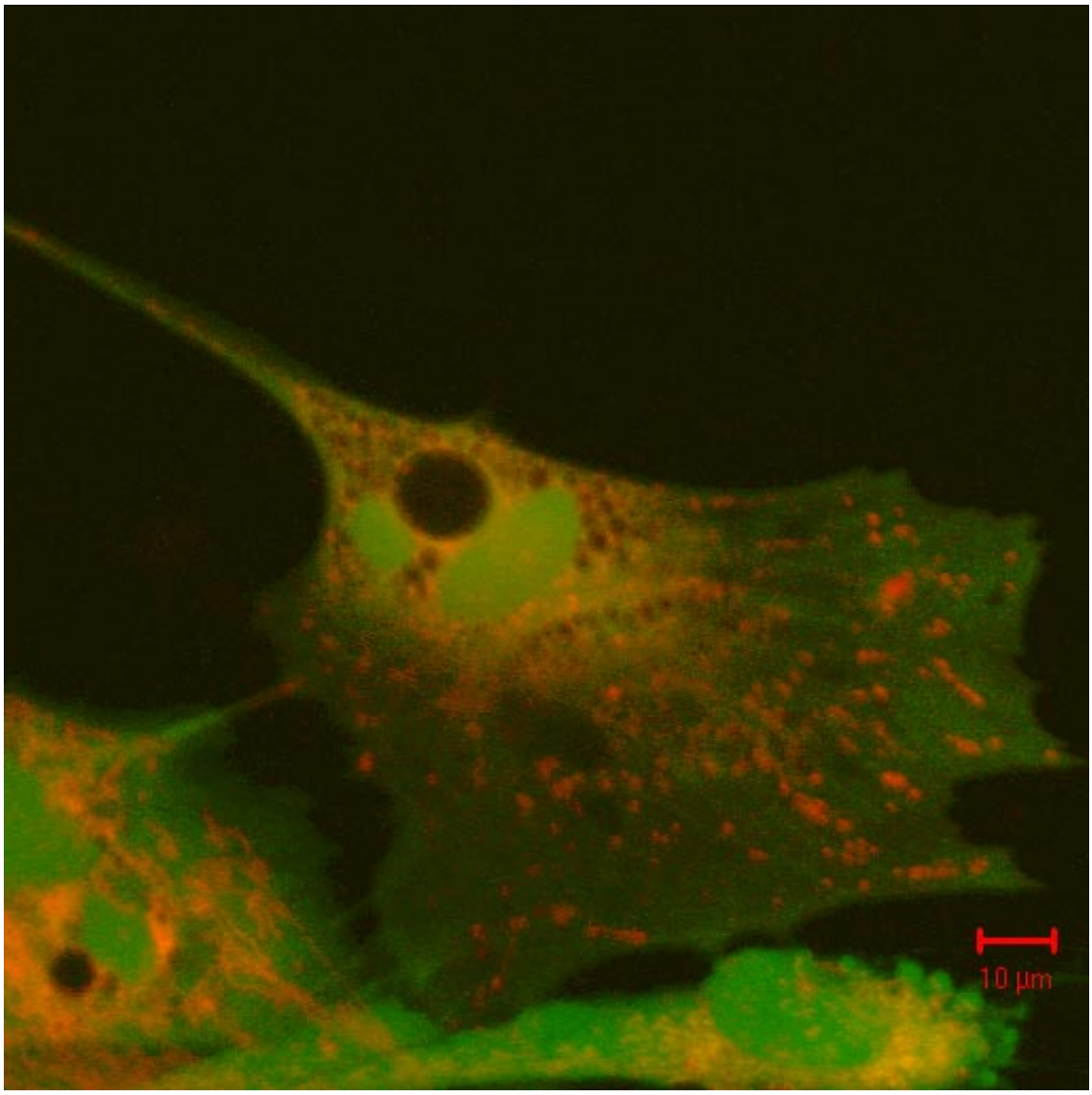

Fig. 3A.

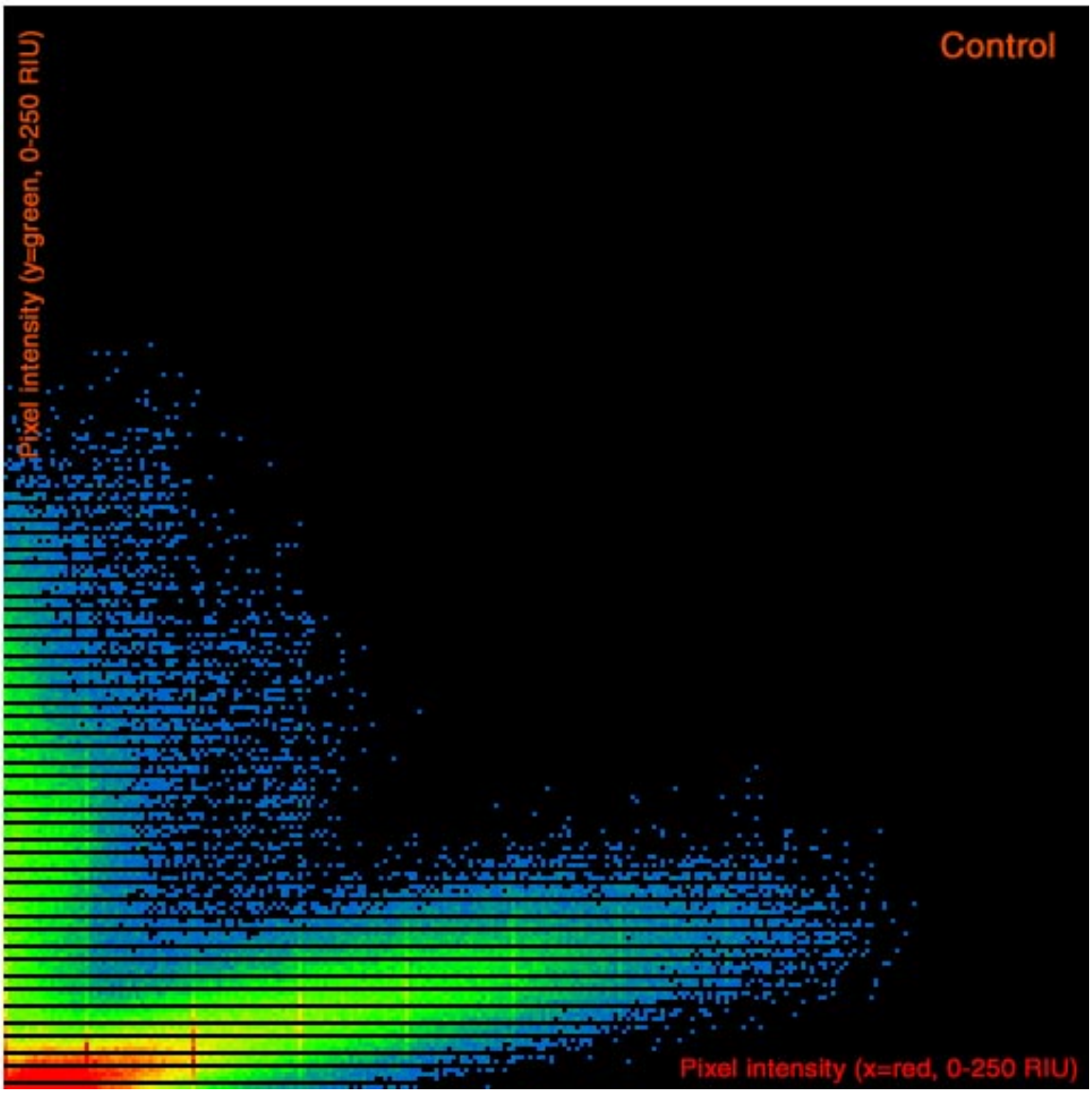
Control
Pixel intensity (y=green, 0-250 RIU)
Pixel intensity (x=red, 0-250 RIU)

Fig. 3B.

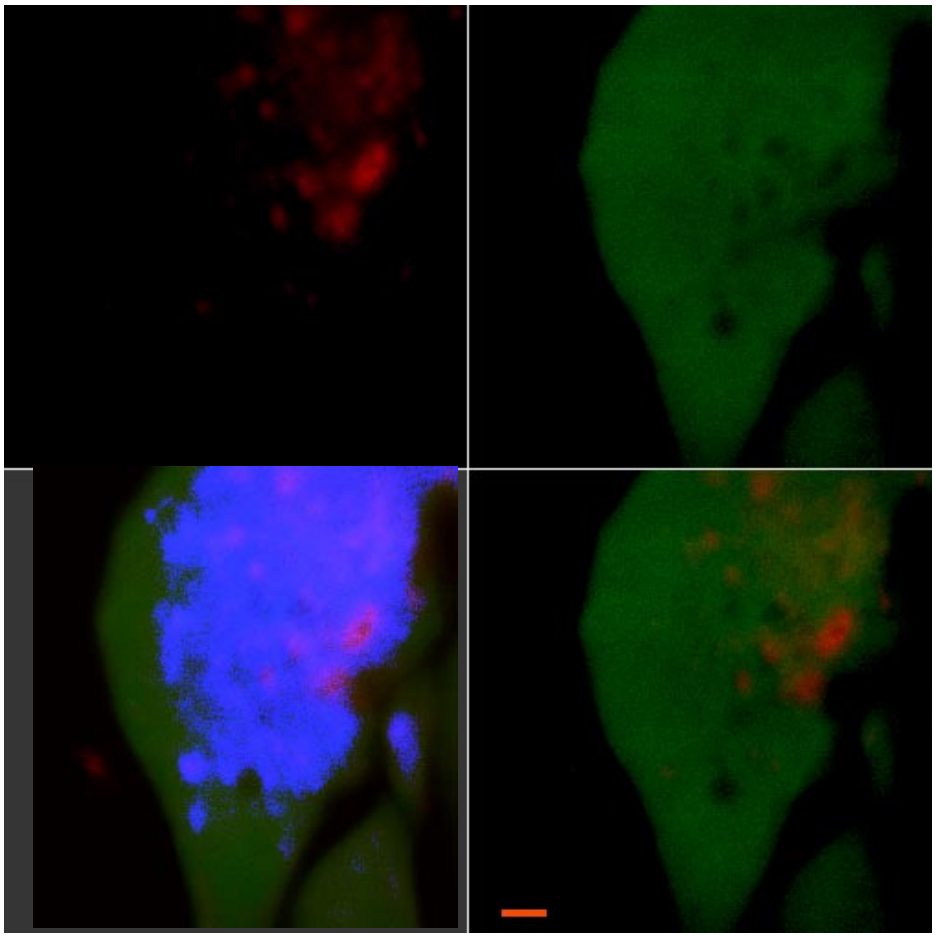

Fig. 4A.

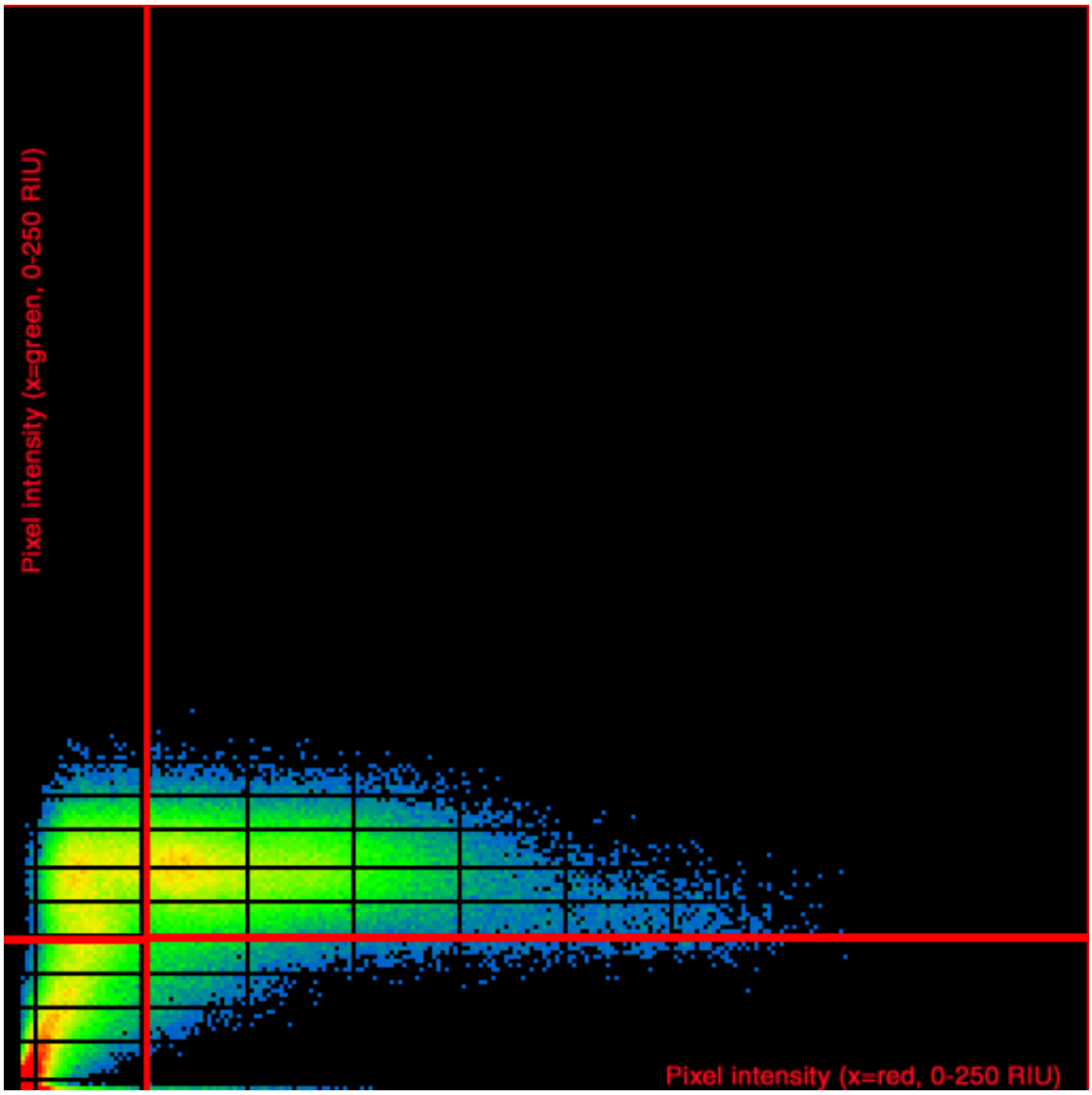
Pixel intensity (x=green, 0-250 RIU)
Pixel intensity (x=red, 0-250 RIU)

Fig. 4B.

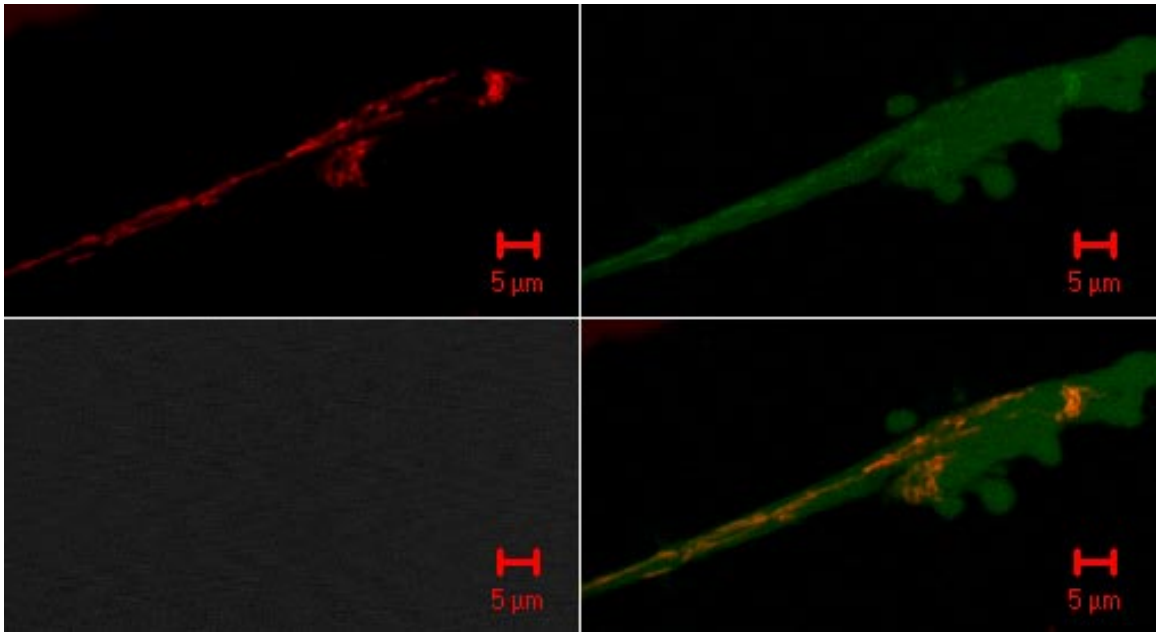

Fig. 5.

RESULTS

PART IV: CHAPTER 5

Effects of Neuropathy-Inducing (OP) Compounds on Mitochondrial ATP Production in Primary Dorsal Root Ganglia Cell Cultures.

Authors:

Christiane Massicotte

Cornelius Van der Schyf

Bernard S. Jortner

Marion Ehrich

Virginia-Maryland Regional College of Veterinary Medicine

Laboratory for Neurotoxicity Studies, VA-MA Regional College of Veterinary Medicine,

1 Duckpond Drive

Blacksburg, VA 24061-0442.

Running title:

Mitochondrial ATP production in OP-exposed DRG

5.1. ABSTRACT

Cultures of dorsal root ganglia (DRG) can achieve neuronal maturation with axons. They have not, however, previously been used to investigate metabolic events that occur following exposure to neuropathy-inducing organophosphorus (OP) esters. Recent studies in other systems demonstrated *in vivo* alterations of ATP concentrations and changes in mitochondrial transmembrane potential ($\Delta\Psi m$) following exposure to neuropathy-inducing OP compounds, suggesting that mitochondrial dysfunction occurs. We report an investigation using chick embryo DRG cultures to evaluate effects on the mitochondrial respiratory chain associated with exposure to these toxicants. This approach uses an *in vitro* neuronal system from the animal species that provides the animal model for OP-induced delayed neuropathy (OPIDN). DRG were obtained from 9-10 day old chick embryos, and grown for 14 days in minimal essential media (MEM) supplemented with bovine and human placental sera and growth factors. Cultures were then treated with 1μM phenylsaligenin phosphate (PSP), mipafox, paraoxon, or the DMSO vehicle. Mipafox and PSP readily elicit OPIDN in hens; paraoxon does not. *In situ* evaluation of ATP production measured by bioluminescence assay in neurons treated with PSP and mipafox, but not paraoxon, showed decreased ATP concentrations. This low energy state was present in several levels of the mitochondrial respiratory chain, including complexes I, III and IV, although complex I was the most severely affected. We conclude that mitochondria are a primary target for neuropathy-inducing OP compounds, resulting in depletion in ATP concentrations.

Key words: organophosphorus; mitochondria; permeability transition; dorsal root ganglia.

5.2. INTRODUCTION

Some organophosphorus (OP) compounds are able to induce delayed neuropathy (OPIDN) after a single exposure in humans and other susceptible species, characterized by distal, non-terminal, axonal degeneration with secondary demyelination (Abou-Donia, 1981; Abou-Donia *et al.,* 1986; Bouldin and Cavanagh, 1979 a, b; Ecobichon, 1994; Ehrich and Jortner, 2001; El-Fawal *et al.,* 1988, 1990; Jortner and Ehrich, 1987; Johnson 1982; Lapadula *et al.,* 1992;). The adult hen has proven to be the most reliable animal model to study the delayed effects of organophosphate intoxication, since it readily shows clinical signs and lesions (US EPA, 1991). The nerve fiber lesions progress over time (1-2 weeks) in a Wallerian-like degenerative pattern (Bouldin and Cavanagh, 1979a). The progressive morphological changes correlate with the development of neurological signs including weakness, incoordination, ataxia, and flaccid paralysis in its most severe form (Massicotte *et al.,* 1999; Randall *et al.,* 1997). The pathogenic mechanisms of OPIDN need yet to be determined.

Metabolic modifications have been documented to occur following exposure of brain, cardiac and bovine chromaffin tissues to OP compounds. These included alterations in mitochondrial respiration and inhibition of oxidative phosphorylation (Sitkiewicz *et al.,* 1980; Holmuhamedov *et al.,* 1996). Some OP compounds have even been reported to interfere with enzyme complexes within the citric acid cycle (Knoth-Anderson *et al.,* 1992) and the glycolytic pathway (Hernandez *et al.,* 1989; Imberti, 1993). These earlier findings suggest that metabolic alterations of free energy production could be an early event involved in mechanisms contributing to OPIDN.

The occurrence of organophosphorus-induced metabolic alterations are supported by preliminary studies conducted *in vivo*. In one case, adenosine triphosphate (ATP)

concentrations were measured in sciatic nerves of adult hens treated with neuropathy-inducing OP compounds (Massicotte *et al.*, 2001). This study revealed variations in ATP concentrations prior to the occurrence of either clinical signs or neuropathological alterations of OPIDN (Jortner and Ehrich, 1987, El-Fawal *et al.*, 1990; Massicotte *et al.*, 2001). However, this preliminary study did not provide information that would localize the sources of ATP concentration changes following OP exposure within the whole sciatic nerve, since the sciatic nerve contains non-neuronal (Schwann cells, fibroblasts, perineurial cells) as well as neuronal cells. Purified neuronal cell cultures (Blood, 1975; Varon *et al.*, 1981; Keithman *et al.*, 1995; Tuler and Bowen, 1989; Wood, 1976) have not yet been used to evaluate the effects of OP compounds on cellular ATP production.

ATP is formed in mitochondria (Mitchell, 1961). Mitochondria contain the respiratory chain, the enzymes of citric acid and fatty acid oxidation, which contribute to oxidative phosphorylation processes in which ATP is formed. Consequently, the cellular role of these organelles is crucial in regard to free energy production. Mitochondria have two membrane structures; the outer permeable membrane facing the cytosolic side, and the highly folded impermeable inner membrane enclosing the centrally located matrix (Fig. 1). Reactions of the Kreb cycle and fatty acid oxidation occur within the matrix, whereas oxidative phosphorylation occurs in the inner membrane. Indeed, the respiratory chain, which consists of 3 proton pumps linked by 2 mobile electron carriers, is present within the inner membrane. Electrons from NADH or $FADH_2$ flow through 3 specific transmembrane complexes called NADH-Q reductase (complex I), cytochrome reductase (complex III) and cytochrome oxidase (complex IV). This electron flow results in the pumping of protons out of the mitochondrial matrix and the generation of a transmembrane potential (Capaldi, 1990; Hofhaus *et al*., 1991, 1996; Weiss *et al*., 1991). ATP is synthesized when protons flow back to the matrix through the ATP synthase enzymatic complex (also known as complex V, or FoF_1-ATPase, or H^+-ATPase) (Penefsky and Cross, 1991; Fillingame, 1992;

Pederson and Amzel, 1993). In this way, the synthesis of ATP is coupled to the flow of electrons from NADH or $FADH_2$ to O_2 by a proton gradient across the inner mitochondrial membrane and simultaneous concentration of ADP present in the system (Babcock and Wikstrom, 1992) (Fig. 2). Structural and functional modifications have been previously reported within mitochondria of cells challenged with OP compounds. These changes include alterations in the mitochondrial transmembrane potential (Ψm) (Holmuhamedov *et al.,* 1996; Carlson and Ehrich, 1999), and inhibition of ATPase in synaptosomal fractions (Barber *et al.,* 2001). Furthermore, earlier studies performed with SH-SY5Y cell cultures showed that modifications in Ψm occurred at much earlier time-points than other indications of cellular damage, such as DNA fragmentation or loss of substrate adhesion (Nostrandt *et al.,* 1992; Carlson and Ehrich, 1999; Carlson *et al.,* 2000). These observations suggest that changes in Ψm could represent an early event in OP-induced cytotoxicity.

Mitochondrial modifications in Ψm could be the result of several mechanisms. For example, impairment of the mitochondrial respiratory electron transport chain could result in reduction of proton gradient across the inner mitochondrial membrane and lead to ATP depletion secondary to uncoupled oxidative phosphorylation. Furthermore, electromotive forces coupled to proton gradients are responsible for the formation and maintenance of Ψm across the inner mitochondrial membrane. Measurements of the mitochondrial respiratory chain have previously been evaluated in the presence of complex-specific inhibitors (I-IV), to investigate the properties of some toxicants (Steyn *et al.,* 2000; Hofhaus *et al.,* 1996; Robinson *et al.,* 1996; Wanders *et al.,* 1993, 1994, 1996; Wolvetang *et al.,* 1990). In fact, electrons from NADH are transferred through complexes I, III, IV, located within the inner mitochondrial membrane, resulting in proton translocation outside the mitochondria. The latter protomotive forces generated by initial electron transfer via these complexes are subsequently used by ATP synthase (Complex V) for ATP synthesis (Weiss

et al., 1991). These results may explain why alterations in mitochondrial oxygen uptake and respiration have been reported in brain synaptosomes following exposure to OP compounds (Sitkiewicz *et al.,* 1980; Skonieczna *et al.,* 1980).

Another mechanism for OP-induced modification of Ψm could also be important. In studies using hepatocytes, cardiac, and brain cells, dosed with t-butylhydroperoxide or other oxidants, severe mitochondrial dysfunction resulted in opening of mitochondrial permeability transition pores (MPT), and caused the protomotive forces to dissipate across the inner mitochondrial membrane (Hunter and Haworth, 1979; Zoratti and Szabo, 1995; Bernardi, 1996: Niemienen *et al.,* 1995). The rapid change of permeability associated with the MPT induced dissipation of the Ψm and uncoupling of oxidative phosphorylation with a secondary reduction of ATP synthesis (Berman *et al.,* 2000; Zoratti and Szabo, 1995; Cassarino *et al.,* 1998). Mitochondrial swelling ensued, along with the release of intramitochondrial ions and proteins (cytochrome *c*) within the cytoplasm (Petit *et al.,* 1997; Lemasters *et al.,* 1998; Cai *et al.,* 1998).

The present study quantifies mitochondrial respiration in purified chick neuronal DRG cell cultures following exposure to OP compounds capable of inducing delayed neuropathy *in vivo*. This was accomplished by measurements of ATP concentration changes associated with exposure to phenylsaligenin phosphate (PSP) and mipafox, direct active esterase inhibitors that cause OPIDN in the hen model, and a nonneuropathic-inducing OP compound, paraoxon, using the luciferin-luciferase bioluminescence assay (Shirhatti and Krishna, 1985; Kutty *et al.,* 1991). The mitochondrial respiratory chain function, evaluated in the presence of agents that act specifically at each complex (Steyn *et al.,* 2000; Hofhaus *et al.,* 1996; Robinson *et al.,* 1996; Wanders *et al.,* 1993; Wolvetang *et al.,* 1990) showed significant alteration in ATP levels in the neuronal cell population.

5.3. EXPERIMENTAL METHODS

5.3.1. Organophosphorus compound preparations.

Phenylsaligenin phosphate (PSP), synthesized by Lark Enterprises (Webster, MA), and mipafox purchased from Chem Services Inc. (West Chester, PA), were used because they induce delayed neuropathy *in vivo* (Carboni *et al.*, 1992; Ehrich and Jortner, 2001). Paraoxon (Chem Services) was used as a non-neuropathic OP control. Stock solutions containing PSP, mipafox, and paraoxon at 100 mM were prepared by dissolving these OP compounds in dimethyl sulfoxide (DMSO). In this study, cytotoxic effects of the OP compounds were determined by using a primary neuronal cell culture exposed to physiological concentrations PSP, mipafox and paraoxon (1 μM). Negative controls received equivalent diluted DMSO vehicle only. The exposure time was 12 hours, based on previous studies that demonstrated OP-induced effects on mitochondria in a neuroblastoma cell line (Carlson and Ehrich, 1999).

5.3.2. Neuronal preparation from dorsal root ganglia cultures.

Dorsal root ganglia obtained from 9-days old chick embryos were dissected under sterile conditions from the lumbar intumescence (Blood, 1975; Wood, 1976; Varon *et al.*, 1981; Kleitman *et al.*, 1995). Under a dissecting microscope, the embryo was laid on its back and the abdominal viscera were removed with care to prevent damage of the DRG underneath. The lumbar DRGs were collected using microdissecting forceps, and transferred to a solution containing L-15 media. Strict sterile procedures were observed during dissections and in all subsequent steps of the purifying processes.

Following DRG collection from approximately 30 embryos, the ganglia were incubated with 0.25% trypsin for 45 min at 37 °C on a rotatory shaker. Trypsin inactivation was achieved by the addition of L-15 media (Sigma Cell Culture Product, L-5520) supplemented with 15-20% fetal bovine serum (FBS). The sample was then centrifuged at 1000 rpm for 5 min, and the pellets resuspended and triturated in 1 ml of serum-containing medium. The volume of this suspension was increased to 5 ml, recentrifuged as before, and resuspended in 10 ml of a solution containing Eagle's minimum essential medium (E-MEM, Sigma Cell Culture Product, M-0643), supplemented with 5% human placental serum (HPS, Scantibodies Laboratory, Inc, Santee, California), 50 ng/ml of nerve growth factor (NGF, fraction 2.5S, murine, natural, Gibco BRL), 5 mg/L y-irradiated and lyophilized bovine insulin (Sigma, I-1882), 10 mg/L human transferrin (98% purity, Sigma, T-3309), 20 nM progesterone (Sigma, P-0130), 30 nM anhydrous sodium selenite s (45% purity, Johnson Matthew Electronics, E-07B17), and 100 μM tetramethylenediamine dihydrochloride (98% purity, Sigma, P-7505). One drop of this suspension was plated in the center of a round 35-mm poly-d-lysine coated glass bottom (no. 1.5) and coverslipped (P35 GC-1.5-10-C, Mat Tek Corporation).

After the cells had been allowed to attach to collagen for 12 hours, the purification procedure was initiated by refeeding the cell culture with a solution containing antimitotic agents (E-MEM, 5 % HPS, 498 mg/dl glucose, 50 ng/ml NGF, 10 mg/L transferrin, 100 μM putrescine, 20 nM progesterone, 5 mg/L bovine insulin, 30 nM sodium selenite, 10 μM uridine, 10 μM FdU). The antimitotic protocol was accomplished by alternating antimitotic feedings with maintenance feedings according to the following schedule: maintenance feeding on days 1, 4-6, 8-10 and day 12 onward, and antimitotic feeding on days 2-4, 6-8, and 10-12. Prior to performing experiments, the purified neuronal cultures were allowed to rest in maintenance media for one week to ensure that no residual FdU remained. These neuronal cultures will often degenerate with FBS when they are kept longer than 21 days;

therefore, since less neuronal degeneration occurs with the use of HPS, this supplement was used to maintain the purified neuronal cell cultures (Kleithman *et al.,* 1995).

5.3.3. Complex-specific inhibition of mitochondrial respiration

For the studies evaluating mitochondrial respiration, each experiment was performed in 14 day-old purified neuronal DRG cultures. The cells were harvested 12 hours post-treatment with 0.25% trypsin and 0.05% (w/v) EDTA, and centrifuged for 5 min at 700 rpm. The cells were resuspended in e-MEM with 15% FBS for 30 min to allow cells to recuperate from the harvesting process. The cells were then washed 3 times in PBS (pH = 7.4) and kept at 4 °C during the incubation time. The quantity of cells present in the each culture system were counted using a cytometer, and diluted with PBS to obtain 10^5 cells/ ml. The cells were then incubated at 37 °C for 15 min to eliminate residual intracellular ATP stores that may be present in the preparations (Steyn *et al.,* 2001).

The effects of OP compounds on the mitochondrial electron transport chain, including enzymatic functions of complexes I, III, and IV, were measured *in situ* in digitonin-permeabilized neuronal DRG cell populations as the amount of ATP produced over time (Ventura *et al.,* 1995; Hofhaus *et al.,* 1996; Robinson *et al.,* 1996; Wanders *et al.,* 1993; Steyn *et al.,* 2000). Reaction mixtures consisted of an isotonic medium [150 mM KCl, 75 mM Tris•HCl, 2 mM EDTA, 10 mM potassium hydrogen phosphate, 0.1% (w/v) bovine serum albumin, final pH = 7.4 with 1 N NaOH], 40 μg/ml digitonin (Sigma) dissolved in sterilized and distillated water, and 1 mM ADP. The cells were added to complex-specific solutions to reach a concentration of 500 cells/ml. Complex-specific substrates necessary for the facilitation of complex-driven ATP synthesis were added separately in concentrations of 10 mM (malate for Complex I; glycerol-3-phosphate for Complex III; N,N,N',N'-tetraethyl-p-phenylenediamine dihydrochloride and ascorbic acid

for Complex IV), and their effects were evaluated individually for each complex. For each individual complex of the respiratory chain function was also determined in the presence of complex-specific xenobiotics (20 μg/ml rotenone for Complex I; 10 μg/ml antimycin for Complex III; 10 mM sodium azide for complex IV). The resulting mixtures described above were then incubated immediately for 30 min. After incubation, the cells were placed on ice, and the reactions were terminated by neutralizing the extracts with 50 μL of 8% trichloroacetic acid and 2 mM EDTA. Following neutralization of these extracts, 500 μL of Tris-buffer•HCl were added to all preparations (Wanders *et al.,* 1993-1994; Hofhaus *et al.,* 1996; Robinson *et al.,* 1996; Steyn *et al.,* 2000, 2001). Complex specific ATP production can be compared between complexes (I, III, IV) to localize the effect of OP compounds at precise enzymatic-complex levels.

5.3.4. Quantification of ATP concentrations

ATP concentrations were determined by using a standardized luciferase-luciferin assay and a semi-automatic bioluminometer, as previously reported for NG 108-15 and murine N-2∝ neuroblastoma cell lines or human leukocytes (Shirhatti and Krishna, 1985; Kutty *et al.,* 1991; Steyn *et al.,* 2000). Addition of 100 μL of a standardized luciferase-luciferin ATP assay mixture (firefly luciferase, luciferin, MgSO4, EDTA, DTT, and bovine serum albumin in tris buffer - purchased from Sigma, no. FL-AAM) was added to 100 μL of the mitochondrial extracts. Chemically, ATP reacts with D-luciferin, releasing diphenyl phosphate (PPi) and adenylyl luciferin. Then, oxygen reacts with the newly formed adenylyl luciferin to produce CO_2, AMP and electronically excited oxiluciferin (Lundin, 2000). The quantity of light emitted during relaxation were measured in photons (562 nm), or relative light units (RLU). External standardization with a known concentration of ATP was used to quantify ATP in the samples. Concentrations of ATP produced were reported as the concentration of ATP (pmol) per neuronal cell. The results were expressed as mean ±

SEM from duplicate experiments, with three different subsamples (n = 6). Statistical significance ($p < 0.05$) of mean ATP concentration values between treatment groups was determined using a one way analysis of variance with the PC-SAS software (version 6.1).

5.4. RESULTS

General effects of OP compounds on mitochondrial function in neuronal chick dorsal root ganglia cell cultures.

The production of ATP by purified dissociated neuronal cell cultures exposed for 12 hours to OP compounds was measured using the bioluminescence assay. Since ATP was the limiting reagent, the light produced was proportional to ATP concentrations. Measurements of RLU corresponded to a linear detection range from 10^{-14} M to 10^{-10} M of ATP ($y = 0.7969 + 11.386$, $r^2 = 0.9998$).

Alterations of overall ATP production were recorded in purified dissociated neuronal cell cultures exposed for 12 hours to OP compounds (Fig. 1). More specifically, OP compounds capable of inducing delayed neuropathy, represented by 1 µM mipafox and 1 µM PSP, decreased free ATP production recorded from the bioluminometer (ATP concentrations [pmol/cell] = 179 ± 5 and 256 ± 14 respectively; mean ± SEM; $p < 0.05$) compared to neuronal cells exposed to DMSO vehicle only (ATP = 307 ± 8). There were no differences noted between 1 µM paraoxon-challenged neuronal cell cultures (ATP = 271 ± 18) and the control cell populations.

Mitochondrial complex-specific alterations following exposure of neuronal chick dorsal root ganglia cell cultures to OP compounds

ATP production in purified neuronal cell cultures was further evaluated 12 hours post-exposure to OP-compounds, using complex-specific xenobiotics. These were rotenone, antimycin, and sodium azide for complexes I, III, and IV, respectively. Measurements of complexes I, III and IV driven ATP production could be made in the presence of complex-specific substrates, which included 10 mM of both glutamate and malate, 10 mM glycerol-3-phosphate, and 10 mM of ascorbic acid added to 200 μM of TMDP, respectively. Complex-specific mitochondrial alterations were determined after challenge with 1 μM paraoxon, mipafox and PSP.

In the presence of xenobiotics acting on complex I, III, and IV, the purified neuronal cells treated with neuropathy-inducing mipafox showed significantly lower ATP production in complexes I, II and IV (174 ± 39, 221 ± 12, 271 ± 29 pmol/cell, respectively, $p<0.05$) when compared to neuronal cell cultures treated with DMSO vehicle or paraoxon (136 ± 34, 271 ± 12, 334 ± 27 pmol/cell, respectively). ATP production was also decreased by the other neuropathy-inducing test compound, PSP (Fig. 2). This indicated that the effects of neuropathy-inducing compounds were not complex-specific on the respiratory chain. Differences in complex-specific ATP production were minimal between control cultures and cultures exposed to paraoxon. Although ATP production differed from controls in all cultures exposed to mipafox and PSP, values obtained for complex I - rotenone preparations were the most severely diminished (Fig. 2).

5.5. DISCUSSION

In this study, neuropathy-inducing OP compounds caused decreases in ATP concentrations. Cell viability is highly dependent on the production and utilization of ATP and mitochondrial synthesis of ATP is essential to maintenance of normal neuronal function (Fiskum 1983, 1985). ATP concentration alterations, therefore, may be a relevant response of neuronal cells to neuropathy-inducing OP compounds.

In this study, the method of Steyn et al. (2001) provided a highly sensitive means for quantification of ATP concentrations by bioluminescence in neuronal cell populations. This approach required a very small number of neuronal cells. Concentrations of substrates, complex-specific xenobiotics, and digitonin required for the selective permeabilization of the neuronal cells used for DRG in this study were those used previously in human leukocytes and N-2α and SH-SY5Y neuroblastoma cells (Steyn *et al.*, 2000; Steyn *et al.*, 2001).

Alterations of ATP concentrations have been previously measured in sciatic nerves of hens treated with the neuropathy-inducing OP compounds phenylsaligenin phosphate (Massicotte *et al*., 2001). In that study, modifications in ATP concentrations suggested dysregulation of mitochondrial-associated cellular energy production, representing early events in the development of OPIDN. Substrates and xenobiotics acting on specific complexes were used to localize the level of the respiratory chain primarily affected by neuropathy-inducing OP compounds. For example, the specific substrate for complex I, malate, was used to confirm appropriate function of complex I. Rotenone, a xenobiotic acting on complex I, was used to determine the extent of complex functional alteration in the presence of OP compounds. Complex-specific substrates and xenobiotics were also used to determine OP-induced effects on complexes III and IV. OP compounds did cause

change in all of these complexes, indicating OP compounds did not have a complex-specific effect. However, results reported in this study support other *in vitro* and *in vivo* models that demonstrated the toxic effects of OP compounds on mitochondria (Carlson and Ehrich, 1999; Massicotte *et al.*, 2001; Mochida *et al.*, 1988; Veronesi *et al.*, 1993). This study is unique in that it specifically evaluates the mitochondrial respiratory chain as an intracellular target for physiological concentrations of neuropathy-inducing compounds in living cells.

Our findings further confirm that OP compounds causing delayed neuropathy reduced ATP production at several levels of the respiratory chain 12 hours post-exposure. These events occurred in our primary cell cultures at the same time-point (12 hours) when mitochondrial Ψm alterations were detected in previous studies using SH-SY5Y cells (Carlson and Ehrich, 1999). The lower energy state seen in the latter study was thought to be related to depolarization of the mitochondrial membrane potentials, since disturbance of electronic charges can abruptly impair the electron transport chain and concomitant pumping of proton across the mitochondrial membrane (Carlson and Ehrich, 1999). Alterations in ATP concentrations occurred as early as 12 hours post-exposure to OP compounds in our primary neuronal cultures, which is considerably earlier than morphological alterations in affected hen axons (Massicotte *et al.*, 2001a). Since ATP production is directly related to the presence of intact mitochondrial function, this reduction in ATP concentrations can be explained by lower numbers of mitochondria or mitochondrial injury following exposure to OP-compounds that are capable of inducing delayed neuropathy.

Compromised mitochondria can trigger cell death through disruption of electron transport, oxidative phosphorylation and ATP production, and opening of MPT pores (Green and Reed, 1998). Disruption of electron transport chain reactions resulting in energy depletion, as was demonstrated in this study, has been recognized as an early feature of cell death (Garcia-Ruiz *et al.*, 1997). In addition, abrupt depolarization of the mitochondrial

membrane associated with dysfunction of its respiratory chain results in mitochondrial swelling and in the release of calcium and apoptotic factors into the cytosol (Halestrup and Davidson, 1990; Minamikawa *et al.,* 1999; Zahrebelski *et al.,* 1995). This could contribute to the subsequent neuronal damage observed later in the course of OPIDN. Another recent investigation demonstrated that mitochondrial permeability transition (MPT) occurred in neuronal dorsal root ganglia cell cultures exposed to neuropathy-inducing OP compounds (Massicotte *et al.,* 2001b). When MPT occurs in a cell, ATP becomes progressively depleted secondary to uncoupling of oxidative phosphorylation and accelerated ATP hydrolysis by mitochondrial ATP synthase. ATP depletion following MTP leads abruptly to necrotic cell death (Farber, 1982; Borgers *et al*., 1983; Lofrumento *et al.,* 1991; Parks *et al.,* 2001; Lemasters *et al,* 1999). On the other hand, energy depletion can lead to mitochondrial swelling, with secondary opening of mitochondrial permeability transition pores. Induction of MPT state has also been associated with the progression of apoptotic cell death, and the release of apoptotic factors (Cai *et al*., 1998; Korge *et al.,* 2001; Lemasters *et al*., 1998; Qian et al., 1997). Therefore, low energy state induced by neurotoxic OP compounds in this study suggests that alteration of free ATP production could lead to cell death by necrosis as well as by apoptosis, secondary to MPT state (Massicotte *et al.,* 2001). These findings support the view that mitochondria are a primary target in the response to exposure to neuropathy-inducing OP compounds, and they are affected by two different mechanisms, mitochondrial permeability transition and energy depletion.

The alterations in ATP production demonstrated in our investigation support other studies showing variations in mitochondrial energy metabolism in cells exposed to OP compounds. Mitochondrial membrane depolarization (Holmuhamedov *et al*., 1996; Carlson and Ehrich, 1999; Poppe *et al.,* 2001), inhibition of mitochondrial oxygen consumption and respiration, and reduction of oxidative phosphorylation have been documented following OP exposure (Spetale *et al*., 1976; Sitkiewick *et al*., 1980; Skonieczna *et al*., 1980).

Mitochondrial membrane depolarization could modify the H+ proton pump across the mitochondrial membrane, causing failure of ATP coupling, and disruption of the mitochondrial respiratory chain reactions (Rustin *et al.,* 1994). Other metabolic pathways affected by OP compounds include oxidation of succinate, α-glycerophosphate, and pyruvate/malate substrates (Holmuhamedov *et al*., 1996), all of which are ATP dependent reactions. Therefore, it is likely that the alterations in ATP concentrations observed in our study are relevant, and possibly central events that could contribute to the pathogenesis of OPIDN observed *in vivo*.

The depletion in ATP concentrations noted in our neuronal cell cultures treated with neuropathy-inducing compounds could participate in the distal, non-terminal neuronal degeneration observed *in vivo*, possibly related to alteration in axonal transport. ATP has been proposed to fulfil an important part of the metabolic and energetic demands required in all phases of axonal transport (Goodrum and Morell, 1992; Tanford, 1983). The long axons spanning the large separation between the cell body and the nerve terminal require specialized axonal transportation systems. Rapid movement of material (rate between 200-400 mm/day) down the axon is defined as fast axonal anterograde transport (Goodrum and Morell, 1992). The motor molecule for anterograde movement is thought to be kinesin, an ATPase consisting of two large subunits (alpha), and two small subunits (beta). Kinesin forms cross-bridges between the moving membranous organelles. The fast anterograde transport system depends on oxidative metabolism, and is independent of the cell body (Kandel *et al.,* 1991). Disruption in retrograde axonal transport has been reported in OPIDN (Moretto *et al.,* 1987). It is likely that the decreased ATP production, as it was observed in our neuronal cells preparations, may lead to disruption of axonal transport, with secondary segmental swelling, and ultimately axonal degeneration.

In conclusion, this study demonstrated clearly that neuropathy-inducing OP compounds cause alterations in ATP production within neuronal cell cultures. Depletion in ATP concentration occurred only after exposure to compounds capable of causing OPIDN. Neuronal mitochondria are the primary site of injury following exposure to neuropathy-inducing compounds, and these mitochondria are being targeted both at the MPT pore and all complexes, particularly complex I, of the respiratory chain. The induction of MPT is likely to result in disruption of the mitochondrial membrane potential, which affect the proton gradient across its membrane, and subsequently cause a reduction in ATP production. These early event can contribute to alteration in neuronal ATP production previously reported in OPIDN. The profound ATP depletion and the induction of MPT can induce the release of apoptotic factors and intramitochondrial ions, leading to axonal damage observed later in the course of OPIDN.

5.6. ACKNOWLEDGEMENTS

The authors gratefully acknowledge the technical assistance of Wen Li, Kristel Fuhrman, Elizabeth Grabeau, and Daniel Ward without whom this work could not have been performed. Virginia-Maryland Regional College of Veterinary Medicine has primarily supported this work.

5.7. REFERENCES:

Abou-Donia, M.B. (1981). Organophosphorus ester-induced delayed neurotoxicity. *Ann Rev. Pharmacol. Toxicol.* **21,** 511-548.

Abou-Donia, M.B., Trofatter, L.P., Graham, D.G., Lapadula, D.M. (1986). Electromyographic, neuropathologic, and functional correlates in the cat as the results of tri-o-cresyl phosphate delayed neurotoxicity. *Toxicol. Appl. Pharmacol.* **83**, 126.

Babcock, G.T., Wikstrom, M. (1992). Oxygen activation and the conservation of energy in cell respiration. *Nature* **356**, 301-309.

Barber, D., Hunt, J., Ehrich, M. (2001). Inhibition of calcium-stimulated ATPase in the hens brain P2 synaptosomal fraction by organophosphorus esters: relevance to delayed neuropathy. *J. Toxicol. Environ. Health* **63,** 101-113.

Berman, S.B., Watkins, S.C., Hastings, T.G. (2000). Quantitative biochemical and ultrastructural comparison of mitochondrial permeability transition in isolated brain and liver mitochondria: evidence for reduced sensitivity of brain mitochondria. *Exp. Neurol.* **164**, 415-425.

Bernardi, P., Scorrano, L., Colonna, R., Petronilli, V., Di Lisa, F. (1999). Mitochondria and cell death. Mechanistic and methodological issues. *Eur. J. Biochem.* **264,** 687-701.

Bernardi P. (1996). The permeability transition pore. Control points of a cyclosporin A-sensitive mitochondrial channel involved in cell death. *Biochim. Biophys. Acta.* **1275,** 5-9.

Bigalow, J.E., Varnes, M.E., Jacobson, B., Koch, C.J. (1983). Factors influencing the oxygen consumption and radiation response of cultured mammalian cells. *Adv. Exp. Med. Biol.* **159**, 347-359.

Blood, L.A. (1975). Scanning electron microscope observations of the outgrowth from embryonic chick dorsal root ganglia in culture. *Neurobiology* **5,** 75-83.

Borgers, M., Thone, F., Van Reempts, J., Verheyen, F. (1983). The role of calcium in cellular dysfunction. *Am. J. Emerg. Med.* **2,** 154-161.

Bouldin, T.W., Cavanagh, J.B. (1979a). Organophosphorous neuropathy. 1. Teased fiber studies. *Am. J. Path.* **94,** 241-247.

Bouldin, W.T., Cavanagh, J.B. (1979b). Organophosphorous neuropathy. *Am. J. Path.* **94**, 253-261.

Cai, J., Yang, J., Jones, D.P. (1998). Mitochondrial control of apoptosis: the role of cytochrome *c*. *Biochem. Biophys. Acta.* **1366,** 139-149.

Capaldi, R.A. (1990). Structure and function of cytochrome *c* oxidase. *Ann. Rev. Biochem.* **59**, 569-596.

Carboni, D., Ehrich, M., Dyer, K., Jortner, B.S. (1992). Comparative evolution of mipafox-induced delayed neuropathy in rats and hens. *Neurotoxicology* **14**, 723-733.

Carlson, K., Ehrich, M. (1999). Organophosphorus compound-induced modification of SH-SY5Y human neuroblastoma mitochondrial transmembrane potential. *Toxicol. Appl. Pharmacol.* **160,** 33-42.

Carlson, K., Jortner, B.S., Ehrich, M. (2000). Organophosphorus compound-induced apoptosis in SH-SY5Y human neuroblastoma cells. *Toxicol. Appl. Pharmacol.* **168,** 102-113.

Cassarino, D.S., Swerdlow, R.H., Parks, J.K., Parker, W.D. Jr., Bennett, J.P. Jr. (1998). Cyclosporin A increases resting mitochondrial membrane potential in SY5Y cells and reverses the depressed mitochondrial membrane potential for Alzheimer's disease cybrids. *Biochem. Biophys. Res. Commun.* **248**, 168-173.

Clark, J.B., Nicklas, W.J. (1970). The metabolism of rat brain mitochondria. *J. Biol. Chem.* **245**, 4724-4731.

Crompton, M. (1999). The mitochondrial permeability transition pore and its role in cell death. *Biochem. J.* **341,** 233-249.

Ecobichon, D.J. (1994). Organophosphorus insecticides. In: DJ Ecobichon and RM Joy (Eds.), *Pesticides and Neurological Diseases* CRC Press Inc., Bocca Raton, FL, 171-249.

Ehrich, M., Jortner, B.J. (2001). Organophosphorus-induced delayed neuropathy. In: *Neurotoxicology Handbook*, Massaro, E.J., ed., Totowa, NJ: Human Press, pp. 17-27.

El-Fawal, H.A.N., Jortner, B.S., Eyre, P., Ehrich, M. (1988). The biventer cervicis nerve-muscle preparation of adult hens: effect of phenylsaligenin phosphate administration. *Neurotoxicology* **9,** 625-636.

El-Fawal, H.A.N, Jortner, B.S., Ehrich, M. (1990). Use of the biventer cervicis nerve-muscle preparation to detect early changes following exposure to organophosphates inducing delayed neuropathy. *Fund. Appl. Tox.* **15,** 108-120.

EL-Fawal, H.A.N., Jortner, B.S., Ehrich, M. (1990). Modification of phenylsaligenin phosphate-induced delayed effects by calcium channel blockers: *in vivo* and *in vitro* electrophysiological assessment. *Neurotoxicology* **11**, 573-592.

Farber, J.L. (1982). Biology of disease: membrane injury and calcium homeostasis in the pathogenesis of coagulative necrosis. *Lab. Invest.* **47,** 114-123.

Fillingame, R.H. (1992). H^+ transport and coupling by the F_0 sector of the ATP synthase: insights into the molecular mechanism of function. *J. Bioenerg. Biomemb.* **24**, 485-491.

Fiskum, G. (1983). Involvement of mitochondria in ischemic cell injury and in regulation of intracellular calcium. *Am. J. Emerg. Med.* **2**, 147-153.

Fiskum G. (1985). Mitochondrial damage during cerebral ischemia. *Ann. Emer. Med.* **14**, 810-815.

Garcia-Ruiz, C., Colell, A., Mari, M., Morales, A., Fernandez-Checa, J.C. (1997). Direct effect of ceramide on the mitochondrial electron transport chain leads to generation of reactive oxygen species. Role of mitochondrial glutathione. *J. Biol. Chem.* **272**, 11369-11377.

Goodrum, J.F., Morell, P. (1992). Axonal transport. In: *Neurotoxicology*, Abou-Donia MB, ed. CRC Press, pp 79-119.

Green, D.R., Reed, J.C. (1998). Mitochondria and apoptosis. *Science* **281**, 1309-1312.

Griffin JW, Watson DF. (1988). Axonal transport in neurological disease. *Ann. Neurol.* **23**, 3-13.

Halestrap, A.P., Davidson, A.M. (1990). Inhibition of Ca^{2+} -induced large amplitude swelling of liver and heart mitochondria by cyclosporine is probably caused by the inhibitor binding to mitochondrial-matrix peptidylprolyl cis-trans isomerase and preventing it interacting with the adenine nucleotide translocase. *Biochem. J.* **268,** 153-160.

Hernandez, A.F., Pla, A., Villanueva, E. (1989). Decreased phosphofructokinase activity during the development of triorthocresyl-phosphate-induced delayed neuropathy. *Toxicol. Lett.* **49**, 35-40.

Hofhaus, G., Weiss, H., Leonard, K. (1991). Electron microscopic analysis of the peripheral and membrane parts of mitochondrial NADH dehydrogenase (complex I). *J. Mol. Biol.* **221**, 1027-1043.

Hofhaus, G., Shakeley, R.M., Attardi, G. (1996). Use of polarography to detect respiration defects in cell cultures. *Methods Enzymol.* **264**, 476-483.

Holmuhamedov, E.L., Wang, L., Terzic, A. (1999). ATP-sensitive K^+ channel openers prevent Ca^{2+} overload in rat cardiac mitochondria. *J. Physiol.* **519,** 347-360

Hunter, D.R., Haworth, R.A. (1979). The Ca^{2+} -induced membrane transition in mitochondria. I. The protective mechanisms. *Arch. Biochem. Biophys.* **195,** 453-459.

Hunter, D.R., Haworth, R.A. (1979). The Ca^{2+} -induced membrane transition in mitochondria. II. Nature of the Ca^{2+} trigger site. *Arch. Biochem. Biophys.* **195,** 460-467.

Imberti, R., Nieminen, A.L., Herman, B., Lemasters, J.J. (1993). Mitochondrial and glycolytic dysfunction in lethal injury to hepatocytes by *t*-butyl hydroperoxide: protection by fructose, oligomycin, cyclosporin A and trifluoperazine. *J. Pharmacol. Exp. Therap.* **265**, 392-400.

Johnson, M.K. (1982). The target for initiation of delayed neurotoxicity by organophosphorus esters. *Rev. Biochem. Toxicol.* **8,** 141-212

Jortner, B.S., Ehrich, M. (1987). Neuropathological effects of phenyl saligen phosphate in chickens. *Neurotoxicology* **8,** 97-108.

Kandel, E.R., Schwartz, J.H., Jessel, T.M. (1991). *Principles of Neural Sciences* (3rd ed). NewYork, Elsever, pp. 49-62.

Kleitman, N., Wood, P.M., Bunge, R.P. (1995). Tissue culture methods for the study of myelination. In: *Culturing Nerve Cells*, Banker G, Goselin K (eds)., Cambridge, Massachussetts Institute of Technology, pp. 545-594.

Knoth-Anderson, J., Veronesi, B., Jones, K., Lapadula, D.M., Abou-Donia, M.B. (1992). Triphenyl phosphite-induced ultrastructural changes in bovine adrenomedullary chromaffin cells. *Toxicol. Appl. Pharmacol.* **112**, 110-119.

Korge, P., Honda, H.M., Weiss, J.N. (2001). Regulation of the mitochondrial permeability transition by matrix Ca^{2+} and voltage during anoxia/reoxygenation. *Am. J. Physiol.* **280,** C517-C536.

Kutty, R.K., Santostasi, G., Horng, J., Krishna, G. (1991). MPTP-induced ATP depletion and cell death in neuroblastoma X glioma hybrid NG 108-15 cells: protection by glucose and sensitization by tetraphenylborate. *Toxicol. Appl. Pharmacol.* **107**, 377-388.

Lapadula, E.S., Lapadula, D.M., Abou-Donia, M.B. (1992). Biochemical changes in sciatic nerve of hens treated with tri-o-cresyl phosphate: increased phosphorylation of cytoskeletal proteins. *Neurochem. Int.* **20**, 247-255.

Lemasters, J.J., Hackenbrock, C.R. (1979). Continuous measurement of adenine triphosphate with firefly luciferase luminescence. *Methods Enzymol.* **56**, 530-544.

Lemasters, J.J., Nieminen, A.L., Qian, T., Trost, L.C., Elmore, S.P., Nishimura, Y., Crowe, R.A., Cascio, W.E., Bradham, C.A., Brenner, D.A,. Herman, B. 1998; The mitochondrial permeability transition in cell death: A common mechanism in necrosis, apoptosis and autophagy. *Biochim. Biophys. Acta.* **1366,** 177-196.

Lemasters, J.J., Qian, T., Bradham, C.A., Brenner, D.A., Casico, W.E., Trost, L.C., Nishimura, Y., Nieminen, A.L., Herman, B. (1999). Mitochondrial dysfunction in the pathogenesis of necrotic and apoptotic cell death. *J. Bioenerg. Biomembr.* **31,** 305-319.

Lofrumento, N.E., Marzulli, D., Cafagno, L., La Piana, G., Cipriani, T. 1991; Oxidation and reduction of exogenous cytochrome c by the activity of the respiratory chain. *Arch. Biochem. Biophys.* **288**, 293-301.

Lundin, A. (2000). Use of firefly luciferase in ATP-related assays of biomass enzymes, and metabolism. *Methods Enzymol.* **305**, 346-370.

Massicotte, C., Inzana, K.D., Ehrich, M., Jortner, B.S. (1999). Neuropathologic effects of phenylmethylsulfonyl fluoride (PMSF)-induced promotion and protection in organophosphorus ester-induced delayed neuropathy (OPIDN) in hens. *Neurotoxicology* **20**, 749-760.

Massicotte, C., Barber, D.S., Jortner, B.S., Ehrich, M. (2001a). Nerve conduction and ATP concentrations in sciatic-tibial and medial plantar nerves of hens given phenylsaligenin phosphate. *Neurotoxicology* **22,** 91-98.

Massicotte, C., Jortner, B.S., Ehrich, M. (2001b). Effects of neuropathy-inducing organophosphorus compounds on mitochondrial permeability transition in primary dorsal root ganglia cell cultures. *Toxicol. Appl. Pharmacol.*, to be submitted.

Minamikawa, T., Williams, D.A., Bowser, D.N., Nagley, P. (1999). Mitochondrial permeability transition and swelling can occur reversibly without inducing cell death in intact human cells. *Exp. Cell. Res.* **246,** 26-37.

Mochida, K., Gomyoda, M., Fujita, T., Yamagata, K. (1988). Tricresyl phosphate and triphenyl phosphate are toxic to cultured human, monkey and dog cells. *Zbl. Batk. Hyg. B.* **185,** 427-429.

Moretto, A., Lotti, M., Sabri, M., Spencer, P.S. (1987). Progressive deficit of retrograde axonal transport is associated with the pathogenesis of di-n-butyl dichlorvos axonopathy. *J. Neurochem.* **49,** 1515-1522.

Nemienen, A.L., Saylor, A.K., Tesfai, S.A., Herman, B., Lemasters, J.J. (1995). Contribution of the mitochondrial permeability transition to lethal injury after exposure of hepatocytes to t-butylhydroxyperoxide. *Biochem. J.* **307,** 99-106.

Nostrandt, A.C., Ehrich, M. (1992). Developement of a model cell culture system in which to study early effects of neuropathy-including organophosphorus esters. *Toxicol. Lett.* **60**, 107-114.

Parks, J.K., Smith, T.S., Trimmer, P.A., Bennett, J.P., Parker, W.D. Jr. (2001). Neurotoxic Abeta peptides increase oxidative stress *in vivo* through NMDA-receptor and nitric-oxide-synthase mechanisms, and inhibit complex IV activity and induce a mitochondrial permeability transition *in vitro*. *J. Neurochem.* **76**, 1050-1056.

Pederson, P.L., Amzel, L.M. (1993). ATP synthases. Structure, reaction center, mechanism, and regulation of one of nature's most unique machines. *J. Biol. Chem.* **268**, 9937-9940.

Penefsky, H.S., Cross, R.L. (1991). Structure and mechanism of F_0F_1-type ATP synthases and ATPases. *Advan. Enzymol. Mol. Biol.* **64**, 173-214.

Petit, P.X., Zamzami, N., Vayssiere, J.L., Mignotte, B., Kroemer, G., Castedo, M. (1997). Implication of mitochondria in apoptosis. *Mol. Cell. Biochem.* **174,** 185-188.

Poppe, M., Reimertz, C., Düßmbann, H., Krohn, A.J., Luetjens, C.M., Böckelmann, D., Nieminen, A.L., Kögel, D., Prehn, J.H.M. (2001). Dissipation of potassium and proton gradients inhibits mitochondrial hyperpolarization and cytochrome *c* release during neural apoptosis. *J. Neurosci.* **21,** 4551-4563.

Qian, T., Nieminen, A.L., Herman, B., Lemasters, J.J. (1997). Mitochondrial permeability transition in pH-dependent reperfusion injury to rat hepatocytes. *Am. J. Physiol.* **273,** C1783-C1792.

Randall, J.C., Yano, B.L., Richardson, R.J. (1997). Potentiation of organophosphorus compound-induced delayed neurotoxicity (OPIDN) in the central and peripheral nervous system of the adult hen: distribution of axonal lesions. *J. Toxicol. Environ. Health.* **51,** 571-590.

Robinson, B.H. (1996). Use of fibroblast and lymphoblast cultures for detection of respiratory chain defects. *Methods Enzymol.* **264**, 454-464.

Rustin, P., Chretien, D., Bourgeron, T., Gerard, B., Rotig, A., Saudubray, J.M., Munnich, A. (1994). Biochemical and molecular investigations in respiratory chain deficiencies. *Clinica. Chimica. Acta.* **228**, 35-51.

Shiratti, V., Krishna, G. (1985). A simple and sensitive method for monitoring drug-induced cell injury in cultured cells. *Anal. Biochem.* **147**, 410-418.

Sitkiewick, D., Skonieczna, M., Krzywicka, K., Dziedzic, E., Staniszewaska, K., Bicz W. (1980). Effect of organophosphorus insecticides on the oxidative processes in rat brain synaptosomes. *J. Neurochem.* **34**, 619-626.

Skonieczna, D., Sitkiewick, D., Bicz, W. (1980). Modification of oxidative phosphorylation in brain mitochondria during development and aging by the oxygen analog of Ronnel. *Pest. Biochem. Physiol.* **14,** 314-318.

Stanley, P.E. (1986). Extraction of adenosine triphosphate from microbial and somatic cells. *Methods Enzymol.* **133**, 14-22.

Steyn, S.J., Mienie, L.J., Van der Schyf, C.J. (2000). β-oxidation of [9, 10(n)-3H] palmitate by human leukocytes: a simple *in situ* assay to assess mitochondrial toxicity in the presence of toxins. *Toxicol. Meth.* **10,** 99-109.

Steyn, S.J., Pieterse, D.J., Mienie, L.J., Van der Schyf, C.J. (2001). Measurement of mitochondrial resipration in permeabilized murine neuroblastoma (N-2α) cells, a simple *in situ* assay to investigate mitochondrial inhibitory properties of toxins. *Toxicol. Methods*, in press.

Tanford, C. (1983). Mechanism of free energy coupling in active transport. *Ann. Rev. Biochem.* **52**, 379-409.

Tuler, S.M., Bowen, J.M. (1989). Toxic effect of organophosphates on nerve cell growth and ultrastructure in culture. *J. Toxicol. Environ. Health* **27,** 209-223.

Varon, S., Skaper, S.D., Manthorpe, M. (1981). Trophic activities for dorsal root and sympathetic ganglionic neurons in media conditioned by Schwann and other peripheral cells. *Dev. Brain Res.* **1,** 73-87.

Ventura, F.V., Ruiter, J.P.N., Ijlst, L., Almeida, I.T., Wanders, R.J.A. (1995). Inhibition of oxidative phosphorylation by palmitoyl-CoA in digitonin permeabilized fibroblasts: implications for long-chain fatty acid B-oxidation disorders. *Biochim. Biophys. Acta* **1272**, 14-20.

Veronesi, B., Ehrich, M. (1993). Using neuroblastoma cell lines to examine organophosphate neurotoxicity. *In Vitro* **6,** 57-65.

Wanders, R.J.A., Ruiter, J.P.N., Wijburg, F.A. (1993). Studies on mitochondrial oxidative phosphorylation in permeabilized human skin fibroblasts: application to mitochondrial encephalomyopathies. *Biochem. Biophys. Acta* **1181**, 219-222.

Wanders, R.J.A., Ruiter, J.P.N., Wijburg, F.A. (1994). Mitochondrial oxidative phosphorylation in digitonin-permeabilized chorionic villus fibroblasts: A new method with potential for prenatal diagnosis. *J. Inher. Meta. Dis.* **17**, 304-306.

Wanders, R.J.A., Ruiter, J.P.N., Wijburg, F.A., Zeman, J., Klement, P., Houstek, J. (1996). Prenatal diagnosis of systemic disorders of the respiratory chain in cultured chorionic villus fibroblasts by study of ATP-synthesis in digitonin-permeabilized cells. *J. Inherit. Metab. Dis.* **19**, 133-136.

Weiss, H., Friedrich, T., Hofhaus, G., Preis, D. (1991). The respiratory-chain NADH dehydrogenase (complex I) of mitochondria. *Euro. J. Biochem.* **197**, 563-576.

Wolvetang, E.J., Tager, J.M., Wanders, R.J. (1990). Latency of the peroxisomal enzyme acyl-CoA: dihydroxyacetonephosphate acyltransferase in digitonin-permeabilized fibroblasts: the effect of ATP and ATPase inhibitors. *Biochem. Biophys. Res. Commun.* **170,** 1135-1143.

Wood, P. (1976) Separation of functional Schwann cells and neurons from normal peripheral nerve tissue. *Brain Res.* **155,** 361-375

Zahrebelski, G., Nieminen, A.L., al-Ghoul, K., Qian, T., Herman, B., Lemasters, J.J. (1995). Progression of subcellular changes during chemical hypoxia to cultured rat hepatocytes: a laser confocal microscopic study. *Hepatology* 21, 1361-1372.

Zoratti, M., Szabo, I. (1995). The mitochondrial permeability transition. *Biochem. Biophys. Acta* **1241,** 139-176.

FIG. 1. Complex-specific ATP production in neuronal cell cultures 12 hours post-exposure to 1 μM of OP compounds in the presence of complex-specific substrates or ADP only. Substrates for complexes I, III, and IV were malate, glycerol-3-phosphate and N,N,N',N'-tetramethyl-p-phenylenediamine, respectively. In the exclusive presence of ADP, neuropathy-inducing mipafox and PSP caused significant reduction in ATP production, compared to controls ($p < 0.05$, indicated by *). Mipafox and PSP also severely diminished complex I (CI*) driven ATP production compared to controls. ATP concentrations were also significantly reduced by mipafox and PSP in complexes III and IV (mean ± SEM, expressed as pmol of ATP/cell; $p < 0.05$, indicated by *). There were no significant differences in ATP concentrations between the controls and paraoxon, an OP that does not induce delayed neuropathy *in vivo*.

FIG. 2. Concentration of ATP produced in neuronal cell cultures 12 hours post-exposure to 1 μM of OP compounds in the presence of complex-specific xenobiotics. ATP produced by complex I, III and IV was measured in the presence of 20 μg/ml of rotenone, 10 μg/ml of antimycin and 10 mM of sodium azide, respectively. Neuropathy-inducing mipafox and PSP had significantly reduced ATP production at all complex levels, when compared to DMSO or paraoxon treated neuronal cell cultures.

Concentrations of ATP following OP exposure

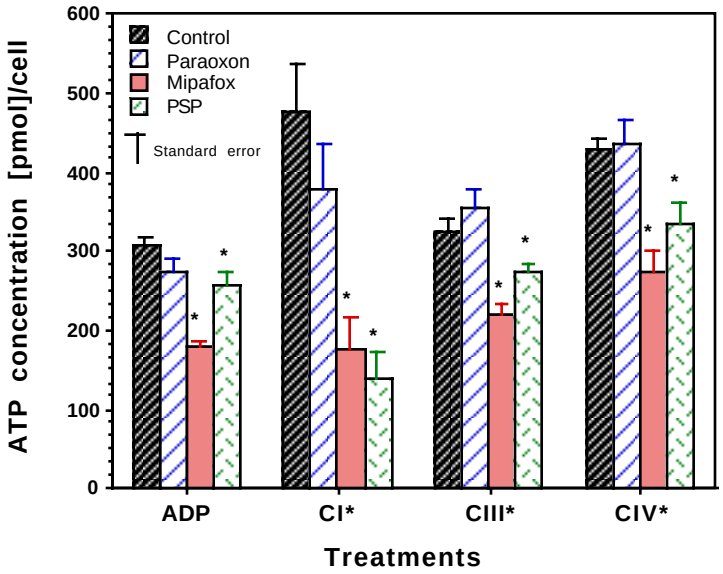

Fig. 1.

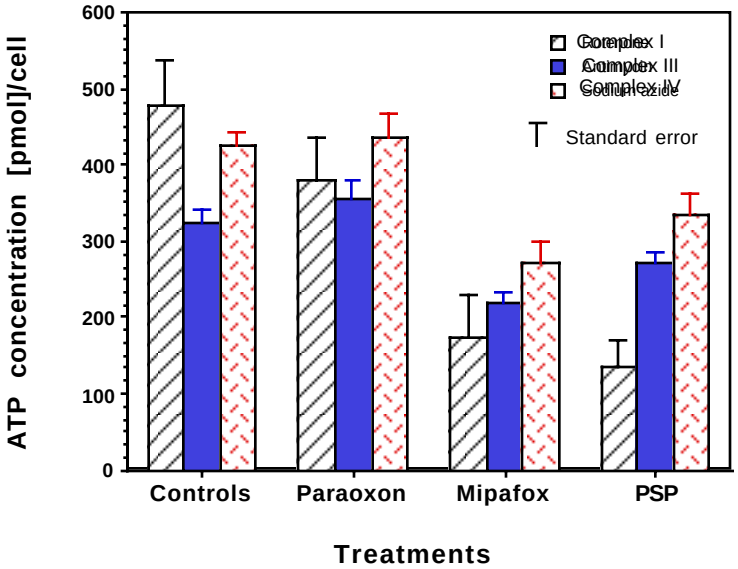
ATP concentration [pmol]/cell
600
500
400
300
200
100
0
Complex I
Complex III
Complex IV
Standard error
Controls
Paraoxon
Mipafox
PSP
Treatments

Fig. 2.

PART IV: CHAPTER 6

MORPHOLOGICAL EFFECTS OF NEUROPATHY-INDUCING (OP) COMPOUNDS IN PRIMARY DORSAL ROOT GANGLIA CELL CULTURES.

Authors:

Christiane Massicotte

Bernard S. Jortner

Marion Ehrich

Virginia-Maryland Regional College of Veterinary Medicine

Laboratory for Neurotoxicity Studies, VA-MA Regional College of Veterinary Medicine,

1 Duckpond Drive

Blacksburg, VA 24061-0442.

Phone: 540-231-4621

Fax: 540-231-6033

Email: marion@vt.edu

Running title:

Morphological alterations in OP-exposed DRG

6.1. ABSTRACT

Chick embryo DRG cultures were used to explore early pathological events associated with exposure to neuropathy-inducing OP compounds. This approach used an *in vitro* neuronal system from the species that provides the animal model for OP-induced delayed neuropathy (OPIDN). DRG were obtained from 9 day old chick embryos, and grown for 14 days in minimal essential media (MEM) supplemented with bovine and human placental sera and growth factors. Cultures were then exposed to 1 μM of OP compounds phenylsaligenin phosphate (PSP) or mipafox, which readily elicit OPIDN in hens, paraoxon, which does not cause OPIDN, or the DMSO vehicle. The media containing these toxicants was removed after 12 hours, and cultures maintained for 4 to 7 days post-exposure. Morphometric analysis of neurites was performed by inverted microscopy, which demonstrated that neurites treated with mipafox or PSP but not with paraoxon had reversible axonal swelling at day 4 post-exposure which reversed by 7 days. Ultrastructural alterations of neurons included mitochondrial swelling and rarefaction of microtubules and neurofilaments. These were more severe following exposure to PSP and mipafox. Paraoxon treated neuronal cell cultures showed no ultrastructural changes compared to DMSO controls. This study supports others that suggested mitochondria are a primary target for neuropathy-inducing OP compounds, and contribute to subsequent axonal swelling.

Key words: organophosphorus, dorsal root ganglia, morphology, and morphometry.

6.2. INTRODUCTION

Some known organophosphorus (OP) compounds can induce delayed neuropathy, resulting axonopathy progressing to myelinated fiber degeneration within peripheral nerves and spinal cord tracts of susceptible animals beginning seven to fourteen days after exposure (Dyer *et al.*, 1991; Ecobichon, 1994; Ehrich and Jortner, 2001; El-Fawal *et al.*, 1988, 1990; Jortner and Ehrich, 1987, 1989; Massicotte *et al.*, 1999). Morphological study of lesions of organophosphorus compounds-induced delayed neuropathy (OPIDN) has been enhanced by techniques such as perfusion fixation, plastic embedding, light microscopy and ultrastructural examination (Bischoff, 1967, 1970; Bouldin and Cavanagh 1979b; Ehrich and Jortner, 2001).

Morphological lesions of OPIDN have been described in different animal species (rats, cats, monkey, sheep, and chickens) using tri-*ortho*-tolyl phosphate (TOTP), diisopropyl-fluoro-phosphate (DFP), phenylsaligenin phosphate (PSP), and mipafox as toxicants (Abou-Donia *et al.*, 1981, 1990; Bishoff, 1967; Bouldin and Cavanagh, 1979; Carboni *et al.*, 1992; Ehrich *et al.*, 1995; Ehrich and Jortner 2001; US EPA, 1991). Chickens were considered the most appropriate animal for the study of OPIDN because they exhibited locomotor deficits associated with distinct, well-defined bilateral lesions in the spinal cord (mainly long tracts), brain stem, cerebellum, and peripheral nerves. Lesions of OPIDN as seen by light microscopy were best observed with appropriately stained sections from epoxy resin embedded tissue. In the early stages of axonal degeneration, there were focal regions of poor axoplasmic staining, swelling, and associated thin myelin sheaths. Dark-staining intra-axonal debris accumulated in the axoplasm, especially in paranodal regions. Fragmentation of damaged fibers ensued as the process evolved into the Wallerian-like stage, with axonal and myelin ovoids, debris accumulation, and phagocytosis by Schwann cells. Axons became shrunken with disorganized and altered myelin sheaths

(Jortner and Ehrich, 1987; Prineas, 1969). The onset and severity of lesions correlated with clinical neurological abnormalities (Ehrich *et al.,* 1995; Massicotte *et al.,* 1999). Using standard single neurotoxic dosages, the first lesions were noted approximately on days 4-7, when a few degenerated fibers were observed (El-Fawal *et al.,* 1988, 1990). By day 21, severe and extensive degeneration was seen in the majority of susceptible subjects exposed to appropriate dosages of neurotoxicants (Ehrich *et al.,* 1995; Jortner and Ehrich, 1987; Massicotte *et al.,* 1999). Lesions in the myelin sheaths were also seen secondary to the axonal alterations. In peripheral nerve, intra-myelin vacuoles were observed within the extra-cellular space of the intraperiod line of the myelinated sheaths, closest to the axon (i.e., between the inner loop of Schwann cell cytoplasm and the most inner dense line of the myelinated sheaths) (Bouldin and Cavanagh, 1979b). The deterioration of the myelin sheaths and axons formed ovoids that were phagocytized by Schwann cells (Bishoff, 1985). Subsequently, Wallerian degeneration occurred with complete loss of the axon and myelin sheath distal to the presumed site of injury. These were replaced by compact bands of proliferative Schwann cells, the so-called Buengner's bands, in peripheral nerve.

Several reports used transmission electron microscopy to describe changes observed in axons, myelin and fiber terminals of animals with OPIDN. In distal levels of affected axons, OP compounds caused early axoplasmic accumulation of branching cisternal membranous structures, resembling agranular reticulum, prior to swelling and further nerve fiber degeneration (Bischoff, 1967,1970; Bouldin and Cavanagh, 1979b; Prineas, 1969). As axonal degeneration proceeded, changes consisted of loss of neurotubules and neurofilaments, degenerated mitochondria, accumulation of vacuoles, membranous structures and dense bodies, granular transformation and reduction of axoplasm were noted (Bischoff, 1967,1970; Bouldin and Cavanagh, 1979b; Lapadula *et al.,* 1992; Prineas, 1969). Marked focal axonal non-terminal, mid internodal vacuoles gave rise to swellings (varicosities), and degeneration associated with paranodal demyelination (Bouldin and

Cavanagh, 1979). End-stage Wallerian-like fiber degeneration revealed the presence of axonal and myelin debris in Schwann cells (Prineas, 1969). It has been postulated that OP compounds produce neuropathy by being bound to unknown proteins of the myelin sheath or axonal membrane, causing membrane damage, altering directly or indirectly the regulation of the transmembrane ionic gradient. Passive influx of water then accumulates within the area of intra-period gaps, forming vacuoles in the intracellular space (Ghadially, 1988). Accumulation and agglutination of proliferated vesicular elements have also been reported to be a common feature in presynaptic endings. These were shown to be mingled with crowded circular membrane complexes and myelin figures. Also, dark presynaptic terminals rich with condensed organelles and tangled filamentous structures were seen (Bishoff, 1970).

In addition to the morphological changes described in animal models with OPIDN, OP-induced cytotoxicity has been demonstrated *in vitro* (Carlson and Ehrich, 1999; Carlson *et al.,* 2000; Ehrich *et al.,* 1997; Mochida *et al.,* 1988). *In vitro* systems have been used to examine the cellular mechanisms associated with the pathogenesis of OPIDN, as such studies are difficult in animal models. For example, immortal cell lines have been used for evaluation of fragmentation of DNA and apoptotic mechanisms (Carlson and Ehrich, 1999; Carlson *et al.,* 2000), and for observation of morphological changes associated with cell death (Harvey and Sharma, 1980; Knoth-Anderson *et al.,* 1992; Tuler and Bowen, 1989). *In vitro* alterations of metabolic processes and energy production have included inhibition of glucose metabolism (Harvey and Sharma, 1980), and decreased incorporation rate of ^{3}H-adenosine into ATP (Knoth-Anderson *et al.,* 1992).

Effects of nerve growth factors and toxicants including OP compounds have been previously described in neuronal cell cultures, using morphometric analysis of processes and growth cones (Argiro *et al.,* 1985; Castellanos *et al.,* 2000; Doane *et al.,* 1992; Kawa

et al., 1998; Oorschot *et al.,* 1991; Saxod and Bizet, 1988; Tosney and Landmesser, 1985; Ventimiglia *et al.,* 1995; Windebank *et al.,* 1985; Yamada *et al.,* 1971). In most of these studies, the length and diameter of growth cones were the most accurate morphometric measurement of neuronal cell dynamics (Nishiyama *et al.,* 1994; Saxod and Bizet, 1988; Unchern *et al.,* 1994). These studies provided rapid, efficient and unbiased approaches to measure conformational modulations of neurons in culture. Although several morphometric investigations evaluated neuronal responses to toxicants, morphometric analysis has not been yet performed for OP compounds causing delayed neuropathy using primary cell preparations.

The morphological effects of OP compound exposure on primary neuronal cell cultures from chicken embryos, the US EPA approved species for OPIDN testing (US EPA, 1991) are described here. Although structural alterations in mitochondria have been previously demonstrated following OP exposure in other cell culture systems (Knoth-Anderson *et al.,* 1992; Antuned-Madeira *et al.,* 1994; Carlson and Ehrich, 1999), specific data related to structural effects following exposure to neuropathy-induced OP compounds in primary DRG cultures are not found in the literature. The present study describes lesions in neuronal cell cultures from chicken DRG after exposure to neuropathy-inducing OP compounds, using inverted and electron microscopic methods of imaging, and morphometric analysis of neurites. Then, these morphological changes were compared to those observed *in vivo*.

6.3. EXPERIMENTAL METHODS

Organophosphorus compound preparations.

Phenylsaligenin phosphate (PSP), synthesized by Lark Enterprises (Webster, MA), and mipafox purchased from Chem Services Inc. (West Chester, PA), were used because they induce delayed neuropathy *in vivo* (Ehrich *et al.,* 1995). Paraoxon (Chem Services) was used as a non-neuropathic OP control. Stock solutions containing PSP, mipafox, and paraoxon at 100 mM were prepared by dissolving these OP compounds in dimethyl sulfoxide (DMSO). In this study, cytotoxic effects of the OP compounds were determined by using a primary neuronal cell culture exposed to physiological concentrations of PSP, mipafox and paraoxon (1 μM). Negative controls received DMSO (0.1%) vehicle only. The exposure time was 12 hours, based on previous studies that demonstrated OP-induced effects on mitochondria in a neuroblastoma cell line in that period of time (Carlson and Ehrich, 1999).

Neuronal preparation from dorsal root ganglia cultures.

Dorsal root ganglia of 9-days old chick embryos were dissected under sterile conditions from the lumbar intumescence (Blood, 1975; Eldrige *et al.,* 1989; Kleitman *et al.,* 1995; Varon *et al.,* 1981; Wood, 1976). Under a dissecting microscope, the embryo was laid on its back and the abdominal viscera were removed with care to prevent damage of the DRG underneath. The lumbar DRGs were collected using microdissecting forceps, and transferred to a solution containing L-15 media. Strict sterile procedures were observed during dissections and in all subsequent steps of the purifying processes.

Following DRG collection from approximately 30 embryos, the ganglia were incubated with 0.25% trypsin for 45 min at 37°C on a rotatory shaker. Trypsin inactivation was achieved by the addition of L-15 media (Sigma Cell Culture Product, L-5520) supplemented with 15-20% fetal bovine serum (FBS). Then the sample was centrifuged at 1000 rpm for 5 min, and the pellets resuspended and triturated in 1 ml of serum-containing medium. The volume of this suspension was increased to 5 ml, recentrifuged as before, and resuspended in the 10 ml of a solution containing Eagle's minimum essential medium (E-MEM, Sigma Cell Culture Product, M-0643), supplemented with 5% human placental serum (HPS, Scantibodies Laboratory, Inc, Santee, California), 50 ng/ml of nerve growth factor (NGF, fraction 2.5S, murine, natural, Gibco BRL), 5 mg/L y-irradiated and lyophilized bovine insulin (Sigma, I-1882), 10 mg/L human transferrin (98% purity, Sigma, T-3309), 20 nM progesterone (Sigma, P-0130), 30 nM sodium selenite anhydrous (Johnson Matthew Electronics, Ward Hill, MA, E-07B17), and 100 μM tetramethylenediamine dihydrochloride (98% purity, Sigma, P-7505). One drop of this suspension was plated in the center of a round 35-mm poly-d lysine coated glass bottom (no. 1.5) coverslip (P35 GC-1.5-10-C, Mat Tek Corporation, Ashland, MA).

After the cells had been allowed to attach to collagen for 12 hours, the purification procedure was initiated by refeeding the cell culture with a solution containing antimitotic agents (E-MEM, 5% HPS, 498 mg/dl glucose, 50 ng/ml NGF, 10 mg/L transferrin, 100 μM putrescine, 20 nM progesterone, 5 mg/L bovine insulin, 30 nM sodium selenite, 10 μM uridine, 10 μM FdU). The antimitotic protocol was accomplished by alternating antimitotic feedings with maintenance feedings according to the following schedule: maintenance feeding on days 1, 4-6, 8-10 and day 12 onward, and antimitotic feeding on days 2-4, and 6-8. Prior to performing experiments, the purified neuronal cultures were allowed to rest in maintenance media for one week to ensure that no residual FdU remained. These neuronal cultures will often degenerate with FBS when they are kept longer than 21 days; therefore,

since less neuronal degeneration occurs with the use of HPS, this supplement was used to maintain the purified neuronal cell cultures (Kleithman *et al.*, 1995).

For morphological studies, the neuronal cells were exposed for 12 hours to 1 μM PSP, mipafox, and paraoxon. Media containing OP compounds were removed at 12 hours, and the culture was kept in the previously described maintenance media for an additional 4 to 7 days prior to analysis. Morphometric data were obtained using inverted microscopy images. Two cultures dishes for each treatment were used (N=2), and several images were recorded from each treated dish (subsample, n=50), using the Oncor Image software system (Gaithersburg, MD). Following further magnification with Photoshop Software, neurites were outlined on the computer (n=50/dish) and analyzed with Adobe Photoshop software (Morphometric Analysis Tool Kit, 3.0). Parameters estimated for the evaluation of axonal integrity 4 and 7 days following OP exposures included the radial length, and maximum and mean diameters (Argiro *et al.*, 1985; Castellanos *et al.*, 200; Doane *et al.*, 1992; Kawa *et al.*, 1998; Nishiyama *et al.*, 1994; Oorschot *et al.*, 1991; Saxod and Bizet, 1988; Unchern *et al.*, 1994; Ventimiglia *et al.*, 1995; Windebank *et al.*, 1985). The actual radial length was calculated from a line drawn parallel to the axon (axonal length), centered at a 90° angle with the axonal membrane (axonal radius). The mean axonal diameter was determined by taking the mean of 20 equally spaced axonal diameter readings within the axon of one neuron, at 90° with the axonal membrane (axonal diameters). The maximum diameter represented the greatest axonal diameter recorded during calculations of the mean axonal diameter. Based on these values, length to diameter ratios representing general swelling (LD = total axonal radial length/mean diameter) and axonal segmental swelling (s = [(maximum axonal diameter - mean axonal diameter)/ mean axonal diameter] X 100) were calculated for each axon evaluated. Random sampling was used for estimation of all parameters (Mayhew, 1990). The cell area chosen were selected by dividing the round bottom dish into four quadrants. Only one of the quadrants, selected prior to cell culture

purification, was evaluated for morphological studies (light and electron microscopy). The results were expressed as mean ± SEM from duplicate experiments (N=2 cell culture dishes), where the diameters and radial lengths of 50 axons were measured for each treated dish (n = 50). Statistical significance ($p < 0.05$) of mean values among treatments regardless of day post-challenge were determined using a one way analysis of variance with the PC-SAS software (version 6.1). Then, a least significant difference (LSD) test was performed to compare the means among treatments within each day (4 and 7) (mean ± SEM, $p<0.05$).

For transmission electron microscopy, the 2.5% gluteraldehyde-fixed cell cultures were post-fixed for 2 hours in 2% OsO_4 in 0.1 M phosphate buffer at pH 7.4, and washed with 0.1 M phosphate buffer solution. Following post-fixation, the tissues were dehydrated in graded concentrations of ethanol (15%, 30%, 50%, 70%, 95%, 100%), and cleared in propylene oxide. The samples were then infiltrated with 50:50 propylene oxide/epoxy resin for 24 hours, followed by 100% epoxy resin for at least 24 hours. Cells were embedded in an epoxy resin and were polymerized in a 60 °C oven for 24-48 hours. Selected blocks were cut at 80 nm, and then placed on new 200 mesh grids (2-3 grids for each block). These thin sections were first stained with 2% uranyl acetate to enhance contrast of nucleic acid-containing structures and subsequent lead citrate staining. The latter staining agent was used to enhance staining of membranes of cellular components. The grids were rinsed with distilled water, dried, and placed in a grid box, with care taken to record grid identity on a grid box form. These thin sections were examined using a JEOL JEM-100CX II transmission electron microscope. For each treated cell culture dish (n=2), 100-125 electron micrographs (axons and perikaryon) were taken and evaluated by two observers, one of whom was blinded to the treatment groups. The morphological changes observed in the treated dishes were compared to controls, and these observations were based on an agreement from both evaluators. The electron microscopy findings were then compared to neuronal cell culture pathology previously described in the literature.

6.4. RESULTS

6.4.1 Morphometric analysis of neurites exposed to OP compounds.

Axonal parameter differences among treatment groups were evident when the neuronal cultures were viewed by inverted microscopy (Fig. 1). In control cultures (N=2), the mean neurite diameters were 0.2330 ± 0.0005 μm at day 4, and 0.24 ± 0.07 μm at day 7 post-exposure. The mean neurite diameters obtained for neuronal populations treated with OP compounds were not different from the controls, and were not significantly altered by the age of the culture. In contrast, lengths of the neurites were significantly altered by the age of the culture, independently of the treatments received. Total radial lengths of neurites in the neuronal cultures exposed for 12 hours to OP compounds were not significantly different than controls at any time during this study (Fig 2a). The overall length to diameter (LD) ratios were significantly greater at day 7 post-exposure compared to day 4, independent of the treatments received. There were significantly lower LD ratios for cultures treated with mipafox (LD = 9.6 ± 0.2) and PSP (LD = 9.4 ± 0.9) compared to control neuronal populations (LD = 14.9 ± 2.6) and cells exposed to paraoxon (12.5 ± 0.4) at day 4 post-exposure. However, no differences were detected among treatment groups at day 7 post-exposure (Fig. 2b). In addition, there was a tendency toward increased swelling of the neurites when the cultures were exposed to OP compounds compared to controls (s = 42 ± 5) at day 7 post-exposure. At this time, cells exposed to paraoxon demonstrated significant segmental axonal swelling (s = 61 ± 2). Cells exposed to mipafox (s = 51 ± 4) showed distinctive segmental swelling of the neurites (Fig. 2c).

6.4.2. Electron microscopic evaluation

Control and paraoxon treated cultures revealed similar morphological features. The perikaryal cytoplasm of their neuronal cell bodies was rich in organelles, with prominent Golgi, polyribosomes, rough endoplasmic reticulum, vesicles, neurofilaments and mitochondria (Fig. 3a). Rough endoplasmic reticulum and most mitochondria ended at the initial segment of each axon (Fig 3b). There was a prominent subplasma membrane mass of polyribosomes and ribosomes. The proximal axon was also rich in neurofilaments. Axonal processes contained dense cores and pale vesicles, microtubules, and smooth endoplasmic reticulum (Fig. 3c). In the course of the axon, structural features observed included mitochondria, dense core and pale vesicles, microtubules, neurofilaments, smooth endoplasmic reticulum, and occasional swellings in small neurites, which usually contained mitochondria. Normal mitochondrial structures were present in these cell cultures, including a smooth and regular double layer membrane surrounding lamellar, tubular and vesicular cristae within the more electron dense matrix. A few mitochondria showed swelling of the matrix, with decreased in electron density, and modest increased mitochondria size. Marked local swelling of the distal regions of axons were occasionally present, with increased separation of microtubules and filaments, dense core and clear vesicles (Fig. 3d). Lysis of plasma membrane, cytoplasmic swelling, altered mitochondria, disordered cristae, matrix dense deposit, membranous debris and increased lipid droplets were present in low numbers. A few putative macrophages were also detected in some samples.

Cultures treated with the neuropathy-inducing OP compounds mipafox and PSP showed different morphological features. For example, numerous and extensive necrotic debris were detected in the PSP treated cultures (Fig 4a). A few viable axonal regions were seen. These neurites had numerous swellings along their course and at their terminals, or growth cones, which were more numerous than in control cells. The swellings contained

increased dense core and clear vesicles, and there was increased separation of microtubules, and granular degeneration of microtubules and neurofilaments (Fig. 4b). Some regions of neurofilament aggregates were seen. These changes progressed to lytic regions, neuritic rupture and debris formation. Some degenerative swelling consisted of masses of membranous cytoplasmic bodies, or of microtubules and neurofilaments (Fig. 4b). Similar observations were made for mipafox treated neuronal cells, although changes were somewhat less severe. In both cases, there was a reduction in microtubule-rich, thin axons, so common in controls. In the OP treated cultures, these neurites often appeared thicker, with numerous mitochondrial swellings. In addition, groups of axons showed a sequence of swelling with increasing separation and dissolution of microtubules and neurofilaments, and mitochondrial degeneration, progressing toward marked cell swelling and degeneration. Neuronal populations treated with mipafox or PSP showed frequent and more severe mitochondrial damage within their cell body and neurites than in the control populations. In the early stage of mitochondrial degeneration, swelling of the matrix was observed frequently, with increased mitochondria size and progressive dissolution of the matrix. More severe signs of mitochondrial degeneration were frequently encountered, including disordered cristae, matrix dense deposit, membranous debris and increased lipid droplets. Advanced stages of mitochondrial injury were frequently observed in these treated neuronal populations, characterized by a dense matrix containing some intramatrical granules. Mitochondrial membranes were irregular, with blebbing of inner and outer membranes progressing to complete disruption, resulting in mitochondrial dissolution.

6.5. DISCUSSION

Cultures of dorsal root ganglia (DRG) can achieve neuronal maturation making them useful for neurobiological studies. They have not, however, previously been used to investigate quantitative and qualitative morphological changes that occur following exposure to neuropathy-inducing organophosphorus (OP) esters. The present study is the first time that electron microscopy was used to evaluate morphological effects of neuropathy-inducing OP compounds in chick DRG neuronal cell cultures. Since the adult hen is considered the most reliable animal model for the study of OPIDN (Abou-Donia, 1981, 1986; US EPA, 1991), this *in vitro* neuronal cell model is unique because it allows investigation of OP compounds in a target species. The DRG, although removed from chicks, which are susceptible to OPIDN but less than adults (Funk *et al.,* 1994), could be used to measure axonal processes in relatively mature neuronal cultures. This primary cell culture preparation is the closest *in vitro* representation for neuronal effects occurring *in vivo*; therefore, it has potential usefulness for studies of pathogenic mechanisms at the cellular level.

This study is also unique because it used a morphological method of imaging in a living neuronal DRG cell culture model. Measurements were taken at day 4 and day 7 post-exposure to OP compounds since the earliest neuropathological changes in hens were observed at day 4 (El-Fawal *et al.,* 1990). OP exposures were only 12 hours in an attempt to mimic loss of OP compounds through biotransformation *in vivo*. This dosing paradigm, which included transient exposure to the toxicant, may be the reason why we were unable to provide statistical significance for the effects on neurite length, although a trend to lesser length was noted. Diameter of the very long, thin DRG neurites did not provide much information, and neurite lengths were affected by day of maturation. Microscopy of DRG cultures and calculation of the LD ratio support the suggestion that exposure to neuropathy-

inducing OP compounds contributed to general axonal swellings. The early changes in LD ratios and the axonal swellings were seen on day 4 but reversed by 7 days post-exposure. Our findings may support previous studies in which axonal regeneration was observed in hens after dosing with OP compounds capable of inducing delayed neuropathy (Jortner *et al.,* 1989). Segmental axonal swelling (s) was also observed in paraoxon treated cultures at day 7 post exposure, and although not statistically significant, the % of segmental swellings were greater at day 7 post-exposure to OP compounds. Overall, the relatively small sampling size and the dosing paradigm chosen in this current study may have resulted in relatively high variability, decreasing the probability for statistical differences of some parameters examined. The small number of plates (N=2) decreased the power of the statistical tests performed in this study, but by increasing the number of neurites analyzed (n=50/plate), we obtained a much better estimation of the means. Large culture plates were required to allow full growth of axons, but the need for many embryos and expensive media containing NGF and human placental serum prohibited an experimental design with a large sample size. Differences between cultures treated with neuropathy-inducing OP compounds and controls were, however, evident when viewing the cultures by inverted light microscopy. Other studies using same parameters measured time-related changes in DRG cell cultures, sometimes in the presence of growth factors (Argiro *et al.,* 1985; Castellanos *et al.,* 2000; Doane *et al.,* 1992; Nishiyama *et al.,* 1994; Ventimiglia *et al.,* 1995). In our study, we also found that time in culture made a difference in measurements since the axonal length of the axon was greater at day 7 compared to day 4.

The current study used a completely computerized procedure for morphometric analysis, allowing standardized quantification of parameters to be evaluated, including length, and complete distribution of axonal diameters. Previous morphometric analysis performed on neurites used a laborious and time-consuming method of parameter assessment in which all neuronal processes were drawn by hand (Argiro *et al.,* 1985; Kawa

et al., 1998; Nishiyama *et al.,* 1994)). The method described here, which utilized a relatively simple software program, greatly facilitated calculations of neuronal parameters of interest compared to previous studies. However, inverted microscopic evaluation of axonal changes is less sensitive than electron microscopic changes and the small sample size for the inverted microscopic method of axonal evaluation may have contributed to variability noted within treatment groups.

Electron microscopy performed on the neuronal DRG cells used in this study provided high resolution of cellular ultrastructure within the perykarion and axon. Using this method, extensive damage to mitochondria and neurites was seen. Lesions of axons and their growth cones previously described in the literature were used as references for the present study (Bray and Bunge, 1981; Bunge and Bunge, 1984; Cheville, 1983; Dyck *et al.,* 1993; Fadic *et al.,* 1985; Fried *at al.,* 1970; Ghadially, 1988; Gray, 1975; Lee and Cleveland, 1994; Liem *et al.,* 1978; Peters *et al.,* 1991; Westrum *et al.,* 1976). The results of this study demonstrate that the DRG cell model is more appropriate to study the effects of neuropathy-inducing compounds than previous studies using immortalized cell lines (Nostrandt *et al.,* 1992; Taylor *et al.,* 1995) because the latter do not allow sufficient neurite outgrowth to provide a substrate for axonal degeneration observed *in vivo*. In fact, there have been some questions whether immortalized cell line neurites contain the same cytoskeletal elements as do true axons (Taylor *et al.,* 1995). Segmental axonal swelling was frequently observed in the neuronal cells described in this study, resembling to the morphological changes previously reported *in vivo*. Severe swellings of the growth cone and segmental axonal swelling were frequently observed in this current study, which corresponded with previous studies showing distal, non terminal axonal degeneration as a primary feature of OPIDN (Bouldin and Cavanagh, 1979). Axonal swellings in the present study were associated with progressive dissolution of microtubules and neurofilaments. This corresponds to the morphological changes described as primary features of OPIDN *in vivo*

(Bishoff, 1970; Prineas, 1969). The accumulation of cisternal membranous structures along the growth cones and the agglutination of proliferated elements within the presynaptic endings observed in DRG treated with neuropathy-inducing OP compounds resembled the early lesions of OPIDN reported *in vivo* models (Bishoff, 1967, 1970; Bouldin and Cavanagh, 1979b; Prineas, 1969).

In addition, the current study supports other *in vitro* and *in vivo* models that demonstrated the toxic effects of OP compounds on mitochondria. For example, a recent study demonstrated that mitochondrial permeability transition (MPT) occurred in neuronal dorsal root ganglia cell cultures exposed to neuropathy-inducing OP compounds (Massicotte *et al.,* 2001a). When mitochondria undergo MPT in a cell, ATP becomes progressively depleted secondary to uncoupling of oxidative phosphorylation and accelerated ATP hydrolysis by mitochondrial ATP synthase (Berman *et al.,* 2000; Crompton, 1999; Farber, 1982; Lemaster *et al,* 1979, 1999; Lofrumento *et al.,* 1991; Parks *et al.,* 2001). ATP depletion has also been noted in DRG cultures exposed to neuropathy inducing OP compounds (Massicotte *et al.,* 2001b). The energy depletion can lead to mitochondrial swelling, with secondary opening of mitochondrial permeability transition pores. Since compromised mitochondria are likely to serve as a precursor of a cascade of events resulting in ultimate neuronal necrosis, the OP-induced damage to this organelle may contribute to the neuropathological changes seen both in neuronal DRG cell cultures and in distal axonal damage observed in animals. Our morphological findings support the idea that the mitochondria are a primary target in the development of OPIDN.

In conclusion, the lesions observed in chick embryos DRG cell cultures exposed to neuropathy-inducing OP compounds were similar to some of the morphological changes described in hens with OPIDN. In future studies, higher dosages or more prolonged exposures might be used since chicks are not as susceptible as adults to the effects of these

toxicants (Funk *et al.,* 1994). However, DRG cultures provide the closest and most differentiated *in vitro* model for evaluation of the effects of neuropathy-inducing compounds at the cellular level.

6.6. ACKNOWLEDGEMENTS

The authors gratefully acknowledge the technical assistance of Virginia Viers, Kathy Lowe, Sandy Hancock, Kristel Fuhrman, Wen Li, Sandy Hancock, and Daniel Ward without whom this work could not have been performed. Virginia-Maryland Regional College of Veterinary Medicine has primarily supported this work.

6.7. REFERENCES

Abou-Donia MB. Organophosphorus ester-induced delayed neurotoxicity. *Ann Rev Pharmacol Toxicol* 1981; 21: 511-548.

Abou-Donia MB, Lapadula M. Mechanisms of organophosphorus ester-induced delayed neurotoxicity: Type I and Type II. Ann Rev Pharmacol Toxicol 1990; 30: 405-440.

Andreyev A, Fiskum G. Calcium induced release of mitochondrial cytochrome *c* by different mechanisms selective for brain versus liver. *Cell Death Differ* 1999; 6: 825-832.

Antunes-Madeira MC, Videira RA, Madeira VMC. Effects of parathion on membrane organization and its implications for the mechanisms of toxicity. *Biochim. Biophys. Acta* 1994; 1190: 149-154.

Argiro V, Bunge MB, Johnson MI. A quantitative study of growth cone filopodial extension. J Neurosci Res 1985; 13: 149-162.

Berman SB, Watkins SC, Hastings TG. Quantitative biochemical and ultrastructural comparison of mitochondrial permeability transition in isolated brain and liver mitochondria: evidence for reduced sensitivity of brain mitochondria. *Exp Neurol* 2000; 164: 415-425.

Bernadi P. The permeability transition pore. Control points of a cyclosporin A-sensitive mitochondrial channel involved in cell death. *Biochim Biophys Acta* 1996; 1275: 5-9.

Bischoff A. The ultrastructure of tri-ortho-cresyl phosphate poisoning. I. Studies on myelin and axonal alterations in the sciatic nerve. *Acta Neuropath (Berl.)* 1967; 9: 158-174.

Bischoff A. Ultrastructure of tri-ortho-cresyl phosphate poisoning in the chicken. II. Studies on spinal cord alterations. *Acta Neuropath (Berl.)* 1970; 15: 142-155.

Bischoff A. The ultrastructure of tri-ortho-cresyl phosphate-poisoning. I. Studies on myelin and axonal alterations in the sciatic nerve. *Acta Neuropath (Berl.)* 1985; 9: 158-174.

Blood LA. Scanning electron microscope observations of the outgrowth from embryonic chick dorsal root ganglia in culture. *Neurobiology* 1975; 5: 75-83.

Bouldin WT, Cavanagh JB. Organophosphorous neuropathy. *Am J Path* 1979b; 94: 253-261.

Bray D, Bunge MB. Serial analysis of microtubules in cultured rat sensory axons. *J Neurocytol* 1981; 10: 589-605.

Bunge RP, Bunge MB. Tissue culture observations relating to peripheral nerve development, regeneration, and disease. In: *Peripheral Neuropathy*, Dyck PJ, Thomas PK, Lambert EH, Bunge RP, eds., Philadelphia, W.B. Saunders Company, 1984, pp 378-399.

Cai J, Yang J, Jones DP. Mitochondrial control of apoptosis: the role of cytochrome *c*. *Biochem Biophys Acta* 1998; 1366: 139-149.

Carboni D, Ehrich M, Dyer K, Jortner BS. Comparative evolution of mipafox-induced delayed neuropathy in rats and hens. *Neurotoxicology* 1992; 14: 723-733.

Carlson K, Ehrich M. Organophosphorus compound-induced modification of SH-SY5Y human neuroblastoma mitochondrial transmembrane potential. *Toxicol Appl Pharmacol* 1999; 160: 33-42.

Carlson K, Jortner BS, Ehrich M. Organophosphorus compound-induced apoptosis in SH-SY5Y human neuroblastoma cells. *Toxicol Appl Pharmacol* 2000; 168: 102-113.

Castellanos JE, Martinez M, Acosta O, Hurtado H. Nerve growth factor and neurotrophin-3 modulate the rabies infection of adult sensory neurons in primary cultures. *Brain Res* 2000; 871: 120-126.

Cavanagh JB. The toxic effects of tri-ortho-cresyl phosphate on the nervous system. An experimental study in hens. *J Neurol Neurosurg Psychiat* 1954; 17: 163-172.

Cavanagh JB. Peripheral nerve changes in ortho-cresyl phosphate poisoning in the cat. *J Pathol* 1964; 87: 365-382.

Cheville NF. Cell degeneration. In: *Cell Pathology* , Cheville NF, 2nd ed., Ames, The Iowa State University Press, 1983, pp 114-129.

Crompton M. The mitochondrial permeability transition pore and its role in cell death. *Biochem J* 1999; 341: 233-249.

Doane KJ, Roisen FJ, Wilson FJ. The effects of nerve growth factor and dibutyryl cyclic AMP on cytoskeletal densities in cultured sensory ganglia. Tissue Cell 1992; 24: 367-378.

Dyck PJ, Giannini C, Lais A. Pathologic alterations of nerves. In: *Peripheral Neuropathy*, Dyck PJ, Thomas PK, eds., Philadelphia, PA, W.B. Saunders company 1993, pp 514-597.

Dyer KR, El-Fawal HAN, Ehrich MF. Comparison of organophosphate-induced delayed neuropathy between branches of the tibial nerve and the biventer cervicis nerve in chickens. *Neurotoxicology* 1991; 12: 687-696.

Ecobichon DJ. Organophosphorus insecticides. In: *Pesticides and Neurological Diseases*, Ecobichon DJ, Joy RM eds., CRC Press Inc., 1994, Bocca Raton, FL, 171-249.

Ehrich M, Jortner BJ. Organophosphorus-induced delayed neuropathy. In: *Neurotoxicology Handbook*, Massaro EJ, ed., Totowa, NJ, Human Press, 2001, pp 17-27.

Ehrich M, Correll L, Veronesi B. Acetylcholinesterase and neuropathy target esterase inhibitions in neuroblastoma cells to distinguish organophosphorus compounds causing acute and delayed neurotoxicity. *Fundam Appl Toxicol* 1997; 38: 1-9

Ehrich M, Jortner BS, Padilla S. Comparison of the relative inhibition of acetylcholinesterase and neuropathy target esterase in rats and hens given cholinesterase inhibitors. *Fund Appl Toxicol* 1995; 24: 94-101.

Eldrige CF, Bunge MB, Bunge R. Differentiation of axon-related Schwann cells in vitro: II. Control of myelin formation by basal laminal. *J Neurosci* 1989; 9: 625-638.

El-Fawal HAN, Jortner BS, Eyre P, Ehrich M. The biventer cervicis nerve-muscle preparation of adult hens: effect of phenylsaligenin phosphate administration. *Neurotoxicology* 1988; 9: 625-636.

El-Fawal HAN, Jortner BS, Ehrich M. Use of the biventer cervicis nerve-muscle preparation to detect early changes following exposure to organophosphates inducing delayed neuropathy. *Fund Appl Tox* 1990; 15: 108-120.

EL-Fawal HAN, Jortner BS, Ehrich M. Modification of phenylsaligenin phosphate-induced delayed effects by calcium channel blockers: *in vivo* and *in vitro* electrophysiological assessment. *Neurotoxicology* 1990; 11: 573-592.

Fadic R, Vergara J, Alvarez J. Microtubules and caliber of central and peripheral processes of sensory axons. *J Comp Neurol* 1985; 236: 258-264.

Farber JL. Biology of disease: membrane injury and calcium homeostasis in the pathogenesis of coagulative necrosis. *Lab Invest* 1982; 47: 114-123.

Funk KA, Henderson JD, Liu CH, Higgins RJ, Wilson BW. Neuropathology of organophosphate-induced delayed neuropathy (OPIDN) in young chicks. *Arch Toxicol* 1994; 68: 308-316.

Fried RL, Samorajsky T. Axon caliber related to neurofilaments and microtubules in sciatic fibers of rats and mice. *Anat Rec* 1970; 167: 379-387.

Garcia-Ruiz C, Colell A, Mari M, Morales A, Fernandez-Checa JC. Direct effect of ceramide on the mitochondrial electron transport chain leads to generation of reactive oxygen species. Role of mitochondrial glutathione. *J Biol Chem* 1997; 272: 11369-11377.

Ghadially FN. Mitochondria. In: *Ultrastructural Pathology of the Cell and Matrix,* Ghadially FN, 3rd ed., London, Butterworths, 1988, pp 191-328.

Ghadially FN. Microtubules. In: *Ultrastructural Pathology of the Cell and Matrix,* Ghadially FN, 3rd ed., London, Butterworths, 1988, pp 937-950.

Goodrum JF, Morell P. Axonal transport. In: *Neurotoxicology*, Abou-Donia MB, ed. CRC Press, 1992, pp 79-119.

Gray EG. Presynaptic microtubules and their association with synaptic vesicules. *Royal Soc B* 1975; 190: 369-372.

Green DR, Reed JC. Mitochondria and apoptosis. *Science* 1998; 281: 1309-1312.

Harvey MJ, Sharma RP. Organophosphate cytotoxicity: The effects on protein metabolism in cultured neuroblastom cells. *J Environ Pathol Toxicol* 1980; 3: 423-436.

Jortner BS, Shell L, El-Fawal H, Ehrich M. Myelinated nerve regeneration following organophosphorus ester-induced delayed neuropathy. *Neurotoxicology* 1989; 10: 717-726.

Jortner, B.S., Ehrich, M. Neuropathological effects of phenylsaligenin phosphate in chickens. *Neurotoxicology* 1987; 8: 97-108.

Kawa A, Stahlhut M, Berezin A, Bock E, Berezin V. A simple procedure for morphometric analysis of processes and growth cones of neurons in culture using parameters derived from the contour and convex hull of the object. *J Neurosci Methods* 1998; 79: 53-64.

Kleitman N, Wood PM, Bunge RP. Tissue culture methods for the study of myelination. In: *Culturing Nerve Cells*, Banker G, Goselin K (eds)., Cambridge, Massachussetts Institute of Technology, 1995, pp 545-594.

Knoth-Anderson J, Veronesi B, Jones K, Lapadula DM, Abou-Donia MB. Triphenyl phosphite-induced ultrastructural changes in bovine adrenomedullary chromaffin cells. *Toxicol Appl Pharmacol* 1992; 112: 110-119.

Lapadula ES, Lapadula DM, Abou-Donia MB. Biochemical changes in sciatic nerve of hens treated with tri-o-cresyl phosphate: increased phosphorylation of cytoskeletal proteins. *Neurochem Int* 1992; 20: 247-255.

Lee MK, Cleveland DW. Neurofilament function and dysfunction: involvement in axonal growth and neuronal disease. *Curr Opin Cell Biol* 1994; 6: 34-40.

Lemasters JJ, Hackenbrock. Continuous measurement of adenine triphosphate with firefly luciferase luminescence. *Methods Enzymol* 1979; 56: 530-544.

Lemasters JJ, Qian T, Bradham CA, Brenner DA, Casico WE, Trost LC, Nishimura Y, Nieminen AL, Herman B. Mitochondrial dysfunction in the pathogenesis of necrotic and apoptotic cell death. *J Bioenerg Biomermbr* 1999; 31: 305-319.

Lemasters JJ, Qian T, Elmore SP, Trost LC, Nishimura Y, Herman B, Bradham CA, Brenner DA, Nieminen AL. Confocal microscopy of the mitochondrial permeability transition in necrotic cell killing, apoptosis and autophagy. *Biofactors* 1998; 8: 283-285.

Liem RKH, Yen SH, Salomon GD, Shelanski ML. Intermediate filaments in nervous tissue. *J Cell Biol* 1978; 79: 637-645.

Lofrumento NE, Marzulli D, Cafagno L, La Piana G, Cipriani T. Oxidation and reduction of exogenous cytochrome c by the activity of the respiratory chain. *Arch Biochem Biophys* 1991; 288: 293-301.

Massicotte C, Inzana KD, Ehrich M, Jortner BS. Neuropathologic effects of phenylmethylsulfonyl fluoride (PMSF)-induced promotion and protection in organophosphorus ester-induced delayed neuropathy (OPIDN) in hens. *Neurotoxicology* 1999; 20: 749-760.

Massicotte C, Barber DS, Jortner BS, Ehrich M. Nerve conduction and ATP concentrations in sciatic-tibial and medial plantar nerves of hens given phenylsaligenin phosphate. *Neurotoxicology* 2001a; 22: 91-98.

Massicotte C, Van der Schyf C, Jortner BS, Ehrich M. Effects of neuropathy-inducing OP compounds on mitochondrial ATP production in primary dorsal root ganglia cell cultures.*Toxicol Appl Pharmacol* 2001b; for submission.

Massicotte C, Jortner BS, Ehrich M. Effects of neuropathy-inducing OP compounds on mitochondrial permeability transition in primary dorsal root ganglia cell cultures.*Toxicol Appl Pharmacol* 2001; for submission.

Mayhew TM. Effecient and unbias sampling of nerve fibers for estimating fiber number and size. In: *Quantitative and qualitative microscopy*, Conn PM ed., San Diego, CA, Academic Press Inc., 1990, pp 172-187.

Minamikawa T, Williams DA, Bowser DN, Nagley P. Mitochondrial permeability transition and swelling can occur reversibly without inducing cell death in intact human cells. *Exp Cell Res* 1999; 246: 26-37.

Mochida K, Gomyoda M, Fujita T, Yamagata K. Tricresyl phosphate and triphenyl phosphate are toxic to culture human, monkey and dog cells. *Zbl Batk Hyg B* 1988; 185: 427-429.

Moretto A, Lotti M, Sabri M, Spencer PS. Progressive deficit of retrograde axonal transport is associated with the pathogenesis of di-n-butyl dichlorvos axonopathy. *J Neurochem* 1987; 49: 1515-1522.

Nishiyama N, Cho SI, Saito H. Malonylginsenoside Rb1 potentiates nerve growth factor (NGF)-induced neurite outgrowth of culture chick embryonic dorsal root ganglia. *Biol Pharm Bull* 1994; 17: 509-513.

Nixon RA, Sihag RK. Neurofilament phosphorylation: a new look at regulation and function. *Trends Neurosci* 1991; 15: 501-506.

Nostrandt AC, Ehrich M. Developement of a model cell culture system in which to study early effects of neuropathy-including organophosphorus esters. *Toxicol Lett* 1992; 60: 107-114.

Oorschot DE, Peterson DA, Jones DG. Neurite growth from, and neuronal survival within cultured explants of the nervous system: a critical review of morphometric and stereological methods, and suggestions for the future. *Prog Neurobiol* 1991; 37: 525-546.

Parks JK, Smith TS, Trimmer PA, Bennett JP, Parker WD Jr. Neurotoxic Abeta peptides increase oxidative stress in vivo through NMDA-receptor and nitric-oxide-synthase mechanisms, and inhibit complex IV activity and induce a mitochondrial permeability transition *in vitro*. *J Neurochem* 2001; 76: 1050-1056.

Peters A, Palay SL, Webster HF. The axon. In: *The Fine Structure of the Nervous System*, Peters A, ed., NewYork, Oxford University Press, 1991, pp 101-137.

Prineas J. The pathogenesis of dying-back polyneuropathies. I. An ultrastructural study of experimental tri-ortho-cresyl phosphate intoxication on the cat. *J Neuropathol Exp Neurol* 1969; 28: 571-597.

Poppe M, Reimertz C, Düßmbann H, Krohn AJ, Luetjens CM, Böckelmann D, Nieminen AL, Kögel D, Prehn JHM. Dissipation of potassium and proton gradients inhibits mitochondrial hyperpolarization and cytochrome *c* release during neural apoptosis. *J Neurosci* 2001; 21: 4551-4563.

Qian T, Herman B, Lemasters JJ. The mitochondrial permeability transition mediates both necrotic and apoptotic death of hepatocytes exposed to Br-A23187. *Toxicol Appl Pharmacol* 1999; 154: 117-125.

Saxod R, Bizet MC. Substrate effects on the dynamics of neurite outgrouwth in vitro: a quantitative multi-parametric analysis. *Int J Dev Neurosci* 1988; 6: 177-191.

Taylor DD, Jortner BS, Walton A, Ehrich M. An immunohistochemical study of the cytoskeleton of SH-SY5Y human neuroblastoma cells, and the effects of acrylamide. *In Vitro Toxicol* 1995; 8: 323-333.

Tosney KW, Landmesser LT. Growth cone morphology and trajectory in the lumbosacral region of the chick embryo. *J Neurosci* 1985; 5: 2345-2358.

Tuler SM, Bowen JM. Toxic effect of organophosphates on nerve cell growth and ultrastructure in culture. *J Toxicol Environ Health* 1989; 27: 209-223.

Unchern S, Nagata K, Saito H, Fukuda J. Reduction of neurite extension by piperine, examined on hippocampal and septal neurons in serum free cultures. *Biol Pharm Bull* 1994; 17: 898-901.

US EPA. Pesticide assessment guidelines, subdivision F. Hazard evaluation: human and domestic animals. Addendum 10: neurotoxicity, series 81, 82, 83. National Technical Information Service, Springfield, VA; 1991: 1-60.

Varon S, Skaper SD, Manthorpe M. Trophic activities for dorsal root and sympathetic ganglionic neurons in media conditioned by Schwann and other peripheral cells. *Dev Brain Res* 1981; 1: 73-87.

Ventimiglia R, Jones BE, Moller A. A quantitative method for morphometric analysis in neuronal cell culture: unbiased estimation of neuron area and number of branch points. J *Neurosci Methods* 1995; 57: 63-66.

Westrum LE, Gray EG. Microtubules and membrane specialization. *Brain Res* 1976; 105: 547-550.

Windebank AJ, Wood P, Bunge RP, Dyck PJ. Myelination determines the caliber of dorsal root ganglion neurons in culture. *J Neurosci* 1985; 5: 1563-1569.

Wood P. Separation of functional Schwann cells and neurons from normal peripheral nerve tissue. *Brain Res* 1976; 155: 361-375

Yamada KM, Spooner BS, Wessells NK. Ultrastructure and function of growth cones and axons of cultured nerve cells. *J Cell Biol* 1971; 49: 614-635

FIGURES:

Fig. 1. Light micrographs of chick DRG cultures for morphometric analysis. (a) Control at day 4 post-dosing (0.1% DMSO). (b). Culture 4 days after a 12 hour exposure to 1μM mipafox showing significant swelling of the neurites compared to controls (20X).

Fig. 2. Results of morphometric studies showing OP compound effects on DRG cultures 4 and 7 days post-exposure. (a). Effects of OP compounds on neurite radial lengths at days 4 and 7 days post-exposure. Radial lengths were calculated for each neurite evaluated (N = 2 plates, per treatment, n = 50 observation/plate). Radial lengths of the neurites were altered by the age of the culture. Total radial lengths of neurites in the neuronal cultures exposed to OP compounds were not significantly different than controls at days 4 and day 7 post-exposure. (b). Effects of OP compounds on the calculated LD ratios at days 4 and day 7 post-exposure. Neurite radial length to diameter ratios (LD = total radial length/mean diameter, LD = mean ± SEM) were calculated (N = 2 plates, n = 50 observations/plate). The LD ratios were significantly smaller for cultures exposed to mipafox (LD = 9.6 ± 0.2) and PSP (LD = 9.4 ± 0.9) compared to control neuronal populations (LD = 14.9 ± 2.6) and cells dosed with paraoxon (12.5 ± 0.4), at day 4 post-dosing. LD ratios of treated cultures were significantly greater at day 7 post-dosing compared to day 4, and no differences were present among treatment groups. (c). Effects of OP compounds were also determined as segmental swelling of the neurites [s = [(maximum diameter - mean diameter)/mean diameter] X 100) at days 4 and 7 post-exposure. Segmental swelling of the neurites was detected 7 days post-exposure to OP compounds, especially paraoxon, compared to controls (s =61 ± 2) (20 X).

Fig. 3. Control neuronal cell population of DRG cultures. (a). The perikaryal cytoplasm is rich in organelles, with prominent Golgi, polyribosomes, rough endoplasmic reticulum, vesicles, and mitochondria. (b). In the initial segment of axon are rough endoplasmic reticulum and neurofilaments. At the proximal axonal level, mitochondria are diminished. Moreover, the proximal neurofilament-rich axon contains prominent subplasma membrane masses of polyribosomes and ribosomes. (c). The neurites contain dense core and pale vesicles, microtubules, and smooth endoplasmic reticulum. The axon has a swelling containing mitochondria. (d). Local swelling of the axon was present, with separation and rarefaction of microtubules and filaments, and increased presence of dense core and clear vesicles. (7000 X)

Fig. 4. Neuronal DRG cultures exposed to 1 μM PSP. (a). Extensive necrotic debris is present (thick arrows). A few viable axonal regions can be seen (thin arrows). These neurites had numerous varicosities along their course (arrowheads). These occurred more frequently in PSP and mipafox-treated cultures than in the controls (7000X). (b). Axonal swelling containing increased dense core and clear vesicle (thick arrows), and increased separation of microtubules, granular degeneration of microtubules and neurofilaments (thin arrow) are seen. (16000X) (c). Axonal mitochondria demonstrate dissolution of the matrix content (thick arrow), to complete degeneration of mitochondria with increase density of the matrix (arrowhead) and rupture of the mitochondrial membranes (thin arrow). These alterations progressed to lytic regions, neuritic rupture and debris formation. (16000X). (d). Varicosity within the neurite included masses of membranous cytoplasmic bodies, microtubules and neurofilaments (thin arrow). (16000X).

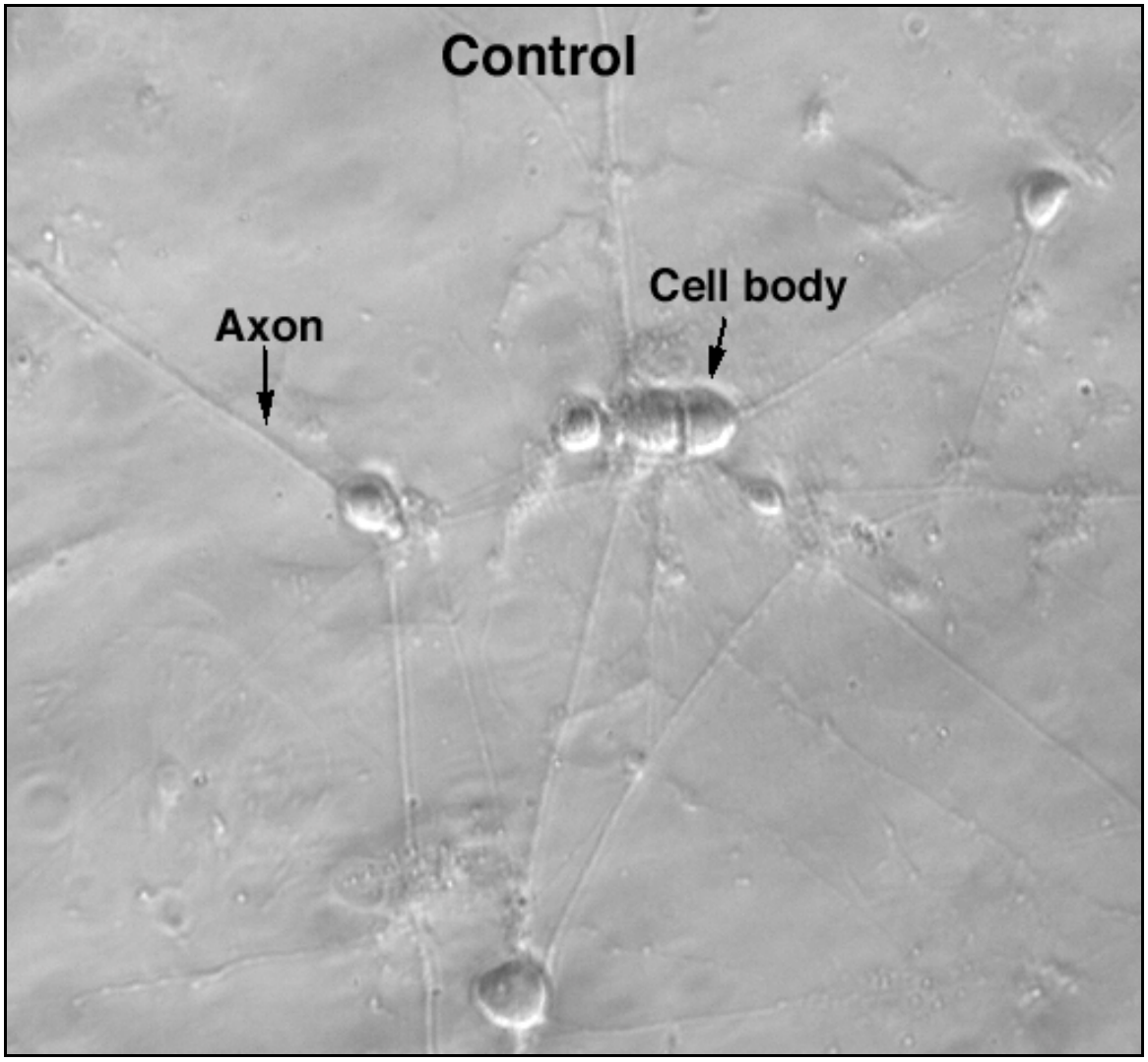

Fig. 1A.

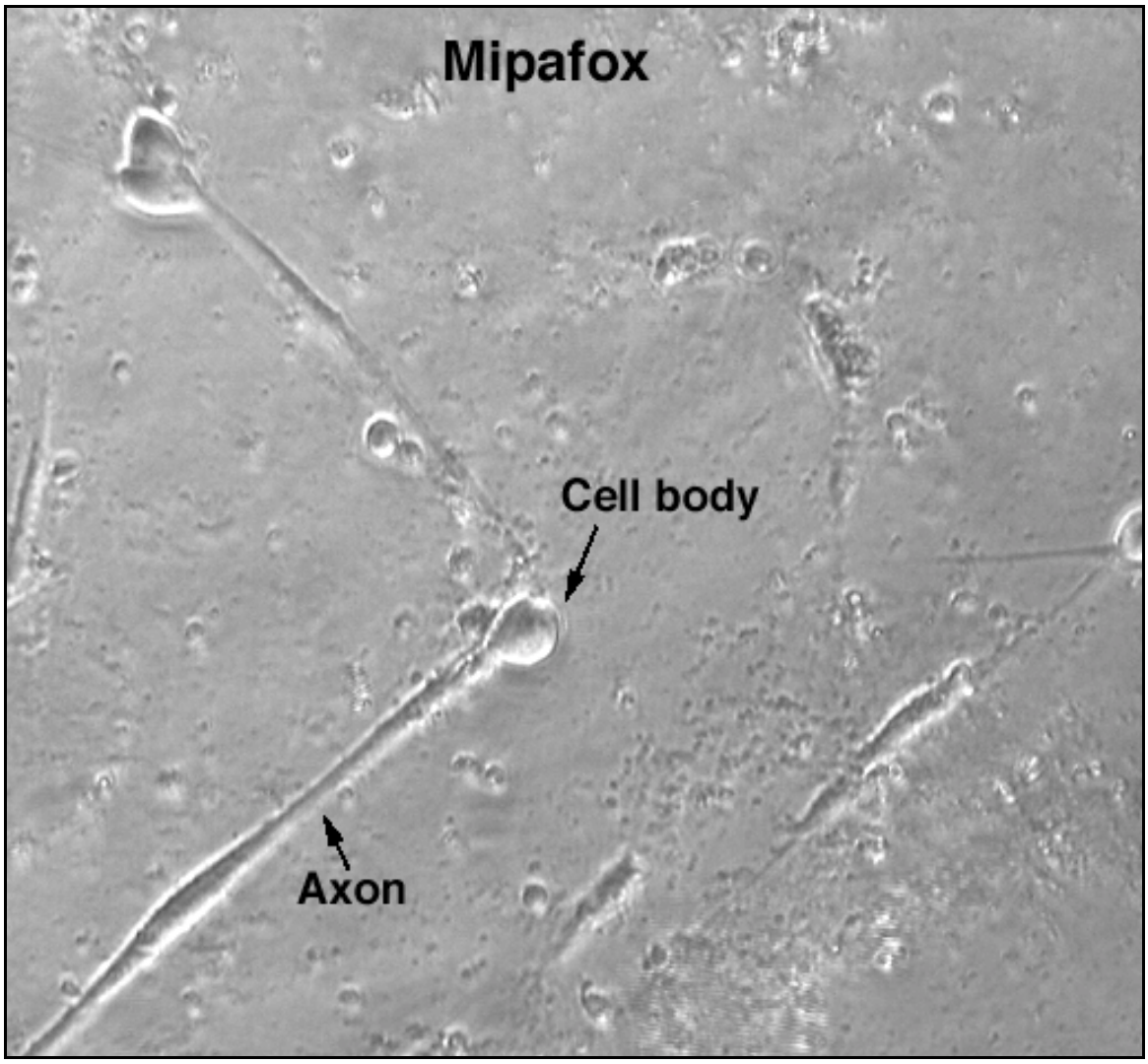

Fig. 1B.

Neuronal growth cone length exposed to OP compounds

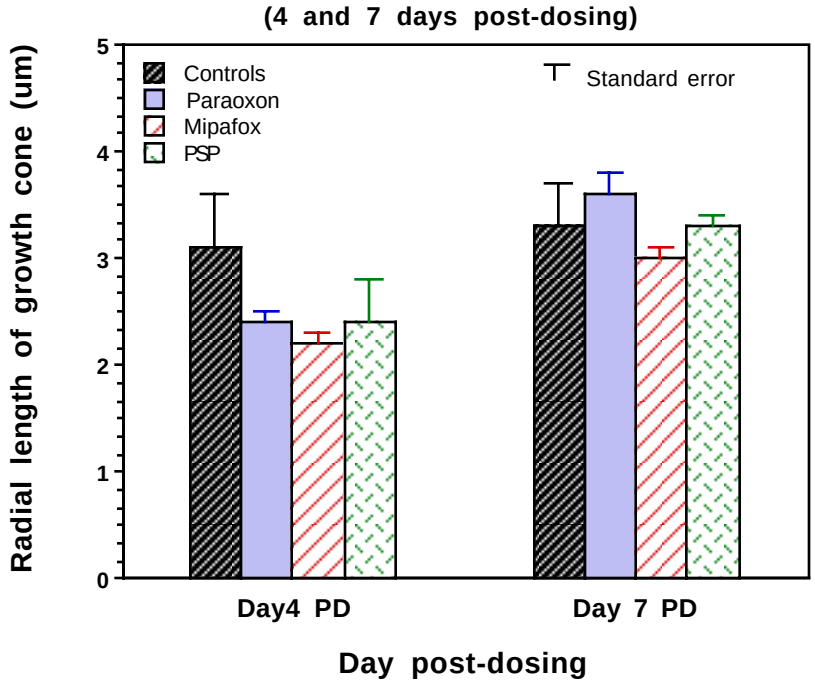

Fig. 2A.

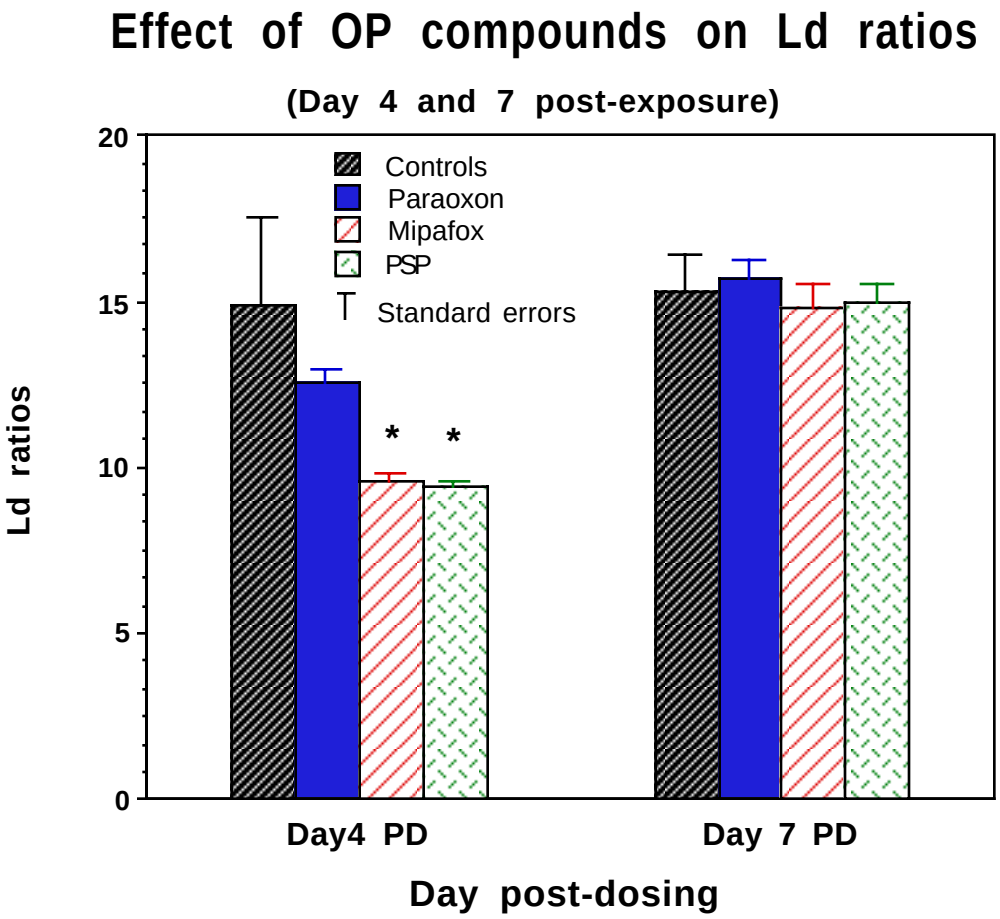
Effect of OP compounds on Ld ratios
(Day 4 and 7 post-exposure)
Controls
Paraoxon
Mipafox
PSP
Standard errors
*
*
Ld ratios
20
15
10
5
0
Day4 PD
Day 7 PD
Day post-dosing

Fig. 2B.

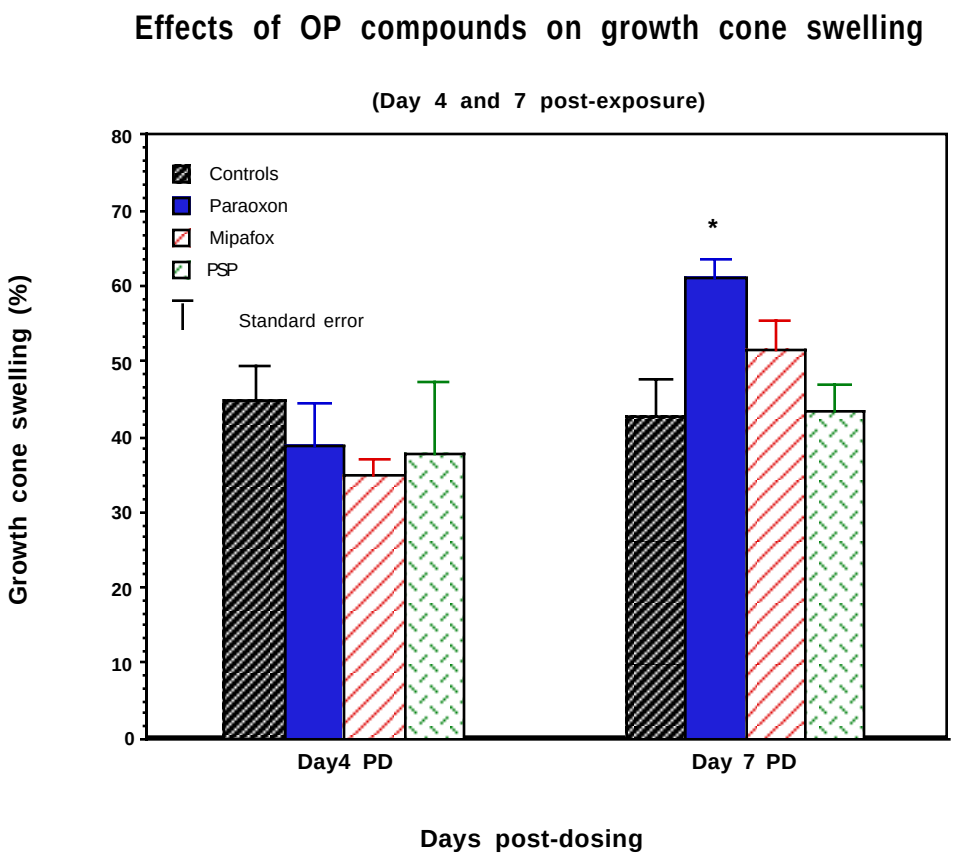
Effects of OP compounds on growth cone swelling
(Day 4 and 7 post-exposure)
Controls
Paraoxon
Mipafox
PSP
Standard error
*
Growth cone swelling (%)
80
70
60
50
40
30
20
10
0
Day4 PD
Day 7 PD
Days post-dosing

Fig. 2C.

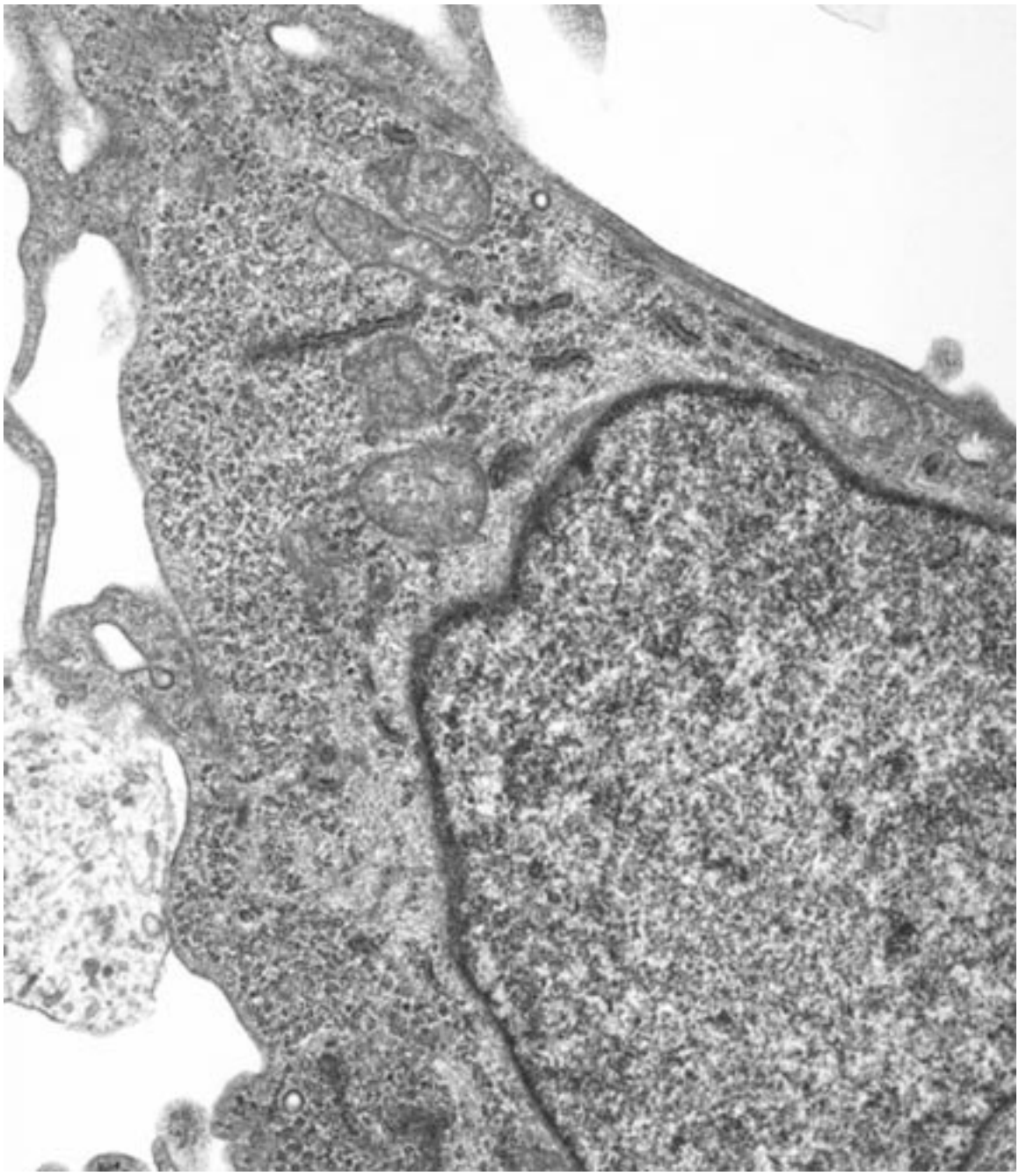

FIG. 3a.

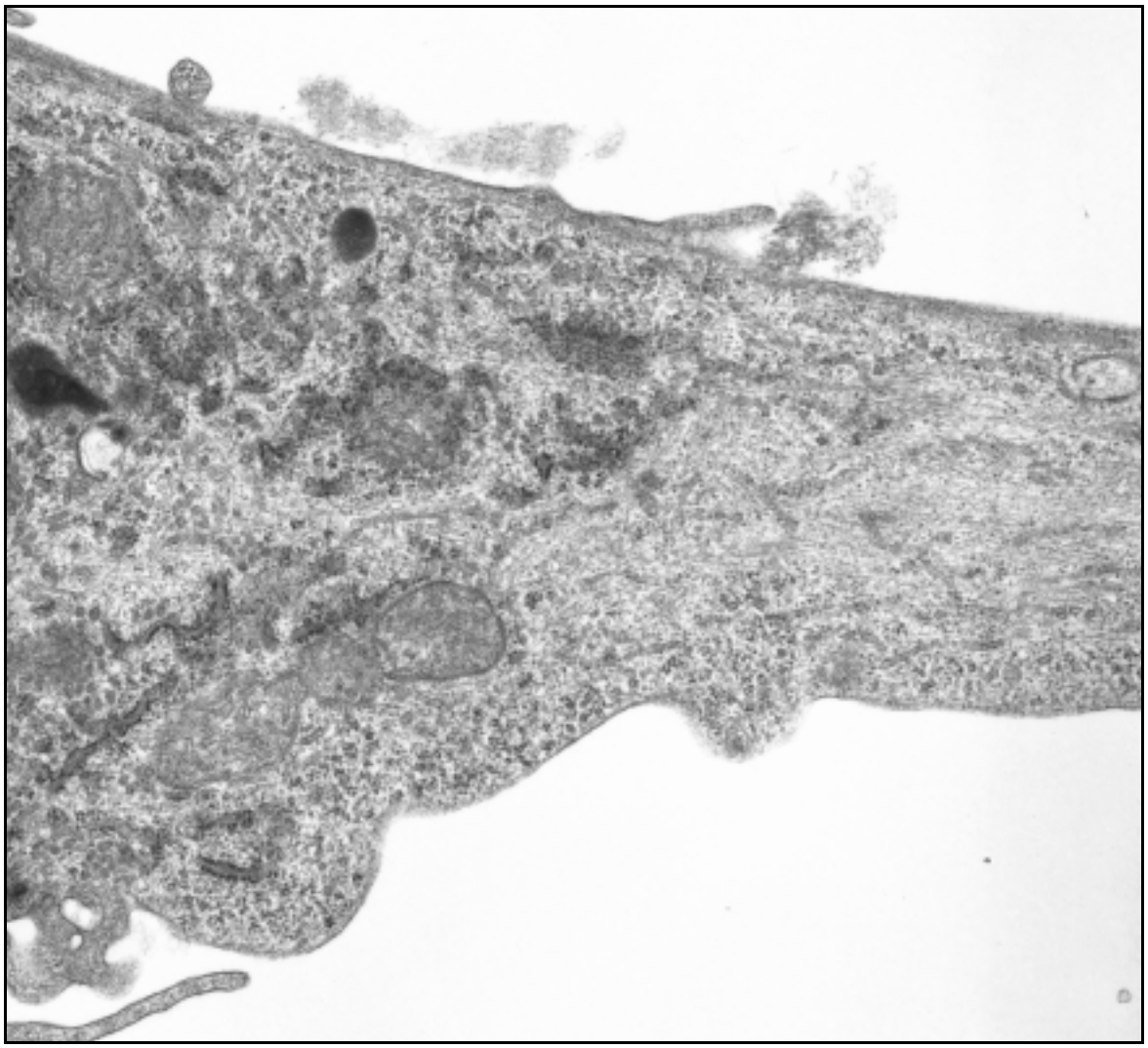

Fig. 3B.

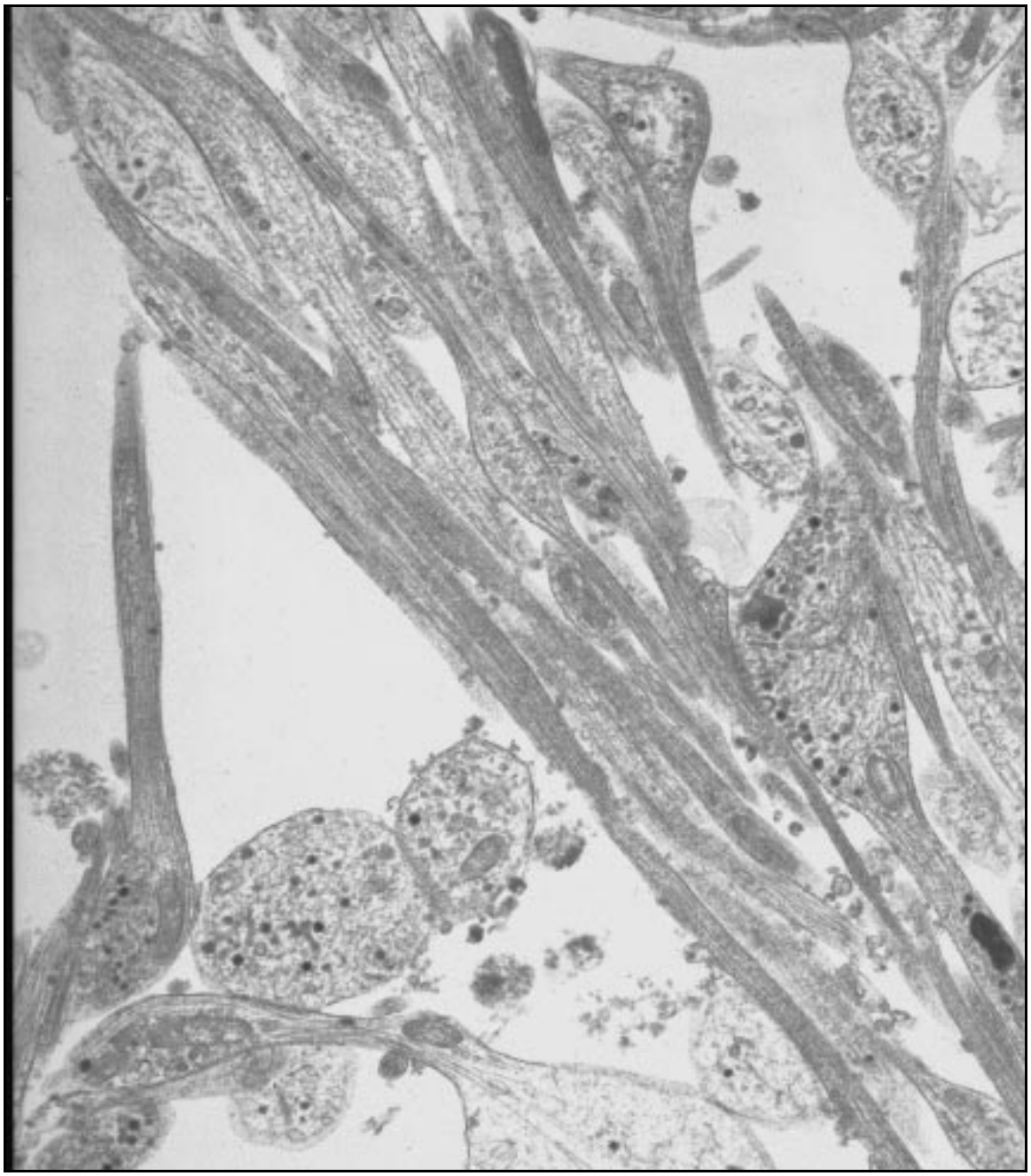

Fig. 3C.

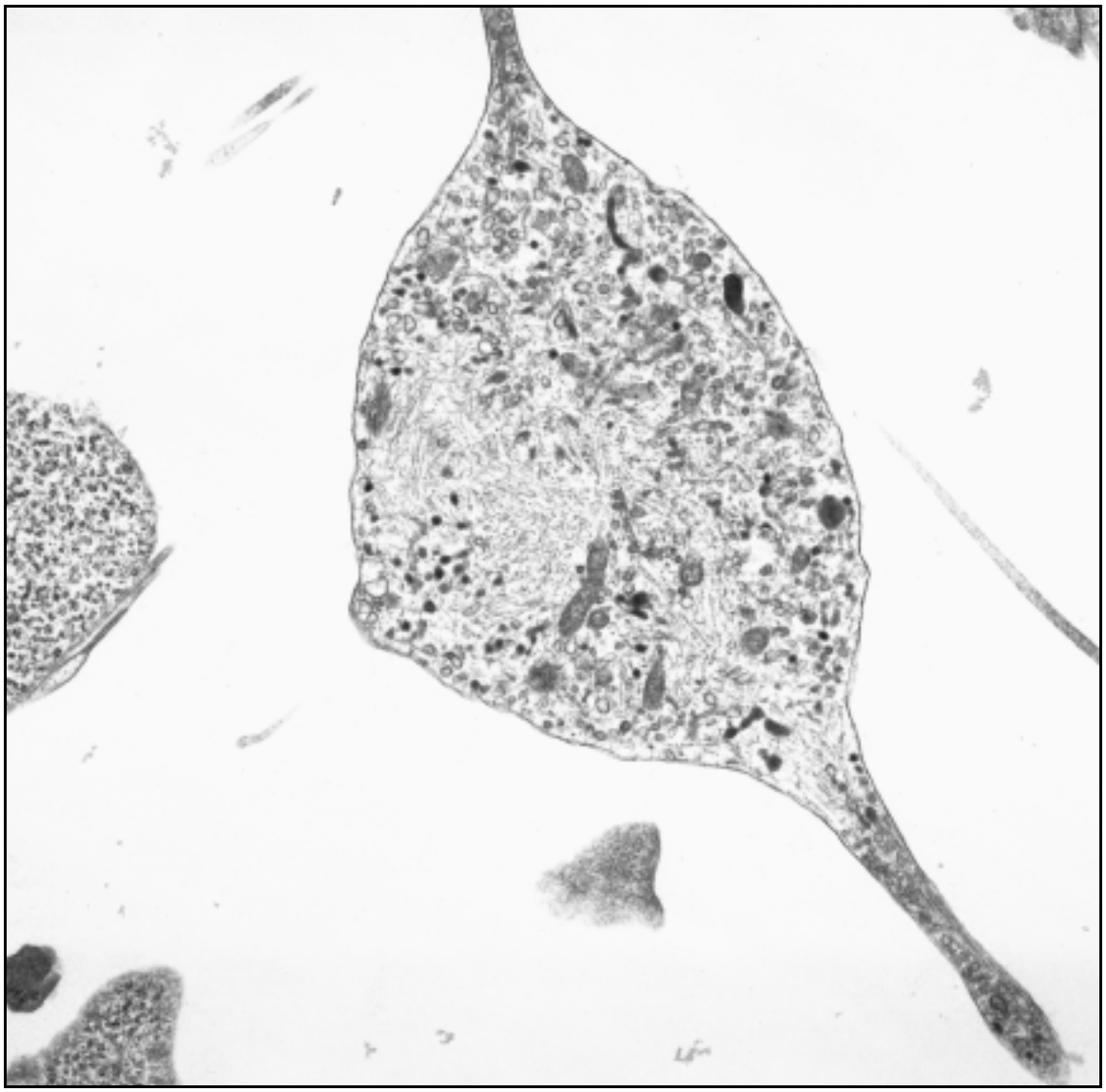

Fig. 3D.

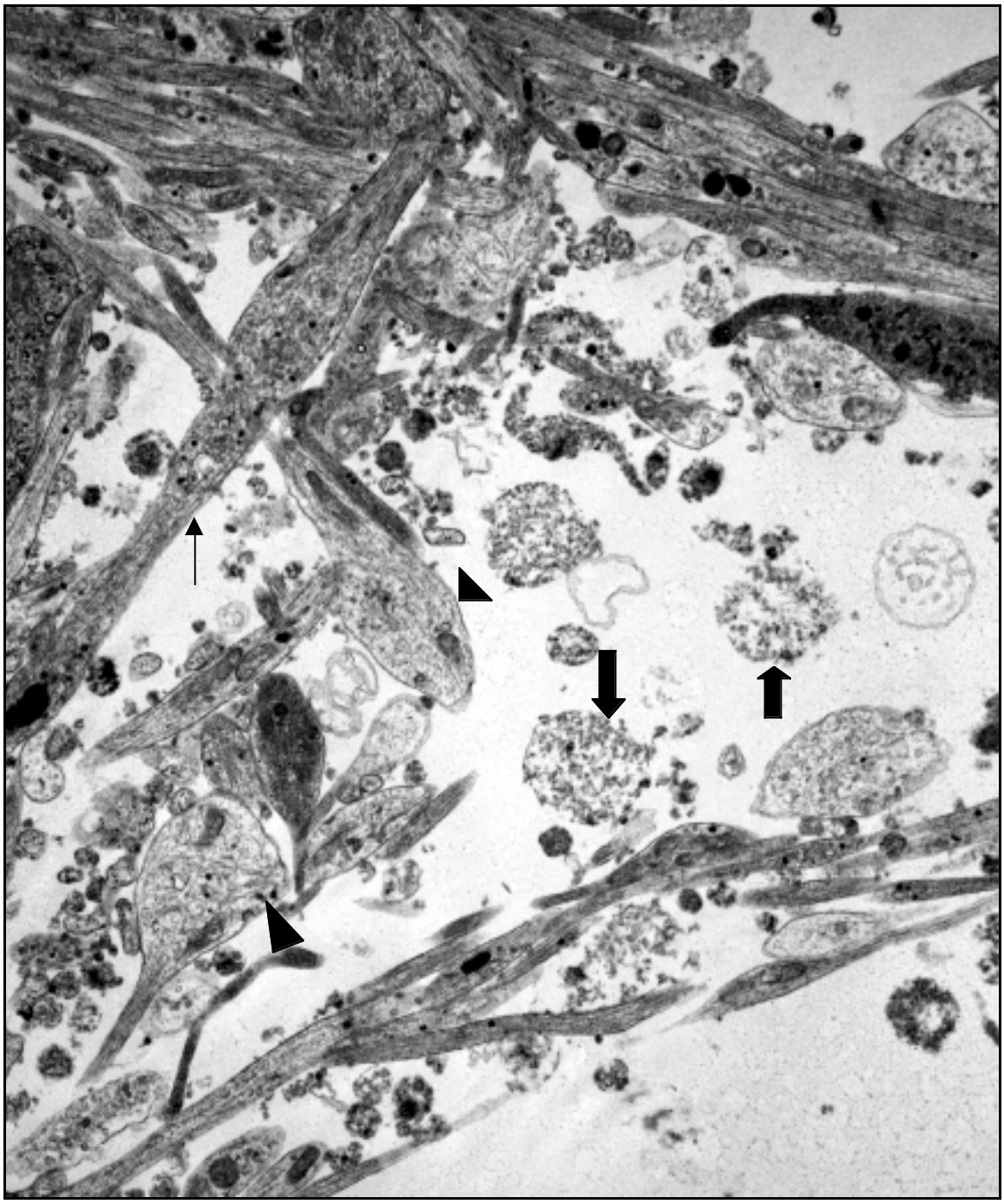

Fig. 4A.